

The role of structures in collective processes

social dynamics and molecular self-assembly

Marta Balbás Gamba



Munich December 2009

The role of structures in collective processes

social dynamics and molecular self-assembly

Marta Balbás Gamba

Dissertation
an der Fakultät für Physik
der Ludwig-Maximilians-Universität
München

vorgelegt von
Marta Balbás Gamba
aus Madrid

München, den 11. Dezember 2009

Gutachter: Prof. Dr. Erwin Frey
Prof. Dr. Stephan Kehrein

Tag der mündlichen Prüfung: 29. Januar 2010

a mi madre

Contents

Zusammenfassung	vii
Abstract	ix
1 Evolutionary social dynamics	1
1.1 Networks	3
1.1.1 Square lattices	4
1.1.2 Random graphs	5
1.1.3 The Watts-Strogatz model	6
1.1.4 Scale free networks	7
1.2 Modelling social systems	10
1.2.1 Evolutionary game theory	10
1.2.2 Opinion models	17
1.2.3 Infection models	22
2 The evolution of mafias	25
2.1 Towards a mathematical description	26
2.2 Deterministic mean field approximation	29
2.2.1 Symmetric model (SM)	29
2.2.2 Fully asymmetric model (FAM)	31
2.2.3 Fully asymmetric policed model (FAPM)	33
2.3 The role of social structures	35
2.3.1 Symmetric model	39
2.3.2 Fully asymmetric model	44
2.3.3 Fully asymmetric policed model	51
2.4 Individuals may move	59
2.4.1 Symmetric model	62
2.4.2 Fully asymmetric model	66
2.4.3 Local mean field approximation in square lattices	70
2.4.4 Fully asymmetric policed model	73
2.5 Conclusion and outlook	79
	iii

3	Pattern diversity in self-assembled monolayers	81
3.1	Self-assembly and order in two dimensional systems	82
3.1.1	The principles of self-assembly of monolayers	82
3.1.2	Fréchet dendrons as building blocks	84
3.1.3	Understanding order in two dimensional systems	85
3.2	Experimental observations	86
3.3	Theoretical model	89
3.3.1	The interaction-site model	89
3.3.2	Theoretically predicted ordered motifs	91
3.3.3	Theory versus experiment	96
3.4	Conclusion and outlook	99
Appendices		
A	Agent based stochastic simulations	101
B	Building uncorrelated scale free networks	103
C	Monte Carlo simulations	105
	Bibliography	108
	List of publications	119
	Acknowledgements	121

List of Figures

1.1	Square lattice	5
1.2	Random and complete graphs	5
1.3	Watts-Strogatz model	7
1.4	Barabási-Albert graph	8
1.5	Scale free graph	9
2.1	SM: bifurcation diagram	30
2.2	SM: stability diagram and separatrix	31
2.3	FAM: bifurcation diagram	32
2.4	FAM: stability diagram and separatrix	33
2.5	FAPM: bifurcation diagram	35
2.6	FAPM: stability diagram and separatrix	35
2.7	Neighbourhoods on structures	37
2.8	Degree distribution of scale free networks	38
2.9	SM: phase portrait for exemplary parameters	39
2.10	SM: deterministic versus stochastic mean field stationary states	40
2.11	SM: stationary state for structures	41
2.12	SM: mafia fraction and extinction probability on structures	42
2.13	SM: extinction as a function of γ on SFN	42
2.14	SM: nucleation process on a lattice	43
2.15	Extinction-coexistence transition as a function of the strength of the mafia	44
2.16	FAM: stationary state for structures	45
2.17	FAM: evolution of an isolated mafioso	47
2.18	FAM: mafia fraction and extinction probability on structures	48
2.19	FAM: nucleation process on a lattice	49
2.20	FAM: mafia fraction on a lattice—heuristic versus simulation	50
2.21	FAM: mafia fractions as a function of γ on scale free networks	50
2.22	FAPM: stationary state for structures	52
2.23	FAPM: stationary state for a square lattice where control elements diffuse randomly	53
2.24	FAPM: snapshot of the population structure on a square lattice	53
2.25	FAPM: mafia fraction and extinction probability on structures	54
2.26	FAPM: extinction-coexistence transition as a function of γ for SFN	55
2.27	FAPM: mafia fraction as a function of γ on SFN	55
2.28	Degree and cumulated degree distribution for a $\gamma = 2.5$ SFN	56

2.29	FAPM: Mafia fraction and extinction probability for police distributions p_1 and p_2	57
2.30	FAPM: preferential police's attachment to hubs	58
2.31	FAPM: extinction transition as a function of p for three distributions of the control elements	60
2.32	FAPM: population fractions for three distributions of the control elements	61
2.33	Active versus passive diffusion	62
2.34	SM: directed diffusion of citizens	64
2.35	SM: directed diffusion of mafia and both species	65
2.36	SM: undirected diffusion of mafia	65
2.37	FAM: directed diffusion of citizens	67
2.38	FAM: directed diffusion of both species as a function of heterogeneity	69
2.39	Neighbourhood configurations on a square lattice	70
2.40	FAM: stability diagram for the local mean field approximation	72
2.41	FAPM: directed diffusion of citizens, mafiosi, and both species	75
2.42	FAPM: undirected diffusion of citizens, mafiosi, and both species	77
2.43	FAPM: directed and undirected mobility in various structures—population fractions	78
3.1	Dendrons chemical configuration	87
3.2	Experimental monolayers	87
3.3	Molecular mechanics energy minimized Fréchet dendron	88
3.4	Interaction-site model	90
3.5	Molecular conformations for a 8/12 dendron	92
3.6	Theoretically predicted supralayers for Fréchet dendrons 8/12 and 8/8	93
3.7	Zig-zag pattern	94
3.8	Stability for the 8/12 molecule as a function of a and T	96
3.9	Exemplary transition from the sawtooth pattern to disorder	97
3.10	Ground state energies for the 8/12 molecule as a function of a	98
C.1	First image algorithm	107

Zusammenfassung

In dieser Dissertation untersuchen wir die Dynamik sozialer Netzwerke und die Dynamik molekularer Monolagen mit Methoden aus der statistischen Physik. In beiden Fällen führt das Zusammenspiel einzelner, mikroskopischer Wechselwirkungen zu kollektiven, makroskopischen Phänomenen, welche stark von der Netzwerk- bzw. Gittertopologie abhängen.

Im ersten Teil untersuchen wir Konflikte in Gesellschaften, in welchen Minderheiten mächtig genug sind, um die Regeln der Allgemeinheit zu diktieren. Unser Ziel ist die relevanten Eigenschaften der sozialen Strukturen und der Beziehungen zwischen den Individuen auszumachen, welche ein tieferes Verständnis der emergenten, kollektiven Phänomene ermöglichen. Insbesondere wollen wir die minimale Größe sowie den Schwellwert für die Stärke einer Minderheit bestimmen, damit sie eine Bevölkerung dominieren kann. Wir entwickeln ein Modell für ein soziales Netzwerk, welches sowohl aus gesetzestreuen Bürgern als auch aus Mafiosi besteht. Die Individuen sind konfrontiert mit der Frage, ob sie die Mafia unterstützen sollen oder nicht. Das Modell berücksichtigt dabei nicht nur die Überzeugungskraft zwischen Bevölkerungsgruppen, sondern auch den Zusammenhalt innerhalb einzelner Gruppen. Weiterhin werden externe Faktoren wie Propaganda und polizeiliche Überwachung einbezogen, welche als *Katalysatoren* für die Wechselwirkungen dienen. Die quantitative Beschreibung des Modells durch nichtlineare Differentialgleichungen stellt einen neuen Ansatz für die Untersuchung sozialer Konflikte dar. Denn in bisherigen Modellen wird der abschwächende Effekt des Gegendrucks, der durch gleichgesinnte Individuen aufgebaut wird entweder gar nicht berücksichtigt oder als additiver Term modelliert anstatt eines Faktor, der die Einflusskraft des Gegners schwächt. Im Mittelpunkt unserer Arbeit steht die Frage, welchen Einfluss die Struktur des Netzwerkes auf die Dynamik des Systems hat.

Wir zeigen, dass das Verhalten beider Gruppen und letztlich das Aussterben der Mafia kritisch von der Heterogenität des Netzwerkes abhängt. Aus unserer Arbeit folgt, dass die Mobilität der Individuen eine wichtige Rolle spielt. Erlaubt man Mitgliedern einer bestimmten Gruppe *sichere* Orte im Netzwerk aufzusuchen, so erhöht sich der Anteil dieser Gruppe im stationären Zustand erheblich. Überraschenderweise stellt ungerichtete Diffusion eine sehr wirksame offensive Strategie zur Stärkung einer Bevölkerungsgruppe dar. Im Grenzfall hoher Mobilität ergibt sich ein gut durchmischtes Netzwerk, das sich eigentlich durch eine Mean-Field-Theorie beschreiben lassen sollte. Da die Entscheidungsfindung jedoch auf der Wechselwirkung zwischen nächsten Nachbarn basiert, führt ein Mean-Field-Ansatz nicht zum Ziel. Es gibt nur eine endliche Zahl an möglichen sozialen Umgebungen. Das Feld, welches die Übergangswahrscheinlichkeiten bestimmt, ist daher diskret. Wir haben dies durch eine *lokale*

Mean-Field-Theorie berücksichtigt, welche die Systementwicklung korrekt nachvollziehen kann.

Der zweite Teil der Arbeit beschäftigt sich mit der Selbstorganisation molekularer Monolagen. Die einzelnen Moleküle, die kurzreichweitig wechselwirken, bilden auf strukturierten Substraten eindrucksvolle makroskopische Muster. Gelänge es diese Prozesse zu kontrollieren, würden sich neue Wege zur Herstellung von Nanodevices auf tun. Vor diesem Hintergrund entwickeln wir ein *Interaction-Site-Modell*, um die Selbstorganisation der Moleküle besser zu verstehen. Ausgehend von der Geometrie der einzelnen molekularen Bausteine, der Symmetrie des zugrundeliegenden Substrates, sowie der Stärke und Reichweite der Wechselwirkungen lassen sich die entstehenden Muster vorhersagen, wie sie in der Gruppe von Bianca Hermann an der LMU München experimentell beobachtet wurden. Weiterhin erlaubt es unser Modell, die Stabilität der Muster und die Art des Schmelzüberganges zu bestimmen.

Abstract

In this thesis we study the dynamics of social systems and molecular monolayers employing tools of statistical physics. In both cases the topological structure underlying the interactions turns out to be the key element in the emergence of collective macroscopic phenomena from the synergy of the individual interactions.

In the first part, we are concerned with the conflicts arising in societies in which minority groups exert enough pressure to impose the rules of the community. We aim at identifying the inherent features of the social structures and individuals' relations which provide further understanding of the emergent collective phenomena. Specifically, we would like to determine the minimal size and threshold strength for such minorities to dominate the population. We develop a model which describes the behaviour of individuals in a society which is split up into two groups, one of lawful citizens and another one of mafia members. Individuals are constantly confronted with the dilemma of supporting the mafia or not. The persuasiveness across different groups is counteracted by the support of peers proportionally to their fractions in a neighbourhood. In addition, the *mafia model* includes the catalytic influence of external elements such as propaganda or control elements for both joining and leaving the mafia. Expressing the probabilities for these actions proportionally to both populations and to the density of control elements, constitutes a novel approach to model the dynamics of social conflicts. In previous approaches the attenuation of the contrary's pressure due to alike individuals is either not taken into account or modelled through an additive term rather than as a factor which effectively weakens the strength of the adversary. We extensively explore the nonlinear dynamics resulting from this approach, emphasizing the role of the specific structure of social networks.

We show how the coexistence of the two groups and the extinction of mafias critically depend on the heterogeneity of the social network. We find that mobility of individuals among the network's nodes plays a crucial role in the dynamics of the system. Enabling agents in a group to rationally seek safer locations greatly enhances their fraction in the stationary state. Surprisingly, undirected diffusion turns out to be a brilliant offensive strategy which drastically affects the system's evolution. If individuals of both groups diffuse much faster than they take decisions, the population becomes well-mixed and one would expect a mean field approximation to reproduce the system's behaviour. However, since decisions are based on interactions with nearest neighbours, we find that such a mean-field approach is always invalid. Since there is only a finite set for the social composition of an individual's neighbourhood, the *field* entering the transition probabilities becomes discrete. We have accounted for this by a *local* mean field theory which captures the system's evolution adequately.

An important direction for further work is the analysis of the role of preferential population distributions in extremely heterogeneous networks, the inclusion of the concept of geometrical distance on top of the topological connections to regulate interactions, and especially the issue of adaptive networks to better resemble the evolution of societies.

In the second part of this work we deal with the *self-assembly of monolayers* constituted by molecular building blocks which interact at the nanoscale level. These blocks, on top of atomic substrates, spontaneously organize into stable supralayers which display intriguing long-range order motifs. These patterning processes, if appropriately controlled, represent a viable route to manufacture practical nanodevices. With this goal in mind, we seek to capture the salient features of the self-assembly process by means of an *interaction-site* model. The geometry of the building blocks, the symmetry of the underlying substrate, and the strength and range of interactions encode the self-assembly process. By means of Monte Carlo simulations, we have predicted an ample variety of ordering motifs which nicely reproduce the experimental results obtained at Bianca Hermann's group at the LMU. We have explicitly explored the phase behaviour of the system in terms of temperature and the lattice constant of the underlying substrate. We have found that various patterns coexist in equilibrium, which melt at temperatures much higher than the room temperature of the experiments. Our method is thus suitable to investigate the stability of the emergent patterns as well as to identify the nature of the melting transition monitoring appropriate order parameters.

The interaction-site model has only been used in the framework of Monte Carlo simulations, needing the indirect input coming from experiments to guess the stable molecular conformations to run Monte Carlo. The theoretical approach developed in this work to predict stable patterns would be greatly improved if genetic algorithms were to supply the stable conformation of the building blocks. This would constitute a straightforward step in further work.

This thesis is structured as follows: The first chapter constitutes an introduction to the theoretical framework of evolutionary sociodynamics. First, a mathematical description of networks is provided. Then, we present an overview of the models developed in the past years to quantitatively understand social problems with the tools of statistical physics.

In the second chapter, we introduce the mafia model. We lay out a mathematical framework from a few simple principles to explain the dynamics of social systems where mafias are present. We investigate the model under a mean field approximation and by means of numerical simulations. We explicitly analyse three possible scenarios and examine the role of structures showing various degrees of heterogeneity. In addition, we study the effect of mobility and provide a local mean field theory which properly captures the essence of the mafia model in regular lattices.

In the third chapter, we address the problem of understanding self-assembly of molecular constituents on top of patterned substrates. We revise the principles of self-assembly and introduce an interaction-site model to theoretically describe it. We discuss the emergent phases for our model as well as their stability. We finally compare our predictions with the experimental results to draw conclusions about the validity of the model.

Chapter 1

Evolutionary social dynamics

I know who I was when I got up this morning, but I think I must have been changed several times since then.

Alice's adventures in wonderland

LEWIS CARROLL

In this thesis we investigate a particular problem in the realm of social dynamical systems where some *actors* interact with each other according to some specific rules. Nature offers many examples of such systems: bees and ants' societies, bacterial cultures, or prey-predator relations to mention just some. But also a variety of problems from economy and human sciences may be understood within the same framework. Evolutionary social dynamics, built on the interactions of discrete agents, addresses questions such as how fast opinions spread in a population, how cooperation emerges in a community, which mechanisms lead an individual to identify himself with some religion or political ideas, how groups follow a fashion trend, or under which circumstances infections spread in a society are examples of social problems whose dynamics is very similar to that of biological systems.

Two features play a relevant role in all the systems above: the relations between individuals¹ and the adaptive capacity of agents. Every system has an underlying structure of connections which determines the groups of interacting agents. In addition, agents are able to adapt their strategies as a result of the interaction with their habitats. The habitat of a given agent contains the interactions with the surrounding actors but also possible external factors, which do not depend on the population.

The adaption process observed in these systems resembles some features of the Darwinian evolution of species. According to this theory, evolution is the set of processes which drives the emergence, change, and extinction of species in biology. Reproduction, selection and mutation constitute the cornerstones of evolution. Over the course of generations individuals reproduce at a given rate. In addition, new features in the species genotype may appear because of the recombination and mutation of the genetic material. When several species compete for the resources in a common habitat only the strongest survive and reproduce. This is *natural selection*. Natural selection drives species to extinction or adaptation.

¹The terms individual, agent, and actor are used interchangeably in this work.

Evolutionary dynamics has turned out to be the proper framework in which to investigate the interaction of populations in a large variety of systems. Several microscopic models have emerged to examine specific features of these complex problems. In them individuals are modelled as *adaptive* agents. A variable accounts for the *state* of agents and takes specific values for every agent which belong to a continuous or discrete range. Depending on the problem considered states may, for instance, represent strategies, species, opinions, or specific qualities. This state evolves in time according to some fixed, environment-dependent rules. The ability of agents to reproduce is quantified by a *fitness function* which is conditioned by the strategy and the environment of the agent.

What is the range of interaction for a given agent? The simplest hypothesis considers interactions are all-to-all. Topologically it corresponds to the case in which individuals occupy the vertices of a complete graph, in which every node is connected to all other nodes and interactions occur between all pairs of agents. This is an example of a *well-mixed* population, a key concept in this work. In a well-mixed scenario individuals experience the same influence they would have in a complete graph. The fractions of the population they interact with belonging to each group are the same as those of the whole society. In real structures this assumption may be made only if individuals diffuse much faster than interactions take place. Mathematically this simplification is equivalent to a global mean field approximation.

However, reality is much more complex and agents usually do not interact with the whole population but only with a subset of it which shows some kind of affinity. To account for the relations between actors one includes different possible topologies in the model. These structures are specifically modelled by regular lattices or heterogeneous networks. In structured societies individuals group according to their interests, opinions, or strategies. The tendency of agents to cluster with alike individuals leads to the emergence of domains.

Sociodynamics is the emerging field devoted to the understanding and quantification of behaviour in social systems. Agent-based models in different architectures are investigated with methods adapted from mathematics and statistical physics, particularly those of nonlinear dynamics and the theory of stochastic processes. Unfortunately, the systems investigated in sociodynamics are often not exactly solvable because of their complexity and the approximations required to solve them analytically may neglect crucial features. Simulations offer a very good experimental setting to investigate the dynamics of many complex systems.

Agent-based algorithms allow to recreate *in silico* the intriguing microscopic interactions which lead to the emergence of macroscopic phenomena. These methods, the so-called *cellular automata*, were pioneered by von Neumann and Ulam in the 1940s [135]. A cellular automaton is an evolving model consisting of a regular lattice or graph whose cells are in a given discrete state among a finite set. The lattice's sites in cellular automata represent interacting agents. Every cell is associated to a particular neighbourhood and interacts with it according to some well-defined, fixed rules. As a result every cell updates its state successively in time until a macroscopic stable equilibrium state is reached.

This chapter is organized as follows: first, in section 1.1 we introduce some notions of graph theory relevant to describe social structures. We then formalize in section 1.2 some concepts of evolutionary dynamics and review some of the most popular models

which deal with social problems. In particular, we discuss the dynamics of social systems in different topologies.

1.1 Networks

The underlying organizations of the systems we are interested in are referred to as social networks and are described by graph theory. The interacting agents occupy the *nodes* of a graph whose *edges* define the possible interactions. Examples of systems with similar architectures are as diverse as airport networks, sexual contacts, the network infrastructure of the internet, the WWW, the metabolic reactions of bacteria, actor or scientific collaborations.

In some networks all nodes have a comparable number of connections. However, many systems show large heterogeneity, meaning that the number of contacts varies significantly from one node to another. Usually these networks contain a non-negligible number of highly connected nodes, the so-called *hubs*. Despite the fact that some of the real networks are very large, all of them exhibit *small-world* character, i.e. the minimum number of nodes between two given nodes is very small compared to the network size. Some examples of actual networks are illustrated in table (1.1) taken from [2] and references therein.

network	nodes	edges	N	$\langle k \rangle$	γ	ℓ	C
movie actors	actors	common films	212250	28.78	2.3	4.54	
www (D)	internet sites	href links	325729	4.51	2.45	11.2	
sexual contacts	persons	sexual relations	2810		3.4		
metabolic E. coli (D)	substrates	reactions	778	7.4	2.2	3.2	
citations (D)	papers	cites	783339	8.57	3		
neuroscience papers	authors	collaborations	209293	11.54	2.1	6	0.76
phone calls	speakers	calls	53×10^6	3.16	2.1		
synonyms	words	synonymy	22311	13.48	2.8	4.5	0.7

Table 1.1: Characteristics of some real networks. The nature of nodes and edges, sample size N , average degree $\langle k \rangle$, exponent of scale free distributions γ , average path length ℓ , and cluster coefficient C are specified if available. (D) stands for directed networks. The observables specified here are defined later in this section. The data are taken from [2], a review which summarizes other works referenced therein.

In this section we define formally the characteristics of the most relevant networks for our work. In particular, we are interested in the degree of heterogeneity of the structures, the average number and variance of connections, the distance between two random nodes, and the possible substructures emerging under a whole network, as for instance clusters or trees.

Networks are represented as graphs, mathematical objects consisting of a set of N nodes connected through n edges. The connections between two nodes may be *undirected* or *directed*. In the first case the established relation between two nodes works in both directions, like the collaboration between two actors; while in the second case the relation is unidirectional, like the transformation from reactants to products in a chemical reaction. The graph is described by a $N \times N$ *adjacency* matrix A , whose entries A_{ij} are 1 if the node i is connected to the node j and 0 otherwise.

Undirected graphs are represented by symmetric matrices. Diagonal elements vanish if there are no self-connections. We define the concepts of average or maximal *path length* between two random nodes, *clustering coefficient* and *degree distribution* and compare them for several kinds of networks.

The **degree** k_i of a particular node i is the number of connections pertaining to it. The degree distribution of a network gives the probability $P(k)$ for a randomly selected node to be connected to k neighbours.

A cluster is a substructure present in a network in which there is a large number of connections among a group of nodes. In particular, one speaks of a cluster around a node i if its neighbours are highly connected among them. Thus, a good measure of the *clustering degree* of a specific node is the ratio between the number of actual, E_i , and possible connections among its neighbours:

$$C_i = \frac{2E_i}{k_i(k_i - 1)}. \quad (1.1)$$

The **clustering coefficient** for the whole network are the clustering degrees of single nodes averaged over the whole network:

$$C = \frac{1}{N} \sum_i C_i. \quad (1.2)$$

The **Hamming distance** between two nodes is the minimum number of vertices between them. This concept of distance is a topological instead a geometrical one. The diameter of a graph is given by the largest distance between any pair of nodes. An alternative measure is the **average path length** ℓ , which is the average distance between two nodes. Both measures characterize the spread of a graph.

In the remainder of this section we describe different network models, paying special attention to the quantities defined above and to the small-world character observed in real networks. First we discuss regular lattices, in particular the square grid. Then we describe random graphs and introduce later the Watts-Strogatz model. Finally we summarize the properties of scale free networks and examine two algorithms to construct them.

1.1.1 Square lattices

A d -dimensional *regular lattice* is a graph whose nodes correspond to the points with integer coordinates in a d -dimensional cartesian space and whose edges connect nodes which are separated by one unit distance. In a regular lattice all nodes have the same degree, namely $k = 2d$. In the topology of square lattices there are no connections among the neighbours of a given node. Therefore there are no clusters in regular grids. The characteristic average path length scales as $N^{1/d}$ for a d -dimensional lattice. As we will see later this is much longer than the path length of random graphs or scale-free networks. Given the lack of clusters and the long path lengths regular lattices do not show the small-world signature observed in actual systems. They are thus not suitable structures to model reality. However, they offer a simple way to study the behaviour of some systems in spatial environments, as for instance bacterial cultures on a petry dish.

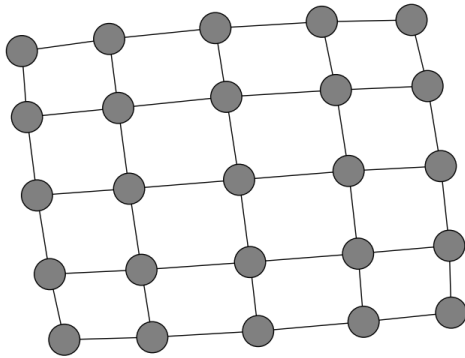


Figure 1.1: Topology of a regular square lattice of size $N = 25$.

1.1.2 Random graphs

A *random graph* is a topological structure in which N vertices are connected among them in a random way. The study of random graphs was pioneered by Erdős and Rényi in the late 1960's [42, 43]. Two equivalent mechanisms were proposed to build these networks. In the first one, n edges are randomly distributed between the $N(N - 1)/2$ possible pairs of nodes among the N nodes of a graph. This mechanism gives rise to $C_{N(N-1)/2}^n$ equiprobable graphs with average degree $\langle k \rangle = n/N$. In the second one, all possible pairs of nodes in a configuration of N vertices are connected with probability p . The expected number of edges is thus $E(n) = pN(N - 1)/2$ and the average degree is $\langle k \rangle = p(N - 1)/2$. An example of a random graph is displayed in the left side of Fig. 1.2.

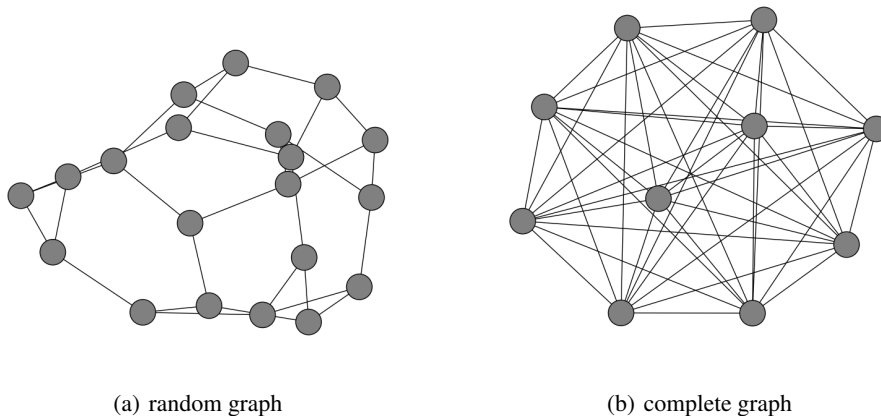


Figure 1.2: Left: Random graph of size $N = 20$ and $\langle k \rangle = 3$. Right: complete graph of size $N = 10$.

A *complete graph* is a special case of a random graph, in which the probability for every pair of nodes to be connected is $p = 1$. As we mention above, this is the underlying structure for a well-mixed population—Fig. 1.2 right.

² C_i^j is the number of possible combinations of size j among i elements.

Several properties of random graphs have been investigated. Special interest has been paid to compute the threshold probabilities p_c for different events to take place such as the emergence of substructures as trees and cycles or percolation phenomena—see [2] for a detailed discussion.

In a random graph, where the probability to build a connection between two random nodes is p , the probability for a node to have a degree k_i follows a distribution with binomial form:

$$P(k_i = k) = C_{N-1}^k p^k (1-p)^{N-1-k}, \quad (1.3)$$

which approaches a Poisson distribution for large sizes N :

$$P(k) \sim \exp(-pN) \frac{(pN)^k}{k!} = e^{-\langle k \rangle} \frac{\langle k \rangle^k}{k!}. \quad (1.4)$$

Since the fluctuations of the degree are small, the number of nodes within a distance l is close to $\langle k \rangle^l$. By equating the number of nodes at the maximal distance with N , one obtains the network diameter, namely the maximal distance between any pair of nodes $\ell \sim \log N / \log \langle k \rangle$. The average path length scales thus logarithmically with the graph size. Random graphs display small-world character.

The probability for the nearest neighbours of a random node to be connected among themselves is proportional to p and the clustering coefficient is thus:

$$C = p = \frac{\langle k \rangle}{N}. \quad (1.5)$$

The average path lengths of the exemplary networks considered in table (1.1) behave in a similar way as those of random graphs, whereas their clustering coefficients are far from those predicted by the Erdős-Rényi model. Although interesting *per se* due to its simplicity, the random graph model is not suitable to describe the complexity of real networks.

1.1.3 The Watts-Strogatz model

Watts and Strogatz introduced a model which better accounts for the properties observed in real networks [143]. It should exhibit small-world properties together with large clustering coefficients like real networks. They proposed a model which is an interpolation between a regular lattice and a completely random graph. First, one builds a one-dimensional ring configuration with N vertices connected to their $2m$ nearest neighbours, m of them in the clockwise and m in the counterclockwise direction—left part in Fig. 1.3. Every link in the clockwise direction is then rewired with probability p to a random node and remains fixed with probability $1-p$ —illustrated in the right side of Fig. 1.3. The result is a graph with a degree distribution similar to that of a random one³, but with very interesting properties. There is a broad region of the parameter p for which the rewired graph exhibits small path lengths and large clustering coefficients. The latter is true for $p \ll 1$ [12], as the clustering coefficient is given by:

$$C(p) \simeq \frac{3(m-1)}{2(2m-1)} (1-p)^3. \quad (1.6)$$

³identical for the limit $p \rightarrow 1$, average degree $\langle k \rangle = 2m$

If $p \gg 1/N$ the typical size of regions between shortcuts is small. Then the average path length is rather small scaling as $\log N$ [16, 15]. Thus, for the parameter region $1/N \ll p \ll 1$ the Watts-Strogatz model reproduces well the features observed in real networks.

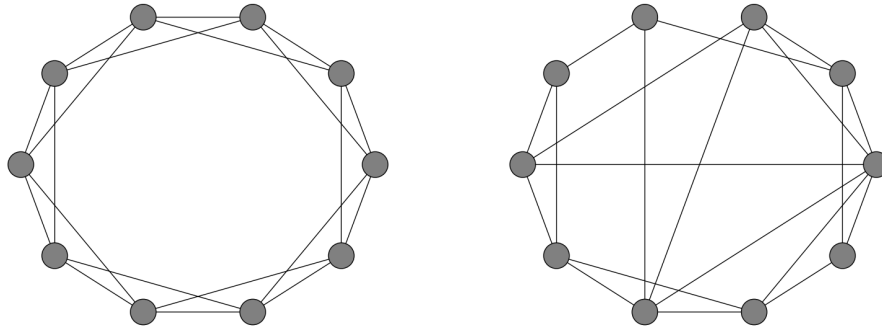


Figure 1.3: Example of a Watts-Strogatz network with $N = 10$ and $m = 2$. The left figure shows the ring configuration before edges were rewired. In the right side the Watts-Strogatz model resulting from rewiring with probability $p = 0.3$.

1.1.4 Scale free networks

In addition to the small-world character, many real networks show heterogeneous connectivity. In particular their degree follows heavy-tailed distributions with a non-negligible number of highly connected nodes or hubs. Such distributions have been recognized, for instance, in air traffic, the WWW, or scientific citation networks. These graphs are described by power law distributions $P(k) \sim k^{-\gamma}$ for which fluctuations around the average connectivity $\langle k \rangle$ are rather large.

A function is called *scale free* (SF) if after rescaling its argument x , the function does not change further than a multiplicative factor, i.e. $f(\lambda x) = \mu f(x)$. Such restriction is only fulfilled by power-law like functions $f(x) \sim x^\gamma$. The scale free property is reflected in the self-similarity of the network: after a coarse-graining process the degree distribution has the same form independently of the length scale. This is a typical feature of fractals. Scale free networks manifest many properties of fractals such as the fractal character of their dimension.

In scale free networks the moments of the degree distribution higher than $\gamma - 1$ systematically diverge for infinite networks. In particular, the second moment of scale free networks with exponent $\gamma < 3$ diverges, which is the reason of many properties of processes such as percolation in these networks.

Cohen and Havlin have shown that scale free networks have path lengths even smaller than those of the Watts-Strogatz model [22, 33]. They were called *ultra small worlds*. For $2 < \gamma < 3$ the diameter of a SF network scales as $\log \log N$, being much smaller than the diameter of random graphs and small-world models; while for $\gamma > 3$ the diameter scales as in the Watts-Strogatz model with $\log N$. For the particular case $\gamma = 3$ the network diameter scales as $\log N / \log \log N$.

What are the mechanisms available to generate scale free networks? The first attempt to solve this question was addressed by Barabási and Albert in the late 90's [10].

The Barabási-Albert model

Barabási and Albert proposed a dynamical process for growing networks which gives rise to scale free graphs [10]. The mechanism is based on two crucial features: growth and preferential attachment. Starting with a configuration of m_0 nodes at every time step Δt a new node is introduced together with $m \leq m_0$ edges to connect the new node with older ones. The main idea is that old nodes with a larger number of links are more likely to be selected for connection than newer ones. Thus, the new node attaches preferentially to vertices with large degree k_i according to the probability

$$\pi(k_i) = \frac{k_i}{\sum_j k_j}. \quad (1.7)$$

After t time steps the network will have $N = m_0 + t$ nodes and mt edges. Simulations and analytical arguments show that evolving networks converge to a stationary state, which displays a power-law degree distribution: $P(k) \sim 2m^2 k^{-\gamma_{BA}}$. The exponent $\gamma_{BA} = 3$ of the power law is found to be independent of the only parameter of the model m . See an example of a Barabási-Albert network in Fig. 1.4.

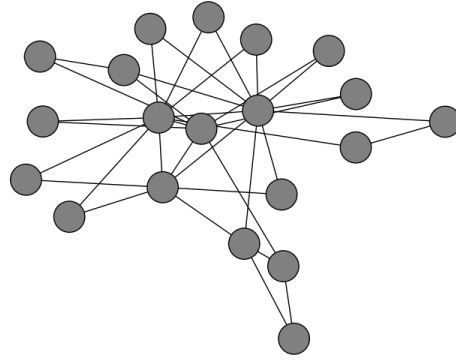


Figure 1.4: Barabási-Albert network for $N = 20$ and $m = 2$.

The average path length of the Barabási-Albert model shows a logarithmic behaviour $\ell \sim \log N / \log \log N$ [21], which is smaller than the average path in random graphs. This result matches that obtained independently by Cohen and Havlin for general scale free graphs [33]. Although there is no analytical prediction for the clustering coefficient in the Barabási-Albert model, it has been observed that it decreases with the network size as $C \sim N^{-3/4}$. This is slower than in random graphs, $C \sim N^{-1}$, but still it does not show the characteristic behaviour of small-world models.

A relevant property of Barabási-Albert graphs is the emergence of correlations between the degrees of connected nodes [73]. Since new nodes mainly attach to old ones with a large degree, the older a node is, the more connections it has. The emerging graph contains thus a substructure of interconnected hubs.

The configuration model and uncorrelated configuration model

The Barabási-Albert model is limited to generate scale free graphs with an exponent $\gamma_{BA} = 3$. Other models have been hence proposed to construct graphs with scale free distributions and arbitrary exponent γ . Molloy and Reed introduced the *configuration model* [93]. Starting with a fixed number of N disconnected vertices k_i stubs⁴ are attached to every node i . The number of stubs per node k_i is drawn from the scale free distribution $P(k)$ with the constraint $m \leq k_i < N$, where m is here the minimal degree of a node. The total number of stubs $\sum_i k_i$ must be even to assure a fully connected graph. Once each node has its corresponding set of free stubs two random stubs are selected to form a permanent bond between the two nodes they are attached to. The process is repeated until no stubs are available. This mechanism guarantees networks free of degree-degree correlations, as the degree of nodes is fixed before nodes are connected with each other. Fig. 1.5 shows an example of a scale free network generated with the configuration model algorithm.

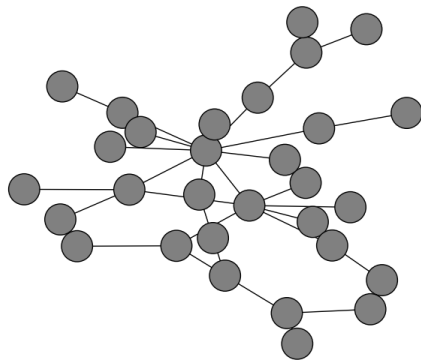


Figure 1.5: Scale free network generated following the algorithm of the configuration model for $N = 30$ and $\gamma = 2.2$.

The configuration model works if the degree fluctuations $\langle k^2 \rangle$ are finite. But this is not the case for $\gamma \leq 3$. For such networks multiple and self-connections emerge. One may explicitly forbid the construction of such connections, but then *disassortative*⁵ degree-degree correlations appear whose origin is due to the *cutoff*—maximum degree—of the network. In order to avoid correlations in scale free networks without multiple and self-connections, it has been shown that the cutoff must be at most $k_s(N) \sim N^{1/2}$ —the so-called structural cutoff [20]. The configuration model considers a cutoff that scales as $k_c(N) \sim N^{1/(\gamma-1)}$, larger than the structural one for $\gamma \leq 3$. Catanzaro et al. proposed a slight modification of the model to get an *uncorrelated configuration* imposing a stronger condition on the possible number of stubs for graphs with $\gamma \leq 3$, namely $m \leq k_i \leq N^{1/2}$. In this way, arbitrary scale free networks are generated without degree-degree correlations, multiple and self-connections [28].

⁴Stub, meaning stumpy end, refers to the still unconnected segments which hang from the nodes according to the given degree distribution, which will then match in pairs to form the definitive connections between nodes.

⁵Highly connected nodes are preferentially connected to low connected ones and vice versa.

1.2 Modelling social systems

In this section we illustrate how some social systems have been modelled in the framework of evolutionary dynamics. We first define some basic notions of evolutionary game theory and briefly discuss the case of finite systems. Then, we introduce the *prisoner dilemma* as a paradigm of game theory, discussing the stable states for different conditions, successful strategies, as well as the role of structures and mobility. We then focus our attention on other important types of processes in social dynamics, namely *contact processes*. In particular, we revisit the most popular opinion and infection models, comparing the results obtained for small variations in the dynamics and constraints of the models and paying special attention to the behaviour of such systems on spatial structures.

1.2.1 Evolutionary game theory

Game theory tackles the problem of getting the highest payoff when playing against others. The players may choose one among many available strategies to try to get the best payoff.

Let $E(S, T)$ be the payoff of an actor playing strategy S against an opponent playing T . The simplest game involves two players and two strategies A and B with four possible outcomes, namely $E(A, A) = a$, $E(A, B) = b$, $E(B, A) = c$, and $E(B, B) = d$. The results of the encounters in *symmetric*⁶ games may be written as a *payoff matrix*

	A	B
A	a	b
B	c	d

whose entries are the payoffs for the column player.

In classical game theory, introduced by von Neumann and Morgenstern in the 40's, individuals play in a *rational* way [140]. This means that they are aware of the game rules and choose the strategy which maximizes their payoffs.

Nash was the first who introduced evolutionary ideas in game theory in his thesis, although they stayed unpublished. The biologist John Maynard Smith and the geneticist Price [87] developed some essential elements of population dynamics in the framework of game theory. The crucial factors they brought into classical game theory are the *frequency* dependent fitness and the lack of rationality. In this framework, individuals take the role of players and species that of strategies. Individuals play a fixed strategy and cannot hence decide which strategy gives the best payoff. Often in social systems individual's actions and rewards depend strongly on others' decisions. The success of a species depends on the composition of the whole population. Actors in large populations play their fixed strategies against all other players. The sum of the payoffs in the encounters is the individual *fitness*, which depends on the population fractions or frequencies, i.e. their own and others' strategies. Individuals' reproduction is proportional to their fitness where the fittest player reproduces faster. In this way, natural selection favours the consolidation of the strongest strategy in game theory. This was the beginning of *evolutionary game theory*.

⁶Symmetric games are those in which all players have the same set of strategies available.

A strategy is said to be an *evolutionary stable strategy* (ESS) if natural selection prevents it from being invaded by other strategies. In other words, if S is an ESS a population of S players cannot be invaded by introducing a few individuals with strategy T , $\forall T \neq S$. In mathematical terms one strategy is evolutionary stable if $E(S, S) > E(T, S)$ or $E(S, S) = E(T, S)$ and $E(S, T) > E(T, T)$, where $E(S, T)$ is the payoff of strategy S against T for the player holding S . Evolutionary stability is a concept which was introduced by Maynard and Price in 1973 [87], although it was preceded by Hamilton's *unbeatable strategy* concept in his sex ratios work [55]. The concept of ESS is the natural evolutionary counterpart to the *Nash equilibrium* strategy [96] in classical game theory. A Nash equilibrium is a strategy such that if every player chooses it, no one can score better with any other alternative strategy. In terms of the payoffs the previous condition reads $E(S, S) \geq E(T, S)$, $\forall T \neq S$. ESS accounts for the selection present in evolutionary games. In fact, every ESS is a Nash equilibrium strategy, whereas the contrary is not always true.

The *replicator equation* [62] describes the selection dynamics as proportional to the individual fitness f_i and frequency x_i of the species i in infinitely large populations. The reproduction of each population i is proportional to the difference between the own and the average fitness $\phi = \sum_i x_i f_i$ and to the fraction of individuals x_i of species i ,

$$\dot{x}_i = x_i(f_i(\mathbf{x}) - \phi). \quad (1.8)$$

For two strategies A and B , because the total population is fixed, i.e. $x_A + x_B = 1$ for all times, the former set of equations reduces to one:

$$\dot{x}_A = x_A(1 - x_A)(f_A(x_A) - f_B(x_A)). \quad (1.9)$$

This equation has three possible solutions: $x_A = 1$, $x_A = 0$, or $x_A = x^*$ such that $f_A(x^*) = f_B(x^*)$. The first corresponds to *dominance* of strategy A , which is stable if $f_A(1) > f_B(1)$. B dominates in the second case, being stable if $f_A(0) < f_B(0)$. The third solution corresponds to *coexistence*, i.e. $0 < x^* < 1$, which is stable if $f'_A(x^*) < f'_B(x^*)$ and unstable otherwise.

Consider a game with two strategies whose payoffs are given by the matrix

	A	B
A	a	b
B	c	d

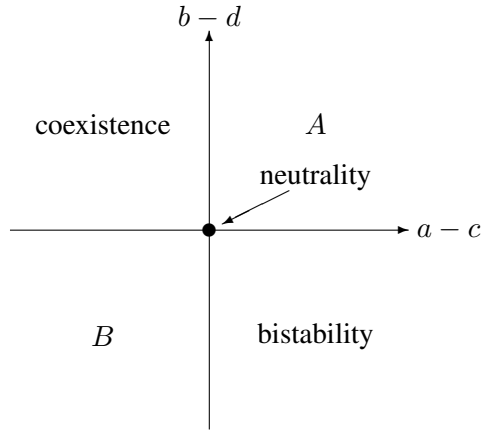
in a large population with a fraction x_A of A players and a fraction x_B of B players. In the framework of evolutionary game theory the fitness functions are equated to the frequency-dependent payoffs, which for the A and B players are:

$$f_A = ax_A + bx_B, \quad (1.10)$$

$$f_B = cx_A + dx_B. \quad (1.11)$$

For these particular fitnesses the solutions of the replicator equation may be dominance or coexistence as discussed before, but the system might also show *bistability* or *neutrality*. The system is bistable if both strategies may dominate the population depending on the initial conditions. For the example considered this occurs if $a > c$ and $b < d$. If the system is neutral the time evolution vanishes for all values of x , as

$f_A(x) = f_B(x)$, so that the system remains at the initial state: all states are stable. The condition for neutrality is $a = c$, $b = d$. The possible regimes in the parameter space are displayed below:



The methods and concepts described up to here tackle the limit of infinite populations but are insufficient to deal with finite populations. In finite populations the stochasticity must be taken into account. In addition, the intensity of selection, i.e. the contribution of the *payoffs* to the general fitness of individuals, plays a specific role which is not present in infinite populations. Thus, when studying finite populations a new concept is required to characterize the system, namely the *fixation probability*. It accounts for the probability that a single player of strategy *A* does not become extinct and overtakes a whole population of $(N - 1)$ *B* players. If the fixation probability is larger than $1/N$ then selection favours the *mutant* agent *A* to take over the population. The condition for the fixation probability to be larger than $1/N$ depends strongly on the system's size N . The concept of evolutionary stable strategies is redefined for finite systems. A strategy *B* is evolutionary stable if selection opposes a mutant strategy *A* invading *B*, i.e. *A* has a lower fitness, and if selection opposes *A* replacing *B*, i.e. the fixation probability of *A* is smaller than $1/N$.

The prisoner dilemma as a paradigm of game theory

The prisoner dilemma is a representative example in game theory. Players may hold one of two strategies: cooperation (C) and defection (D). The outcomes of the encounters between two players are defined by the following payoff matrix

	C	D
C	R	S
D	T	P

where $T > R > P > S$: temptation T is a better payoff than the reward R of cooperating, which is larger than the punishment P of defecting and this still better than the sucker's payoff S . Clearly, defection is a Nash equilibrium and also an evolutionary

stable strategy, $E(D, D) > E(C, D)$. Thus, in games where players only meet once and play a fixed strategy defectors dominate cooperators.

However, in games with repetition, where two players meet more than once, some mechanisms enhance the dominance of cooperation. This is what came out in the contest organized by Axelrod [9]. Many participants submitted new strategies some of which turned out to be able to dominate defection. *Direct reciprocity* refers to mutual cooperation based on the belief that if we meet again you might cooperate later if I cooperate now. It was observed that direct reciprocity yields some dominant strategies. The first winning strategy found under this premise was the popular *tit-for-tat* where players cooperate in the first encounter and then do whatever the opponent did in the previous round. This strategy accumulates better payoffs than the defecting one, and is very successful if players do not make errors. However, if mistakes are considered, then the tit-for-tat players can indefinitely choose defection. In this case the tit-for-tat cannot invade defectors in the thermodynamic limit, but still outperform them in intermediate finite populations [102]. Another strategy, the *generous tit-for-tat*, which randomly cooperates sometimes even if the contrary defects, is a better choice to correct mistakes. But they both are outperformed by the *win-stay, lose-shift* strategy [98], for which the players cooperate if the previous round was successful in terms of payoff (CC or DD) and defects otherwise. This strategy is also able to undergo mistakes and pretty well resembles human behaviour. Cooperation may become an ESS in the case of direct reciprocity if the probability of another encounter exceeds the benefit to cost ratio b/c^7 .

There are other mechanisms available to promote cooperation such as *indirect reciprocity*, *group*, or *kin selection*. Indirect reciprocity refers to the reputation that individuals build by cooperating independently of meeting the same player later. Group selection alludes to mechanisms in which there are two levels of competition: between individuals in a group and between groups. The abundance of cooperators favours the groups to sum a larger fitness and outperform other groups. Kin selection names a dynamics in which some grade of relatedness exists between players establishing altruistic cooperation [54]. For a short review on these strategies see Nowak in [99].

Spatial games and games on networks

Games as the prisoner dilemma inevitably lead to extinction of cooperators in unstructured populations. Only refined strategies as the tit-for-tat, win-stay-lose-shift, kin selection, or indirect reciprocity are able to promote cooperation. However, nature shows numerous examples where cooperation is established without any special strategy. Interactions in real systems take place in organized structures. This fact attracted the attention of game theorists to study the behaviour of games on spatial structures.

The frequencies of the species with which individuals interact are no longer the result of averaging over the whole population, but those of the specific composition of their neighbourhoods. Because of this local character of the interactions spatial games are not expected to show the same behaviour as games in well-mixed populations. Structures favour the formation of new mechanisms not present in the cases which operate under the well-mixed assumption. In particular, spatial structures allow the

⁷If individuals benefit b from a cooperator and cooperators pay a cost c for cooperating, one may rewrite the previous payoffs as $R = b - c$, $S = -c$, $T = b$, and $P = 0$.

formation of domains according to the agents' interests and the rules of the game. Equilibrium states not observed for unstructured systems may now emerge as a result of the dynamics taking place at interfaces. The strategy with the highest payoff is not necessarily the one invading the whole population if other mechanisms favour faster replication due to the spatial constraints. This is possible because of the locality of decisions. Individuals are not influenced by the whole population, but by their nearest neighbours. The local conformation determining individual decisions may turn out to be different than the global one.

Following Axelrod's ideas on the role of structures in cooperative games [8], Nowak and May pioneered the study of games on regular lattices. In their first work they investigated the behaviour of fixed cooperators and defectors on a square grid [86]. Individuals play against every agent in a *Moore neighbourhood*⁸ and accumulate the payoffs of all interactions, i.e. the agents' fitness is the sum of the payoffs of all encounters. All agents update their states simultaneously, following the strategy of the individual with the highest fitness in his vicinity. This simple dynamics shows many regimes in which coexistence or majority of cooperators are stable outcomes, contrary to the defection unavoidably found in well-mixed populations. The equilibrium state reached may be either a static or a dynamic configuration.

However, it was later found that defection invades the population if one takes a more realistic approach like *asynchronous update* [65]. Spatial games thus do not suffice to explain the outcome of cooperation. Further researches of Nowak et al. included stochasticity in their model in two main ways: asynchronous updating and probabilistic strategy change [100, 101]. *Probabilistic strategy change* means that one individual adopts the strategy of his fittest neighbour only with a given probability depending on the fitness. Surprisingly, they found that cooperators do not get extinct if the strategy change is probabilistic even when considering asynchronous update.

In spatial games the dynamics taking place at interfaces between domains plays the main role in the system's evolution. Counter-intuitive results have been observed due to this fact. Later investigations showed, for instance, that cooperators with a higher global payoff than defectors may get extinct because they are worse off at interfaces [100]. In a related sense, the specification of the update process plays a determinant role in the evolution. In addition, if individuals' payoffs are considered as a mortality rate rather than a reproductive one defectors dominate the game. In this case individuals are selected to die with probability inversely proportional to their fitness. When an agent dies the vacant place left is invaded by a randomly selected neighbour. In the sites where species may expand—at interfaces—cooperators are more likely to be selected to die, because their payoffs there are smaller than those of defectors [95]. This particular updating rule hinders cooperation at interfaces leading defectors to dominate the population.

In games with three strategies the local character of spatial games also changes the stationary state of the system. In the *rock-paper-scissors* game three species show a cyclic dominance: *A* dominates *B*, *B* outperforms *C*, and *C* wins over *A*. In well-mixed populations—as experiments in a flask—only one species survives when equilibrium is reached. But the theoretical [104] and experimental [71] works on the spa-

⁸A Moore neighbourhood consists of the eight nearest neighbours, i.e. the cells available to the king's movements in a chess board.

tial game found that the three species coexist on a regular lattice—or Petry dish in the laboratory. They form beautiful spirals in equilibrium states.

Further findings on the evolution of games on grids are summarized in a short review from Nowak and Sigmund [103].

Although much closer to reality than the assumption of a well-mixed population, the regular lattice does not reflect the whole complexity of actual systems. The next step is thus to study games in more heterogeneous structures such as complex networks. The most important consequence of the heterogeneity introduced by networks is that players with more connections participate more often in games and are therefore more influential.

Enhancement of cooperation has been recently observed in networks. Santos et al. explored the outcomes of different games in various graphs: complete, random, Barabási-Albert, and general scale free networks [117, 118]. They performed simulations in which every agent plays with all his neighbours accumulating the obtained payoffs in its fitness. After the rounds are finished, one randomly selected agent compares his payoff with that of a random neighbour and imitates him with a given probability if he were better off⁹. The simulations show that the more heterogeneous a structure is, the better it promotes cooperation. Moreover, the Barabási-Albert network especially promotes cooperation compared with other scale free networks. Due to the preferential attachment growth mechanism, which enhances connectivity between the oldest and most connected nodes, these most influential nodes are interconnected. If cooperators access these nodes, their influence is enhanced and they dominate the population easily.

In particular, one finds that cooperators dominate in the classical prisoner dilemma in regular, random, and scale free graphs when the benefit to cost ratio is larger than the average graph degree $\langle k \rangle$ [105]. This generalization, which is based on pair-pair approximations and was also confirmed with numerical simulations, is indeed true for a death-birth update. In death-birth updates a random individual dies and his vacancy is occupied with the offspring of the fittest neighbour. But again different update rules yield very different scenarios. A birth-death update promotes defection. Individuals, which are selected for reproduction proportionally to their fitness, leave their offspring at a random neighbouring site. The relevant changes take place when individuals invade sites that had a different strategy, i.e. at interfaces. But at interfaces cooperators are worse off and therefore seldom selected to reproduce, which brings about the invasion of defectors.

According to the results discussed in this section, one could conclude that structures promote cooperation in the prisoner dilemma game. However, this is not a robust result. For we have seen that the stationary state strongly depends on the updating mechanism and is very sensitive to the presence of noise in the system.

Mobility

When studying collective behaviour of structured populations one is interested in the role of individual displacements in the system dynamics. The local organization

⁹Note that the process of imitating others' strategies is different to the general one, in which one agent compares his payoff with those of all his neighbours. However, as the authors also simulated the complete graph with this mechanism their results are consistent.

present in spatial games, which favours the emergence of cooperation, is lost when the population randomly diffuses. Indeed, high mobilities produce well-mixed populations for which one expects to recover mean field behaviour for the well-mixed assumption, i.e. the complete graph. Although mobility is an interesting feature in spatial games, very few results have been reported on it.

A work of Dugatkin and Wilson investigates the role of mobility in a *patch* distributed population of individuals playing tit-for-tat and defection [40]. A patch organization is a rather crude spatial distribution in which the population is arranged in groups of $M + 1$ individuals. The tit-for-tat strategy dominates defectors in such a conformation. But if individuals are allowed to randomly diffuse from patch to patch, the system then recovers the mean field behaviour, in which defectors dominate.

Recently Vainstein et al. have investigated the effect of random diffusion for the prisoner dilemma on a grid [136]. They consider a model with empty places and a population density ρ . Individuals are allowed to randomly move to empty sites. The imitation process in this model is deterministic, i.e. individuals invariably adopt the strategy of the fittest. They explore two different mechanisms: combat-offspring-diffusion (COD) and combat-diffusion-offspring (CDO). In the former, after playing with all its neighbours, an individual imitates the fittest one and then diffuses, while in the latter the agent diffuses after playing and then imitates the individual with the highest payoff in the new vicinity. For the COD mechanism it turns out that cooperators get extinct for low densities. Above a threshold density coexistence appears. Cooperators are found to be better off for lower mobilities, though for intermediate densities moderate mobilities yielded a larger fraction of cooperators than the immobile scenario. For the CDO dynamics more drastic effects have been observed. Below a critical density cooperators get extinct by diffusion, for intermediate densities defectors die out for any mobility rate, and for large densities coexistence is observed.

Does this imply that the mean field behaviour is not recovered? The rate at which individuals move is effectively lowered for high densities, since individuals may only move to empty places. The loss of cooperation for low densities and cooperation enhancement by low mobilities suggest that mobility destructs cooperation. Mechanisms in which agents may swap their positions increasing the effective mobility rate might drive to the extinction of cooperators recovering the mean field limit. However, to our knowledge this case has not yet been investigated and the results reported here do not suffice to draw conclusions. In our view, the problem of random diffusion in the prisoner dilemma remains unclear.

A recent work of Reichenbach et al. analyzes the role of diffusion in the rock-paper-scissors game including several levels of stochasticity [111]. They found that the spiral patterns where species coexist are lost above a critical mobility rate. The characteristic wave length of the spirals grows with increasing mobilities up to a point where they burst and only one species survives. In this case the mean field limit has been proved to be recovered for well-mixed populations on regular lattices.

Helbing and Yu recently reported a different problem [60, 59]. They were interested in the possible promotion of cooperation through *success-driven* mobility. In a regular lattice with probabilistic imitation individuals may emigrate to the empty places in their neighbourhoods in which they get the highest possible payoff. The dynamics consists of emigration, game encounters, and imitation. Their simulations showed that a combination of emigration and imitation in fact enhances cooperation. Within this

mechanism cooperation is even resistant to the stochastic effects of including noise in the system, be it in form of mutation probability or random displacements. The success of the mechanism to enhance cooperation is due to the promotion of grouping. Domains make cooperators stronger against defectors' invasion. Moreover, the mutual attraction between cooperators is stronger than the defector-cooperator attraction¹⁰. Thus, the movements bringing cooperators closer are more likely to happen than any other directed displacement.

1.2.2 Opinion models

Opinion models, which are examples of contact processes, deal with the spread of opinions and beliefs in a population due to the interaction between neighbouring actors. In *contact processes* the state of an agent changes if it contacts individuals in different states according to specific rules. Several variations of opinion models have been investigated introducing, for instance, modifications in the interaction rules or number of possible opinions. We review the results of the most popular model, the *voter model*, and discuss some relevant variations of it. We finally stress the modifications observed when considering different structures in which the interacting agents might be arranged.

The voter model

The voter model was first investigated by Clifford and Sudbury in 1973 [32] and named by Holley and Liggett in 1975 [64]. It has become one of the most popular models on opinion dynamics. Despite its simplicity, it is of great theoretical interest because it is exactly solvable in many dimensions [110].

In its most elementary variation, agents located at the vertices of a square grid may hold two different opinions encoded in a binary variable $s_i = \pm 1$. The updating rule simply states that a randomly selected agent i will adopt the opinion of a randomly chosen neighbour j . In the voter model the second agent adopts the state of the first one. This updating step is repeated until an equilibrium is reached. The main questions addressed in the voter model are whether consensus is achieved, under which conditions, and on which time scales.

The change in the state of an agent due to the neighbours' influence is analogue to a spin flip in the zero-temperature *Ising* model due to ferromagnetic interaction. This beautiful analogy allows understanding the dynamics as the trend to minimize the energy cost of the interfaces between domains of different opinions. However, the coarsening process is not exactly the same. In the ferromagnetic *Ising* model the neighbourhood directly influences the energy of every agent and therefore rough interfaces have a high energy cost. In contrast, in the voter model the influence of the neighbourhood composition is probabilistic—the larger the fraction of neighbours with another opinion, the higher the probability for a given agent to change his opinion—but the whole neighbourhood does not conform one agent's decision simultaneously.

¹⁰Attraction between cooperators is proportional to $2R$ in terms of the payoff matrix used before, while cooperator-defector interaction is proportional to $T + S$. Note that in the prisoner dilemma is often established that $2R > T + S$.

For a given system configuration S on a d -dimensional regular lattice the transition rate for an individual i to change his state from s_i to $-s_i$ is [46]:

$$w_i(S) = w(s_i \rightarrow -s_i) = \frac{d}{2} \left(1 - \frac{1}{2d} s_i \sum_j s_j \right). \quad (1.12)$$

An agent has a rate d to change his opinion if surrounded by neighbours with another opinion and a rate 0 if its neighbours have the same opinion. Because this transition rate yields solvable equations for the correlation functions, it represents a good choice for the transition rates.

Frachebourg and Krapivsky have shown that in the thermodynamic limit the system converges to consensus as a power law in time for $d < 2$ and logarithmically for $d = 2$ [46]. But for larger dimensions the voter model exhibits a constant density of domains and thus coexistence of different opinions. Finite systems invariably reach consensus in a time which scales as N^2 for $d = 1$, as $N \log N$ for $d = 2$, and as N for $d > 2$ [72, 82]. Although consensus is achieved for all dimensions, differences are observed in the dynamics. While in small dimensions, $d \leq 2$, consensus is the result of a coarsening process, in larger ones consensus emerges due to big random fluctuations [35].

An essential feature of the voter model is that the *ensemble average magnetization* is conserved. This is a consequence of the *up-down* symmetry of the model. It explicitly means that the magnetization, i.e. the average value of the individual spins $m = \sum_{i=1}^N s_i/N$, vanishes when averaging over many realizations of the system. In the voter model, it implies that both opinions have the same likelihood to be the consensus opinion.

Generalization and variations

Oliveira and coworkers introduced a generalization of the voter model in two dimensions [38]. They redefine the transition rate $w_i(S)$ for a given configuration S in terms of an odd function $f_i(s)$, which depends only on the sum over the states of the neighbouring agents $s = \sum_{j \in \text{nn}} s_j$:

$$w_i(S) = \frac{1}{2} (1 - s_i f_i(s)). \quad (1.13)$$

The function $f_i(s)$ preserves the up-down and spatial symmetries. For the exemplary case of a square lattice $f_i(s)$ has three values: $f_i(2) = -f_i(-2) = a$, $f_i(4) = -f_i(-4) = b$, and $f_i(0) = 0$. The spins sum is 0 or ± 2 at interfaces and ± 4 inside domains. Therefore the parameter a accounts for the probability to change the state at interfaces and b in domains. The values $a = 1/2$ and $b = 1$ correspond to the deterministic case. For these particular values, an agent surrounded by three neighbours with different opinion has a transition rate $1/2(1 + a) = 3/4$ for changing his, while one surrounded by three neighbours sharing his opinion has a rate $1/2(1 - a) = 1/4$ to change his state. The case $a = 1/2$ and $b = 1$ correspond thus to the voter model defined by equation (1.12). Here opinion changes are deterministic after every contact process between a pair of agents and the probability of holding one or the other opinion is proportional to their relative abundance. On the other hand, the case in which

$a = b = 1$ describes the *majority-vote* model discussed later, in which the decision-maker adopts the opinion of the majority. The general case $b = 2a < 1$ accounts for the *noisy* voter model, in which individuals have a certain probability to change their mind even if they are fully surrounded by actors with their opinion. The further a and b deviate from $1/2$ and 1 , respectively, the more noise is introduced in the system. Consensus is never achieved for this case.

Modifications of the voter model are numerous in the literature. The first natural extension included many opinions [125]. A special case of this model was introduced by Vázquez et al. [138]. In their model actors may hold three different opinions A , B , and C , but interactions may only occur through the *central* one, B —interactions between two agents with opinions A and C are forbidden. Both consensus and coexistence of opinions may be reached in this model as a function of the initial conditions.

Lambiotte and Redner investigated the dynamics of *vacillating* voters [75]. The non-confident decision-maker tests the opinion of a second neighbour if the first one shares his opinion. This process favours the growth of minorities, because the probability for minority opinions to be imitated is increased with respect to the direct probability proportional to the frequencies of opinions. It thus results in a bias to a zero magnetization state almost for all initial conditions. Hence, although consensus is also achieved the time needed to reach the stationary state is significantly longer scaling exponentially with N .

Dall'Asta and Castellano substituted the immediate opinion change when meeting a different one with a mechanism which depends on scoring in a positive or negative *counter* [36]. More concretely, the agent's opinion is modified when one of the counters reaches a threshold value. This is no longer a one-to-one contact process, but indirectly depends on the local field. Therefore, using the terminology of fluid dynamics, *surface tension* induces a *curvature-driven* coarsening process in the system.

Curvature-driven coarsening was also found by Castelló et al. in his model for the coexistence of two languages A and B [27]. A central state AB represents bilingualism. Although direct transitions from A to B are forbidden, the transition probabilities from one of the monolingual states $i = A, B$ to bilingualism AB do depend on the densities of the other language in the vicinity, σ_i : $P_{A \rightarrow AB} = 1/2\sigma_B$ and $P_{B \rightarrow AB} = 1/2\sigma_A$. The system evolves towards monolingualism fast destroying the bilingual domains, which are reduced to the interfaces between A and B clusters.

Interesting as well, the studies of Mabilia and coworkers on the effects that a *zealot*—a fanatic one with a fixed opinion—induces in the voter-model [89, 90, 91]. For small dimensions, $d \leq 2$, the zealot imposes consensus around his opinion, whereas for higher dimensions different opinions coexist. In the coexistence state a domain of zealot's opinion is observed around him.

The majority rule model

In which a population of N agents in the nodes of a complete graph hold one of two possible opinions $s_i = \pm 1$ [49]. The key of this model resides on the decision process: opinion changes take place in groups. In a group of g randomly selected agents, all individuals adopt the opinion of the majority. When ties occur in groups of even sizes the system may bias one of both opinions. The average magnetization in this model is not conserved, unlike in the voter model, because of the many-body interactions. For

the majority rule model consensus is always reached, but what is the generalized opinion in equilibrium? The opinion s_i whose initial frequency n_0^i is larger than a critical fraction n_c , $1/2$ for unbiased systems, will be the consensus opinion in equilibrium. The time to reach consensus has been observed to scale with $\log N$ [74, 29].

Consensus is also achieved for the majority rule model in regular lattices. Here interacting groups are built by selecting one random site and its vicinity. In one dimensional lattices the behaviour is rather complex. Minorities may overtake the population, but consensus time is rather long—proportional to the square of the system's size N^2 [30]. In two and larger dimensions, homogeneous initial conditions $n_0^+ = n_0^- = 1/2$ may lead to metastable states which significantly slow down the dynamics. The time to reach consensus scales as a power of N which depends on the dimension.

In the similar *rumour spreading* model several group encounters take place simultaneously [51, 49]. The particularity of the model is that groups may have different sizes. For this system, the critical fraction n_c and the consensus time depend on the groups' size distribution, as well as on the largest size allowed.

Other variations of the model as multi-state opinions [29], variable group sizes [133], inclusion of zealots [51], or individuals and groups favouring one opinion [50] have been explored.

Other models

Close variations to the majority rule model are the *majority-minority* model [92] and the *majority-vote* model [82]. In the former a group of individuals adopts the majority opinion with probability p and the minority one with probability $1 - p$. There is a critical probability p_c such that for $p < p_c$ the system reaches a zero magnetization, while it evolves to consensus for probabilities above the critical one. In the latter model a single agent adopts the opinion of the majority in his neighbourhood with probability $1 - n$, where n is a noise parameter. For this model a phase transition between consensus and coexistence of opinions takes place for a critical value of the noise parameter. Consensus is achieved in the absence of noise [37].

In a slight modification of the majority-vote model the opinion of the updating agent is also taken into account for the establishment of the majority [122]. Simulations for different topologies show that both opinions may coexist in all of them. The composition of the coexistence state depends on the initial configuration. Both opinions may coexist either in a fully disordered state or arranged in domains.

The *Sznajd model* aimed to introduce a new information flux in the spreading of opinions. Whereas in the previous models the flux is directed from the neighbourhood to an individual, in the new model there is a flux from a pair of central individuals to the vicinity. In the first variation of the Sznajd model, if two neighbours in a one dimensional lattice have a common opinion they impose it to their neighbours or impose it to the other's neighbour if the opinions are different. The complicated process failed in introducing new features as it was proved to be equivalent to the voter model [131]. In a new version of the Sznajd model two neighbouring agents impose their opinion to their whole neighbourhood if they share it. But in this case the system remains unchanged if the agents do not have the same opinion. This model reaches consensus at $m = \pm 1$ for initial magnetizations larger, respectively smaller than zero. A sharp

transition between both possible consensus states at the critical initial magnetization $m_0 = 0$ is found in many extensions of the model and for several topologies [126].

Among all the models developed in this field, perhaps that which address the questions closer to our interests is the *social impact theory*. It was brought in by Latané in 1981 [78] and extended later [79, 81]. Individuals with two possible opinions $s_i = \pm 1$ update their states as the result of the interplay between the social impact $I_i(t)$ of their vicinity and a local field h_i accounting for external factors like mass media influence, for instance. The updating rule for a single individual is $s_i(t+1) = \text{sgn}(s_i(t)I_i(t) + h_i)$. The impact factor depends on the difference between the sum of the supportiveness of neighbours with the same opinion as the updating agent and the sum of the persuasiveness of neighbours with the contrary one, all weighted with the distance to the updating individual. Both, supportiveness and persuasiveness are random for each actor. The distance between two agents may be geometrical or topological, the latter based on any kind of relatedness. Consensus never emerges for this model. If the local field vanishes, many stable states with domains of both opinions may be observed. The majority opinion in the stationary state depends on the initial magnetization. In the presence of the local field metastable states are found in which the minority domains shrink after long times to fall in another metastable configuration.

The voter model in networks

The behaviour of the voter model in networks has received much attention during the past years. In highly heterogeneous structures as scale free graphs, for instance, the average magnetization¹¹ is not conserved. This supposes an essential difference with respect to the model in homogeneous lattices. In fact, individuals with a large number of connections are more likely to be picked out when another agent randomly selects a neighbour to imitate. Instead the average magnetization a degree-weighted magnetization $\Sigma(t) = \sum_i k_i s_i(t) / \sum_i k_i$ is conserved [129].

Vázquez and Eguíluz investigated the behaviour of the model in uncorrelated random graphs [137]. They found that consensus is achieved exponentially fast for networks with average degree $\langle k \rangle < 2$, while for $\langle k \rangle \geq 2$ the system undergoes a metastable active coexistence state which finally relaxes into consensus within a time proportional to the system size.

Castellano et al. found that the voter model in small-world networks behaves very similarly as in one-dimensional regular lattices [26]. The system reaches metastable states in which it spends a time proportional to its size. Thus, consensus is not achieved in the thermodynamic limit. However, in finite systems consensus might be reached faster as in the one dimensional regular lattice.

In scale free networks¹² consensus is found for the voter model in finite graphs, but not for the thermodynamic limit [128]. The consensus time scales as N for $\gamma > 3$, as $N^{(2\gamma-4)/(\gamma-1)}$ for $2 < \gamma < 3$, as $(\log N)^2$ for $\gamma = 2$, and as $\mathcal{O}(1)$ for $\gamma < 2$. Initial distributions favouring one opinion to occupy the highest connected nodes have been observed to bias the final consensus towards this opinion [129, 130].

¹¹Remember that the conserved quantity is the ensemble average magnetization.

¹²Scale free networks follow a power law distribution $p(k) \sim k^{-\gamma}$.

A mechanism which conserves the average magnetization is the *link-update* algorithm. In randomly chosen links one of the nodes in the extremes adopts the opinion of the other. For this model consensus times are proportional to the system size independently of the degree of heterogeneity of the scale free network [129].

Castellano [25] and Sood [127] have investigated the *reverse voter*, in which the first selected agent imposes his opinion to one of his neighbours. They found the consensus time to scale linearly with the system size for $\gamma > 2$.

Benczik et al. explored a simple-majority like dynamics in an adaptive network with a fluctuating number of links [17]. Equal states are connected with a probability p , while different are linked with probability q . The state of every agent and the connections are updated at every time step. An intriguing phase diagram arises. For the thermodynamic limit consensus, majority of one opinion or a tie may arise as a function of the probabilities p and q and depending on the initial configuration. In finite systems consensus is always reached, but the system undergoes metastable states during long times.

1.2.3 Infection models

Infection models are another type of contact processes which deal with the spreading of diseases in human populations. They were first introduced in the late 70's by May and Anderson [5, 84, 6, 7] and Diekman, Heesterbeek and Metz [39]. Healthy individuals are *susceptible* (S) of being infected if they get in touch with *infected* individuals (I). The evolution of this process has been discussed in several models, including small variations, e.g. birth-death processes, age or social grouping, or seasonality. They all aim to provide a strong prediction power with the smallest possible number of parameters. Here we will briefly overview two of these models: the susceptible-infected-susceptible (SIS) and the susceptible-infected-recovered (SIR) models. In both variations susceptible individuals are infected at a rate β , if they are in contact with infected agents and heal at a rate μ independently of their environments. The difference between the models resides in the healed individuals. They either could be infected again and are therefore susceptible (SIS model) or are resistant to further infections joining a recovered population (SIR model).

Let s , i , and r be the frequencies of susceptible, infected, and recovered individuals in the population and n the average number of individuals with whom one agent is in contact. The time evolution of the fraction of infected individuals in a mean field approximation for the SIS model is given by:

$$\dot{i}(t) = \beta n i(t) (1 - i(t)) - \mu i(t). \quad (1.14)$$

Given that the infected and susceptible individuals sum the whole population, $s = 1 - i$. The mean field behaviour for the SIR model is described by the set of equations:

$$\dot{s}(t) = -\beta n s(t) i(t) \quad (1.15)$$

$$\dot{i}(t) = \beta n i(t) s(t) - \mu i(t) \quad (1.16)$$

$$\dot{r}(t) = \mu i(t). \quad (1.17)$$

Considering a small initial fraction of infected individuals $i_0 \ll 1$, there is an epidemic threshold for the infection to spread. Infection leads to epidemic outbreak if

the average number of secondary infections $R = \beta n / \mu$ —the “offspring” of infected individuals in every generation in colloquial terms—is larger than one. In other words the infection rate β should be larger than the *epidemic threshold* $\beta_c = \mu / n$ for the epidemic to affect a significant population fraction. Under this assumption the growth of infected individuals in the early stages of the contact process is exponential $i(t) \sim i_0 \exp(t/\tau)$, with $\tau^{-1} = \beta n - \mu$.

If $\beta > \beta_c$ the infection spreads and the system reaches a point where the number of infected individuals is no longer small enough for the approximation $i_0 \ll 1$ to be valid. The dynamics taking place in later stages depends on the specific model considered.

It was only in the 90’s that Rhodes and Anderson investigated the role of a regular grid in infection models [115]. They investigated how the disease transmission in a SIR process depends on the population density and mobility. They found that high densities and large mobilities favoured the propagation of diseases. In particular they were able to find threshold densities for several mobilities below which the population does not get infected.

The topology of networks accounting for the population structure has a great impact on the behaviour of epidemic spreading [69, 41, 68, 70]. Recent reviews on the role of topology are found in [11] and in Pastor-Satorras and Vespignani in [22].

Pastor-Satorras and Vespignani have studied the behaviour of the SIS model in Barabási-Albert scale free graphs [106]. The SIS model is suitable to describe the spreading of viruses in the WWW network, for example. Remember that the degree distribution of a scale free graph is of the form $p(k) \sim k^{-\gamma}$ with $\gamma = 3$ for the Barabási-Albert network. Simulations and analytical calculations showed that there is no epidemic threshold in Barabási-Albert networks. The virus propagates for all transmission rates. They also found that in the early stages the spread of the epidemic is algebraic in Barabási-Albert graphs. The algebraic spreading is in better agreement with the actual data of diseases contagion than the exponential behaviour found for unstructured populations. Their studies predict a stationary infected population in the long time limit which exponentially decreases with small ratios of the transmission and recover rates $\lambda = \beta / \mu$: $i \sim \exp(-2 / \langle k \rangle \lambda)$.

Similar findings were made by May and Lloyd for the SIR model [85]. In the thermodynamic limit there is no epidemic threshold in Barabási-Albert graphs. They observed the same type of stationary infected population for infinite large Barabási-Albert graphs. This result was also found by Moreno et al. who state that the epidemic threshold is inversely proportional to degree fluctuations $\lambda_c \sim 1 / \langle k^2 \rangle$ in Barabási-Albert graphs [94]. Therefore, for finite systems the threshold is recovered, since $\langle k^2 \rangle \sim \log N$. For general scale free networks in the thermodynamic limit their calculations yield that for $\gamma < 2$ no epidemic threshold exists and the long time behaviour of the recovered individuals goes as $r_\infty = \lambda^{1/(3-\gamma)}$, while for $3 < \gamma < 4$ a threshold for the spreading of the epidemic is observed and the fraction of recovered individuals at large times goes as $r_\infty \sim (\lambda - \lambda_c)^{1/(\gamma-3)}$. For $\gamma > 4$ the general behaviour in well-mixed populations is recovered, $r_\infty \sim (\lambda - \lambda_c)$. Nevertheless, in finite populations an epidemic threshold is observed in all cases. In their work they also numerically investigate the role of specific distributions of infected individuals in the network. It turns out that the maximal fraction of infected population considerably increases when the epidemic starts in individuals located at highly connected nodes.

Chapter 2

The evolution of mafias

Life is nothing but a competition to
be the criminal rather than the victim.

BERTRAND RUSSELL

This project was inspired by the film “Gomorra” by Matteo Garrone, based on the homonym book by Roberto Saviano, which describes how mafias rule the south of Italy. Inevitably, after watching the film, I asked myself whether there were any means by which the expansion of mafias could be somehow hindered. Indeed, mafias permeate all levels of society in such a way that to escape their influence seems rather difficult, if not impossible. These thoughts led me to conceive a model aiming at understanding the evolution of mafias in societies.

Modern societies strongly depend on the apparently irrational but certain power exerted by some minority groups, which in occasions can destabilize their smooth running. Fanaticism, extremist political groups, terrorists, or mafias are various examples. Despite their tiny fraction compared to the whole population, such groups can exert a strong enough pressure to dictate the rules of the commons instead of diluting in the seemingly dominant mass. Motivated by this paradox, we develop a model to analyse which features of societies, groups, and individual relations can provide further understanding of these collective phenomena.

The *mafia model* is born in the context of evolutionary social dynamics. We pursue modelling the dynamics of such systems as simply as possible by capturing the generic features of the subtle relations of pressure, support, and protection taking place among individuals and social groups. There are many interesting questions to be addressed in the endeavor to characterize such social systems. We here specifically seek to understand the mechanism which pushes individuals to join or leave mafias. For example, we would like to find out how large and strong a minority group must be to survive, grow, or even dominate a society; or whether it matters, and to what extent, if members of different groups arrange in clusters or, in contrast, are dispersed in a mixed society. We also aim at identifying and understanding the dynamics which gives rise to the emergence of cliques as well as their subsequent evolution in time. In this sense, we are particularly interested in determining the role of the network of contacts between individuals in the establishment of mafias. Another set of questions concern the effectiveness of the means that societies provide to regulate their conflicts—what we will signify as control elements—in protecting the society against the damage of mafias.

Finally, we want to find out whether allowing individuals to rationally escape from the adversary's influence modifies the evolution of the system, and if so, with which frequency individuals are forced to run away.

In this chapter we first develop a mathematical framework to quantitatively characterize the society. To this end, we begin by determining the essential variables and parameters in the model which serve to describe the interactions between mafia and citizens. We then explicitly derive and solve a set of non-linear differential equations for the deterministic evolution of the system in a well-mixed population. Later, we investigate the mafia model in spatial and social structures. In particular we pay attention to the impact of different distributions of external control elements, like a police body, in heterogeneous social structures. Finally, we study the role of mobility. Here we focus on random diffusion of individuals as well as on mobility directed to improve the success of both strategies.

2.1 Towards a mathematical description

The evolution of the mafia model is determined by the interactions among individuals in topological structures which account for the society. We distinguish two populations or strategies: citizens not belonging to the mafia and mafiosi.

In the course of evolution every individual is confronted with the decision of joining or leaving the mafia as the result of the interactions with his environment. The *social pressure* of the society conditions its decision, in particular it depends on the fraction of neighbours belonging to each population and the persuasiveness of the adversary. Mafiosi and citizens have different persuasiveness accounted for by strength parameters. Furthermore, the model also includes the reproduction and death of individuals. New born individuals are supposed to be neutral and therefore join the group of citizens.

In many actual systems external controlling agents¹ fight mafias' growth. They prevent citizens from joining mafias by weakening their strength and persuade mafiosi to leave their gangs. Consequently the decision of individuals about their strategy also depends on the presence of control elements. They are accounted for by their fraction and strength, which are the same for the whole society as they are homogeneously distributed in the system.

A society may have a maximal number N of individuals, *carrying capacity*. The population density ρ is the sum of the citizen and mafia populations divided by the carrying capacity, i.e. the sum of the frequencies of citizens c and mafiosi m : $\rho = c + m$. The fraction of empty places is thus $\phi = 1 - \rho$, so that

$$c + m + \phi = 1. \quad (2.1)$$

A random initial configuration $\{c_0, m_0, \phi_0\}$ evolves in time through individual, asynchronous actions. Individuals die at a rate d and are born in empty places at a rate b . Citizens join the mafia and mafiosi leave it with reaction rates $w_{c \rightarrow m} = w_{cm}$, respectively $w_{m \rightarrow c} = w_{mc}$. All actions are stochastic, i.e. they take place with probabilities proportional to their respective rates.

¹Throughout the chapter we speak of control elements, control agents, police elements, and police as all referring to the same concept.

The per capita reaction rates to adapt the opposite strategy depend strongly on the composition of the social neighbourhood. The decision of a given agent depends on the fraction of citizens and mafiosi in his neighbourhood and on the strength (persuasiveness) attributed to the strategy of the opponent, s_c or s_m . If control elements were present, the reaction rates also depend on their fraction p and strength s_p .

In a well-mixed population the probabilities for a mafioso to become a citizen and vice versa are proportional to the following per capita reaction rates:

$$w_{c \rightarrow m} = w_{cm} = s_m m (1 - p)(1 - c), \quad (2.2)$$

$$w_{m \rightarrow c} = w_{mc} = (s_c c + s_p p)(1 - m). \quad (2.3)$$

The terms $s_c c$ and $s_m m$ account for the social pressure of those neighbours with a different strategy. They depend on both the fraction of neighbours and their strength. The strengths s_c and s_m are parameters of the model, identical for all individuals holding the same strategy. The support provided by individuals with the same strategy is accounted for by the factors $(1 - c)$ and $(1 - m)$. Alike individuals basically attenuate the pressure exerted by the adversary, proportionally to their fraction. These terms introduce non-linear dynamics in the model. Finally, the control elements play a two fold role: protecting citizens and persecuting mafiosi. They *inhibit* the reaction $c \rightarrow m$ through the factor $(1 - p)$ and activate the reaction $m \rightarrow c$ proportionally to their abundance and strength $s_p p$.

In the mafia model the strategy adopted by an individual may be other than the majority strategy in his neighbourhood. This is the case either if the strategy in minority is stronger or if the protection provided by the neighbourhood or control elements is sufficient to overcome the pressure of the majority. The way the model captures the self protection and the catalytic role of external elements, giving rise to a nonlinear dynamics, constitutes a novel approach to the description of social conflicts with respect to the models developed up to now [24]. In the voter model and its variants individuals simply adopt the strategy of a random neighbour or that of the majority or minority population [64, 49]. In the social impact theory, the support of individuals belonging to the same group is accounted for by an additional term, unlike the multiplicative factors which lessen the influence of the opponent in our model. This theory also considers external factors, but they are represented by a site-dependent field [81, 78]. In our view the mafia model improves the understanding of social conflicts in terms of a reduced set of parameters.

One particular case of the mafia model is when citizens have no strength to influence the mafia's behaviour, $s_c = 0$. In this case only the control elements influence the mafia's decision. This might be a more realistic scenario for cases where mafias are extraordinary strong and the population cannot resist their strike. In general, models which aim to describe the competition between two different opinions do need to associate relative strengths to both parties.

With these elements in place, we are ready to formulate a mathematical description

for the deterministic dynamics in a well-mixed environment, namely

$$\frac{dc}{dt} = b\phi + w_{mc}m - w_{cm}c - dc, \quad (2.4)$$

$$\frac{dm}{dt} = -w_{mc}m + w_{cm}c - dm, \quad (2.5)$$

$$\frac{d\phi}{dt} = -b\phi + d(1 - \phi). \quad (2.6)$$

It is instructive to rewrite these equations in a dimensionless form, where time is measured in units of the typical death time $1/d$: $\tau = td$, $\dot{x} = dx/d\tau$, $\beta = b/d$, $\sigma_i = s_i/d$ and $\omega_{ij} = w_{ij}/d$. One is left with the set of differential equations:

$$\dot{c} = \phi\beta + m\omega_{mc} - c\omega_{cm} - c, \quad (2.7)$$

$$\dot{m} = -m\omega_{mc} + c\omega_{cm} - m, \quad (2.8)$$

$$\dot{\phi} = -\phi\beta + (1 - \phi), \quad (2.9)$$

where the dimensionless reaction rates (2.2) and (2.3) are rewritten as

$$\omega_{c \rightarrow m} = \omega_{cm} = m\sigma_m(1 - p)(1 - c), \quad (2.10)$$

$$\omega_{m \rightarrow c} = \omega_{mc} = (c\sigma_c + p\sigma_p)(1 - m). \quad (2.11)$$

The carrying capacity is taken into account by explicitly modelling the empty sites $c + m + \phi = 1$ and thus $\dot{\phi} = -(\dot{c} + \dot{m})$. This allows the computation of the fraction of empty places in equilibrium—obtained by equating (2.9) to zero—which is completely independent of the dynamics encode by ω_{cm} and ω_{mc} :

$$\dot{\phi} = -(1 + \beta)\phi + 1 = 0, \quad (2.12)$$

$$\phi = \frac{1}{1 + \beta}. \quad (2.13)$$

The birth rate controls the number of empty places in the stationary state. Introducing ϕ in equations (2.7) and (2.8) one gets that citizen and mafia populations are related in equilibrium as follows:

$$c + m = \frac{\beta}{1 + \beta}. \quad (2.14)$$

It follows that the population density in equilibrium, *effective carrying capacity*, only depends on the dimensionless birth rate β :

$$\rho = m + c = \beta/(1 + \beta) = b/(b + d). \quad (2.15)$$

Taking into account the solution for the fraction of empty places ϕ and (2.14) the set of equations (2.7), (2.8), and (2.9) reduce to one single equation for the mafia evolution. The stationary states or *fixed points* (FP) of the system are the solutions of the following implicit equation:

$$-m\omega_{mc}(c, m, p) + (\rho - m)\omega_{cm}(c, m, p) - m = 0, \quad (2.16)$$

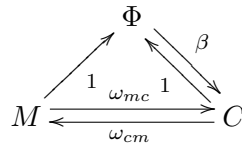
for which the explicit form of ω_{mc} and ω_{cm} depends on the specific model considered.

2.2 Deterministic mean field approximation

In this section we analyze the mafia model within a mean field approximation for well-mixed populations. One assumes that the population is well-mixed if the mobility of individuals is much higher than the frequency of interactions. Under this assumption the local *field*—fraction of different species (strategies) in the vicinity of an agent—which every agent experiences is the same as the global field. The latter is given by the average of frequencies over the whole population. A *well-mixed* population is equivalent to a population on a complete graph, where every agent is connected and interacts with all other agents. This simplification allows analytical calculations which shed some light on the problem's characterization. In particular, we identify the fixed points (FP) and their stability for three particular instances of the mafia model. We also classify possible bifurcations and compute the stability diagram as a function of the parameters of the model.

2.2.1 Symmetric model (SM)

In the symmetric model both species have the same strength $\sigma_c = \sigma_m = \sigma$ in a society without control elements. This particular case models, for instance, the membership to groups such as religions, assuming the dynamics to be biased, so that new born individuals belong to a given group depending on the culture. Another example is the competition between two beliefs or opinions where new individuals hold an a-priori opinion. The dynamics of such systems is outlined in the diagram below, where C , M , and Φ denote the total number of citizens, mafiosi, and empty places:



Mafiosi may become citizens and vice versa with reaction rates ω_{mc} and ω_{cm} respectively, both populations die at rate 1, and only citizens are born in empty places at rate β . The reaction rates to change strategy now read:

$$\omega_{c \rightarrow m} = \omega_{cm} = \sigma m(1 - c), \quad (2.17)$$

$$\omega_{m \rightarrow c} = \omega_{mc} = \sigma c(1 - m), \quad (2.18)$$

leading to the nonlinear differential equations for citizens and mafiosi:

$$\dot{m} = -m\sigma c(1 - m) + c\sigma m(1 - c) - m, \quad (2.19)$$

$$\dot{c} = \phi\beta + m\sigma c(1 - m) - c\sigma m(1 - c) - c, \quad (2.20)$$

where $\phi = 1 - c - m$. Evolution is described by two parameters: the birth rate β and the interaction strength σ .

Since in the stationary state $\rho = c + m = \beta/(1 + \beta)$ the fixed points are given by

$$m^0 = 0, \quad m^\pm = \frac{3\rho \pm \sqrt{\rho^2 - 8\Sigma}}{4}, \quad (2.21)$$

where $\Sigma := \sigma^{-1}$. The fixed point m^0 is an absorbing state, at which the mafia becomes extinct, while the points m^\pm are coexistence states. In the limit of infinite strength, i.e. $\sigma \rightarrow \infty$, $m^- \rightarrow \rho/2$, which constitutes an activation barrier. If the initial fraction of mafiosi is smaller than this barrier, they invariably die out.

At the critical interaction strength

$$\sigma_{\text{sn}}^* = \frac{8}{\rho^2} = 8 \frac{(\beta + 1)^2}{\beta^2} \quad (2.22)$$

a saddle-node bifurcation separates a regime with three fixed points for $\sigma > \sigma_{\text{sn}}^*$, from another regime with only a single stable point, the absorbing one, for $\sigma < \sigma_{\text{sn}}^*$. For the critical strength a saddle-node fixed point exists at $m = 3\rho/4$ —see Fig. 2.1.

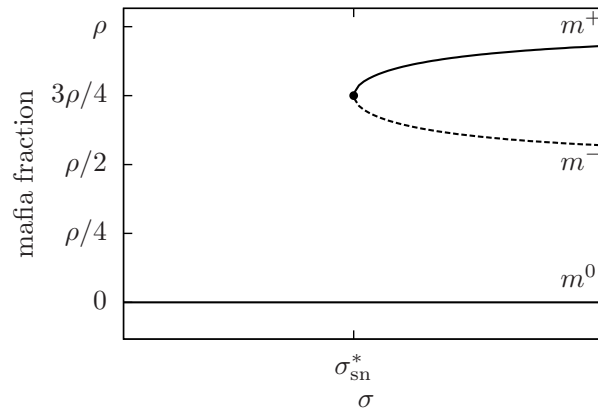


Figure 2.1: SM: Bifurcation diagram for the symmetric model as a function of the strength parameter σ . The solid lines represent the stable FP m^+ and m^0 and the dashed line stands for the unstable node m^- . At the point σ_{sn} a saddle-node bifurcation takes place. For values $\sigma < \sigma_{\text{sn}}$ the node $m^0 = 0$ (mafia's extinction) is the only solution.

The linear stability analysis reveals that the absorbing node is stable for the whole parameter region. The coexistence solutions are a stable and unstable node—see the graphical representation in Fig. 2.1. The coexistence points have physically meaningful values, i.e. $0 \leq m^\pm \leq 1$, for the whole parameter region where they are real because $\rho < 1$.

Fig. 2.2 (left) displays the stability diagram in terms of the birth rate β and the strategy strength σ . Two different regimes are observed. In the first one only the extinction of mafiosi represents a stable solution for the problem. The second regime exhibits bistability; here coexistence of both species and mafia's extinction are possible stable solutions, depending on the initial conditions. In the plot the line separating both regimes represents the saddle-node bifurcation.

We have found that there is a critical strength $\sigma_{\text{sn}}^* = 8/\rho^2$ below which mafia get extinct. In the limit of small birth rates, and consequently small population densities $\rho \rightarrow 0$, the strength required to achieve coexistence is asymptotically large $\sigma_{\text{sn}}^* \rightarrow \infty$. For very small birth rates, the population density is so low, that interactions with other individuals are very seldom and the rates to change strategy result thus very weak.

Instead, the dynamics is governed by the birth-death process. As only citizens are born, the mafia unavoidably dies out.

The separatrix of the system, i.e. the values of the parameters (β, σ) for which the unstable fixed point m^- takes a specific value, are plotted in the right panel of Fig. 2.2. For given initial condition m_0 larger or smaller than the value of the unstable fixed point m^- , the system evolves towards coexistence or extinction. This is graphically displayed in the diagram, where coexistence or extinction are achieved for the parameter region above or below, respectively, the corresponding separatrix with $m^- = m_0$.

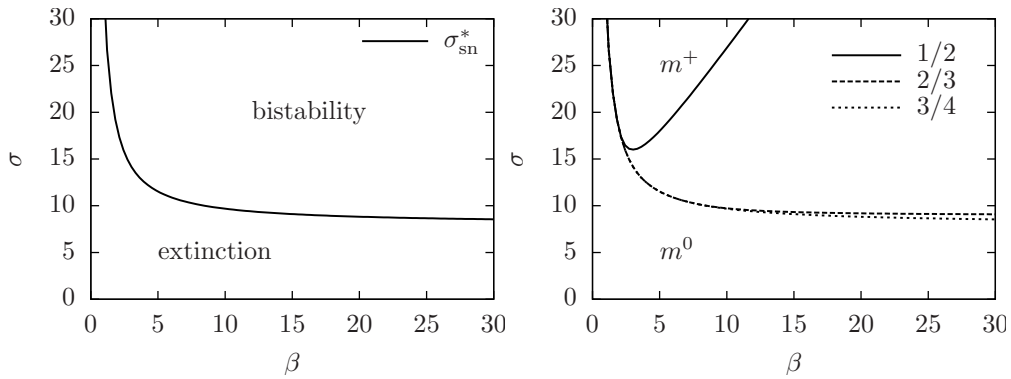
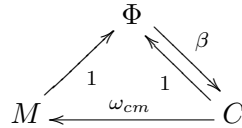


Figure 2.2: SM: Stability [left] and separatrix [right] diagrams as a function of the birth rate β and strength σ . The system is bistable above the line, and monostable—extinction is the only stable state—below it. Along the line separating both regimes a saddle-node bifurcation takes place. In the right part the separatrix for various initial conditions are plotted in the right figure.

2.2.2 Fully asymmetric model (FAM)

We address now the asymmetric case in which citizens do not influence the decision of the mafia, i.e. $\sigma_c = 0$. As long as there are no control elements either, no direct strategy *conversion* from mafioso to citizen is possible. However, mafiosi become citizens indirectly via death-birth processes. The reaction scheme is illustrated below:



The reaction rates for this case

$$\omega_{cm} = \sigma m(1 - c), \quad (2.23)$$

$$\omega_{mc} = 0, \quad (2.24)$$

yield the following differential nonlinear equations for the evolution of the system:

$$\dot{m} = \sigma m(1 - c)c - m, \quad (2.25)$$

$$\dot{c} = \beta\phi - \sigma m(1 - c)c - c. \quad (2.26)$$

They have three fixed points

$$m^0 = 0, \quad m^\pm = \frac{1}{2} \left(2\rho - 1 \pm \sqrt{1 - 4\Sigma} \right), \quad (2.27)$$

with $\Sigma = \sigma^{-1}$.

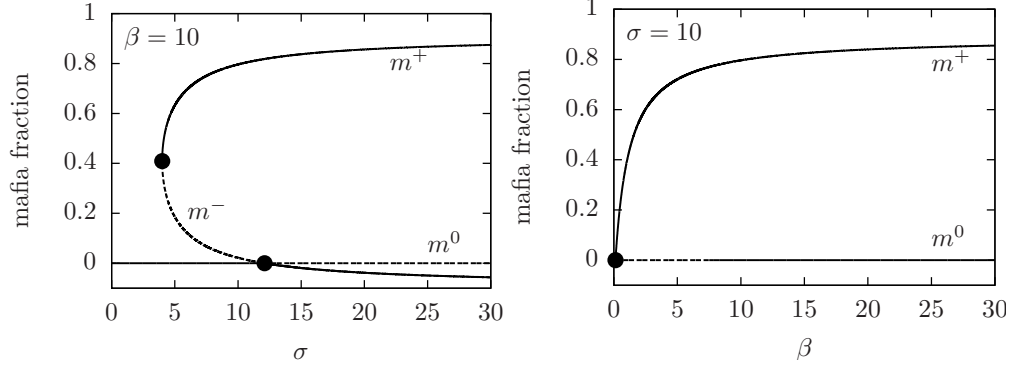


Figure 2.3: FAM: Bifurcations are shown as a function of the strength σ for a fixed birth rate [left] and as a function of the birth rate β for a fixed strength $\sigma = 10$ [right]. The solid and dashed lines represent the stable and unstable fixed points, respectively. The full points represent saddle-nodes.

The stability analysis indicates that the absorbing FP m^0 , where mafiosi die out, is a stable node for

$$\beta = 0, \quad \forall \sigma \quad \text{or} \quad (2.28)$$

$$\beta \neq 0 \quad \text{and} \quad \sigma < (1 + \beta)^2 / \beta, \quad (2.29)$$

and unstable otherwise. As for the coexistence fixed points, m^+ is a physically meaningful stable node for the parameter regions

$$0 < \beta \leq 1 \quad \text{and} \quad \sigma > (1 + \beta)^2 / \beta \quad \text{or} \quad (2.30)$$

$$\beta > 1 \quad \text{and} \quad \sigma \geq 4, \quad (2.31)$$

whereas m^- is unstable for the interesting parameter intervals—see bifurcation diagram in Fig. 2.3.

At the critical value $\sigma_{\text{sn}}^* = 4$ a saddle-node bifurcation separates the bistable region from the monostable one where extinction is the only stable node: the coexistence solutions m^\pm become complex. In addition, at the curve $\sigma_{\text{tc}}^* = (1 + \beta^2) / \beta$ a transcritical bifurcation occurs, where the fixed point m^0 changes its stability. The stability diagram in Fig. 2.4 illustrates both bifurcations. The right panel shows the separatrix for three different values of the unstable node m^- in the bistable regime. The model evolves to coexistence or extinction in the regions above or below the separatrix line with m^- corresponding to the initial conditions, i.e. $m_0 = m^-$.

We have learned that the mafia needs a minimal strength $\sigma = 4$ to survive. Below this threshold mafiosi die out independently of the birth rate. Above this value coexistence of both species may be achieved, although the required strength for the mafia to

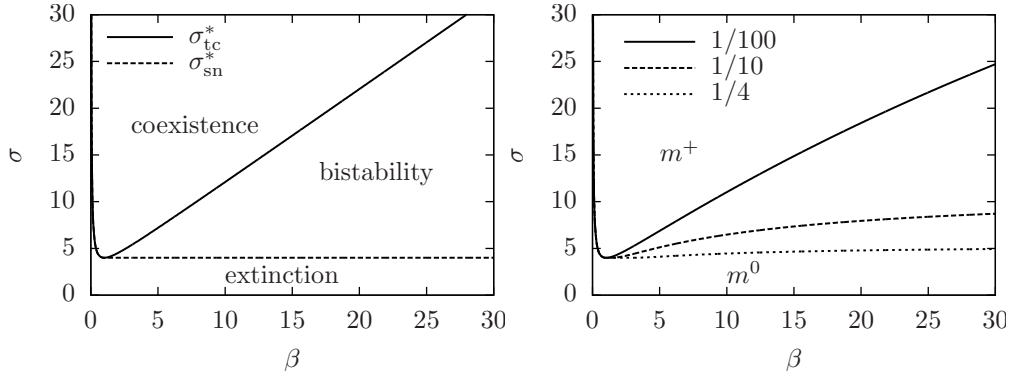


Figure 2.4: FAM: Stability [left] and separatrix [right] diagrams as a function of the birth rate β and strength σ . One can distinguish two regions where the system achieves coexistence m^+ or mafia's extinction m^0 , as well as one region which shows bistability. In the right figure the separatrix for various initial conditions are plotted.

survive increases in this regime with the birth rate. The stationary fraction of mafiosi grows also with the strength of the mafia for a fixed birth rate up to the asymptotic value $m^+ = \rho$ for infinite strength $\sigma \rightarrow \infty$. For a given strength, the mafia fraction in the stationary state is also enhanced with the birth rate, as a consequence of the increment of the whole population, until the saturation value $m^+ \rightarrow 1/2(1 + \sqrt{1 - 4\Sigma})$ for infinite birth rates and population density $\rho \rightarrow 1$.

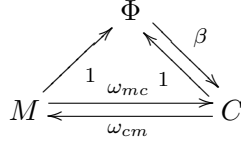
2.2.3 Fully asymmetric policed model (FAPM)

There are many social situations and personal decisions which are influenced by external factors unrelated with the interactions between individuals: mass media, personal beliefs, economical factors, coercion, or police control to mention only some. These external influences differ from agent to agent. We model all these factors as control elements which modify the local field enhancing or inhibiting decisions in certain directions. In a mean field scenario all individuals in a group are equally subject to these external factors, even though they exert different influences on members of mafia and citizens.

In the mafia terminology, a fixed fraction p of control elements enters the asymmetric model with a double function: protecting citizens from the mafia's strike and persuading mafiosi to leave the mafia with strength σ_p .

To keep the problem feasible we reduce the number of parameters equating the police and mafia's strengths with the birth rate²: $\sigma_m = \sigma_p = \beta = \sigma$ and $\sigma_c = 0$. The direct transition from mafioso to citizen is now possible thanks to the mediation by the control elements (police). The reaction scheme below represents the possible reactions in this scenario:

²This corresponds to a particular line, i.e. the diagonal line, in the stability diagram for the fully asymmetric model without police—Fig. 2.4. Hence for $p = 0$ there is a transition from extinction to bistability as in the FAP model. If one were to a different line, one could even observe two transitions.



The distinguishing feature of this instance of the model is that the transition rates between both species do depend on the police fraction p :

$$\omega_{c \rightarrow m} = \omega_{cm} = \sigma m(1-p)(1-c), \quad (2.32)$$

$$\omega_{m \rightarrow c} = \omega_{mc} = \sigma p(1-m), \quad (2.33)$$

yielding the corresponding differential equations for the population:

$$\dot{m} = -\sigma p(1-m)m + \sigma m(1-p)(1-c)c - m, \quad (2.34)$$

$$\dot{c} = \beta\phi + \sigma p(1-m)m - \sigma m(1-p)(1-c)c - c. \quad (2.35)$$

The stationary state is characterized by three fixed points:

$$m^0 = 0, \quad (2.36)$$

$$m^\pm = \frac{(1-2p-\sigma)\sqrt{\sigma}}{2(p-1)\sqrt{\sigma}(1+\sigma)} \mp \frac{\sqrt{1+\sigma}\sqrt{-4-3\sigma+\sigma^2+4p^2\sigma(2+\sigma)-4p(-1+\sigma+\sigma^2)}}{2(p-1)\sqrt{\sigma}(1+\sigma)}. \quad (2.37)$$

The absorbing state m^0 is a stable node for the whole parameter region. The coexistence fixed points m^\pm are stable, respectively unstable nodes with values in the interval $0 \leq m \leq 1$ for

$$\sigma = 4 \quad \text{and} \quad p = 0 \quad \text{or} \quad (2.38)$$

$$\sigma > 4 \quad \text{and} \quad 0 \leq p \leq p_{\text{sn}}^*, \quad (2.39)$$

where

$$p_{\text{sn}}^* = \frac{1}{2\sigma(2+\sigma)} \left(-1 + \sigma + \sigma^2 - \sqrt{1 + 6\sigma + 9\sigma^2 + 3\sigma^3} \right). \quad (2.40)$$

In Fig. 2.5 a bifurcation diagram for a fixed police fraction $p = 0.1$ displays the stability of the three critical points as well as that for the saddle-node bifurcation.

In particular, as illustrated in the stability diagram in figure 2.6, a saddle-node bifurcation takes place for $p = p_{\text{sn}}^*$ where the number of solutions reduces from three to one.

At this line the system's stability changes from bistable to monostable. The more control elements p there are, the larger the interaction strength σ must be to achieve coexistence of both species. The separatrix for $m_0 = 1/2$ is plotted in the right panel.

Summarizing, the presence of control elements increases the strength needed by the mafia to survive with respect to the unpoliced case. This threshold strength grows with the fraction of control elements p . Above a critical fraction of control elements p_{sn}^* , however, mafiosi unavoidably die out independently of their strength. If the police fraction is below this value and mafiosi survive, their stationary fraction grows with their strength as we have seen in the bifurcation diagram of Fig. 2.5.

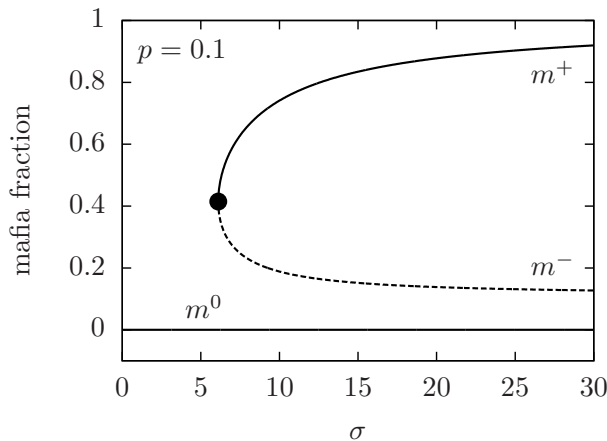


Figure 2.5: FAPM: Bifurcation for a fixed police fraction $p = 0.1$. Two stable nodes [solid lines], m^+ and m^0 , and the unstable m^- [dashed line] are shown as a function of the strength σ . Note that at the saddle-node point [filled point] a saddle-node bifurcation takes place below which extinction m^0 is the only stable fixed point.

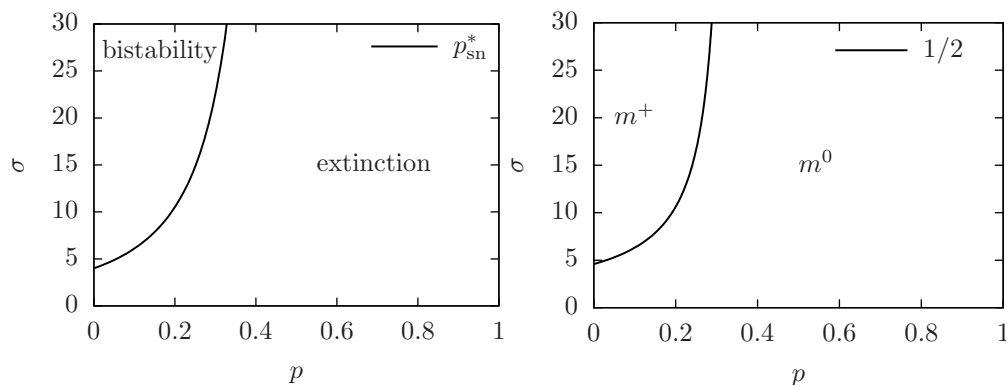


Figure 2.6: FAPM: Stability [left] and separatrix [right] diagrams as a function of the fraction of control elements p and the strength σ . In the stability diagram two regimes are recognized: bistability and extinction of mafiosi. The black line represent the saddle-node bifurcation taking place along the transition from the bistable to the monostable regime. In the right figure the separatrix for $m_0 = 1/2$ is plotted. Note that $\sigma_m = \sigma_p = \beta = \sigma$.

2.3 The role of social structures

The focus of our work is to investigate the role of social structures in conflicts such as the problem of mafias. We are interested in the evolution of the three cases described above for individuals interacting in spatial and social structures. Does the system modify its behaviour with respect to the well-mixed population? We want to identify the features which characterize and dominate the dynamics of societies in structures. In particular, we wonder whether specific social structures may hinder or strengthen the power of mafias. We also investigate the role of specific distributions of the control elements in heterogeneous systems.

We study the dynamics of the mafia model for two kinds of structures: two dimensional regular lattices and scale free networks. Square regular lattices are homogeneous structures where all agents have the same number of neighbours. We consider *von Neumann* neighbourhoods including the north, south, east, and west neighbours. On the other hand, scale free networks exhibit large heterogeneity. Their degree dis-

tribution, i.e. the fraction of nodes with k neighbours, is proportional to a power law $p(k) \propto k^{-\gamma}$. The degree of heterogeneity is related to the exponent γ of the power law. In scale free graphs a relevant phenomenon takes place which is not present in homogeneous structures as random graphs and lattices: Because of the network's heterogeneity agents located in highly connected nodes exert a stronger influence in the society to which they belong. They take part in a larger number of interactions persuading a larger number of individuals.

What are the restrictions introduced by structures? Agents interact with their nearest neighbours. While birth and death rates are the same for all individuals independent of the structure considered and their location, the reaction rates ω_{cm} and ω_{mc} do depend on the composition of the neighbourhood.

Both population and police frequencies are needed to compute the transition rates ω_{cm} and ω_{mc} . For the mean field approximation these fractions are those of the total population. In structured societies, lattice and networks, the population fractions are those of the neighbourhood. Since the number of connections of a given node to its neighbours is finite, the possible values for c and m entering the reaction rates are discretized. There is a finite number of possible neighbourhoods. The smaller the node degree is, the less neighbourhoods are available. This scenario is qualitatively different from the mean field approximation, which averages over the total population and supposes that all individuals interact with the same neighbourhood. In the well-mixed assumption all population frequencies in the continuous range between zero and one are available. Instead, in structures individuals interact with their nearest neighbours, varying for each site or node. The composition of the neighbourhood does not include the strategy of the agent for whom the neighbourhood is computed. Deviations from the behaviour predicted by the mean field approximation are thus expected for populations on lattices and networks.

Not only the frequencies of species, but also the fraction of control elements are specific for every agent. The control elements are located at the edges connecting two nodes—see Fig.2.7. Every edge attached to a given site can thus be occupied or not by a control element, under the constraint that the total number of edges allocating control elements is pN_E , where N_E is the total number of edges. Therefore the fraction of control elements in an agent's neighbourhood is the number of policed edges over the total number of edges. This fraction is different for every node.

We explore the mafia model in some structures beyond the mean field approximation by means of stochastic simulations. In particular, we investigate the system's evolution on regular lattices and scale free networks (SFN) for different initial frequencies (c_0, m_0) and values of the parameters: reaction strength σ , birth rate β , and police fraction p .

The initial configuration is a random distribution of the population according to the initial conditions: $c_0 N$ citizens, $m_0 N$ mafiosi, and $(1 - c_0 - m_0) N$ empty places. The society evolves in time until it reaches a state which is quasistationary. In fact, after a given time τ , the system enters a regime in which the population fractions do not change any longer. Since there exists an absorbing state, i.e. mafia's extinction, if one would wait a time long enough the state of the system would unavoidably evolve towards it. However, we have found that there is a large enough window of time for which the system's state is quasistationary. All the investigations we address in this

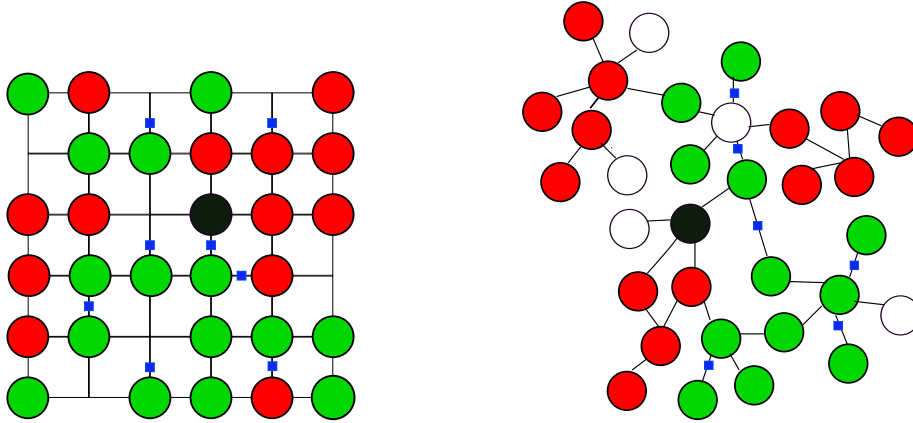


Figure 2.7: Neighbourhoods on structures: regular square lattice and scale free graph. The green nodes are occupied with citizens, the red with mafiosi, the vacant sites in the lattice or uncoloured nodes in the network are empty places. Blue squares account for the control elements. For illustration, one can calculate that the composition of the neighbourhoods (von Neumann for the lattice) of the nodes in black are: $(c, m, \phi) = (1/4, 1/2, 1/4)$ and $p = 1/4$ in the lattice and $(c, m, \phi) = (1/4, 1/2, 1/4)$ and $p = 0$ in the graph.

chapter are therefore carried out for this quasistationary state, that we will refer to as stationary for the sake of simplicity.

In the course of time individuals change their strategies. The sites, where they are allocated, are randomly chosen for updating. Every site updates on average once at each time step $\Delta\tau$. Therefore, a time step consists of N asynchronous single updates. If the site is empty, a citizen is born with probability $\beta\Delta\tau$. If an individual occupies the site he can either die with probability $\Delta\tau$ or change his strategy with probabilities $\omega_{mc}\Delta\tau$ or $\omega_{cm}\Delta\tau$.

As we discussed above the reaction rates are site and time-dependent, encoding the features of the structure considered, i.e. accounting for the local conformations at every node of the lattice or graph. The corresponding reaction rates ω_{mc} and ω_{cm} are thus computed at every time step and for each updating agent as given in equations (2.10) and (2.11)³. In particular the fractions c , m , and p entering the reaction rates for a given individual are those of his vicinity, i.e. the number of citizens, mafiosi, and control elements divided by the total number of neighbours or node's degree k .

We measure for various observables both their time evolution and stationary value, to quantify the questions we are interested in. All the observables discussed in this chapter are averages over the results of thousand of simulations with different initial configurations. We will define specific observables for different purposes, but populations frequencies and extinction probabilities will be relevant throughout this section.

We define the extinction probability as the probability that mafia has gone extinct after a waiting time τ [111]. This probability is measured through many simulations starting with the same initial conditions. The time for which we measure extinction probabilities is within the quasistationary window that the system undergoes defined

³See appendix A for a detailed description of the algorithm.

above.

The extinction probability is also a good quantity to measure the effect of stochasticity. For some initial conditions, the average fractions of mafiosi observed in the stationary state are very small, without necessarily meaning that this is the stationary state, but just an effect of averaging over samples in which extinction takes place due to stochastic fluctuations.

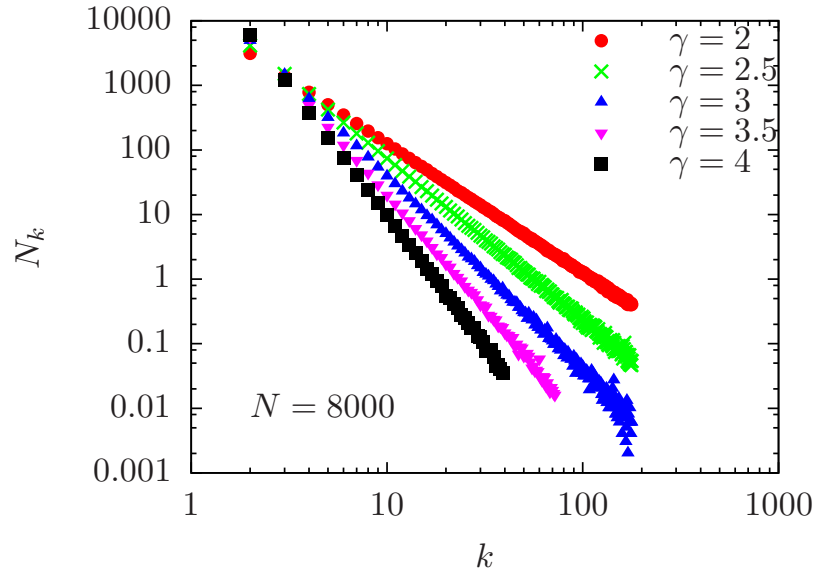


Figure 2.8: Degree distribution for scale free networks. Number of nodes N_k with k neighbours for networks with exponents γ ranging from 2 to 4.

The section outline is the following: we first simulate the complete graph, i.e. the well-mixed mean field approximation, to investigate the effect of stochastic fluctuations due to finite populations. Then, we introduce spatial structure through a square regular lattice with a constant number of neighbours. Finally, we investigate the role of more complex topological structures as scale free graphs⁴. They better account for the heterogeneity of actual social networks. In a SFN the number of neighbours differs from one node to another. In Fig. 2.8 the degree distribution for the different networks used are compared. We will often refer to networks by their exponent γ of their degree distribution, $p(k) \propto k^{-\gamma}$. Networks with small γ exhibit a larger heterogeneity as well as larger average degree, i.e. number of neighbours. They also have a non-negligible tail in their distribution, meaning that there is a finite number of nodes with a high number of connections, the so-called hubs. In addition, the average path lengths of very heterogeneous networks are rather small. For a more detailed discussion on the properties of scale free networks see section 1.1.4. The table below shows the average degree $\langle k \rangle$ of these networks for several sizes and exponents γ .

⁴The network is generated according to the algorithm implemented by Heiko Hotz following the uncorrelated configuration model described in appendix B.

γ	2	2.5	3	3.5	4
$N = 10000$	7.63	4.31	3.16	2.69	2.45
$N = 8000$	7.45	4.29	3.16	2.69	2.45
$N = 6000$	7.23	4.26	3.15	2.68	2.45
$N = 4000$	6.97	4.21	3.11	2.68	2.45

In what follows, we investigate the three cases of the mafia model described in section 2.2: the symmetric model (SM), the fully asymmetric model (FAM), and the fully asymmetric policed model (FAPM). We will pay special attention to possible stochastic effects and explore in detail the role of different distributions of the control elements in the network.

2.3.1 Symmetric model

The stability analysis for the mean field approximation predicts a bistable and a monostable region in the parameter space. In the former, coexistence and mafia extinction are both stable solutions, whereas extinction is the only stable fixed point in the latter.

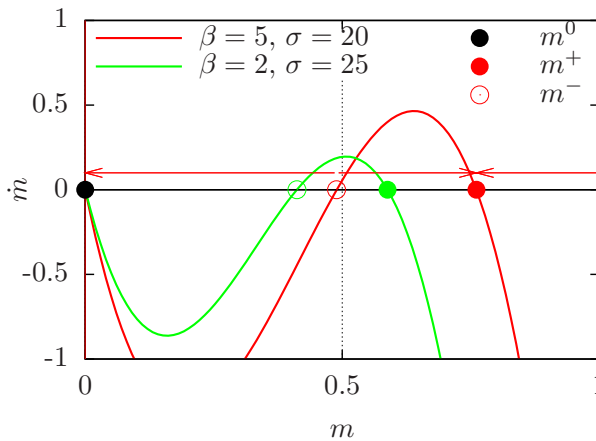
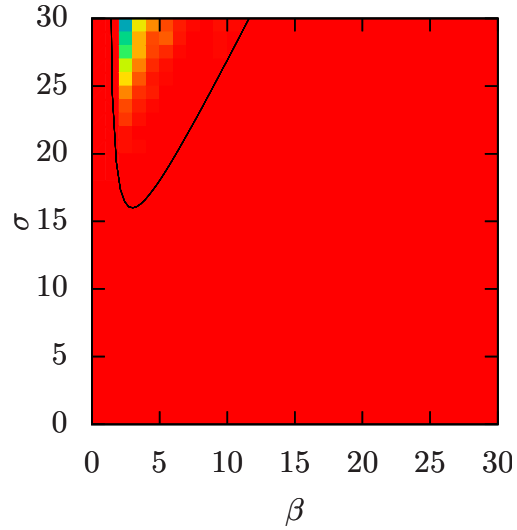


Figure 2.9: SM: Stable [filled] and unstable [empty] nodes for two points (β, σ) in parameter space where coexistence was predicted by the deterministic MF theory. Since the initial conditions are very close to the unstable point, fluctuations easily drive the system to extinction.

We first test the effect of stochasticity due to the finite size of the system in the well-mixed assumption. The simulations show that for initial conditions close to the unstable fixed point m^- fluctuations drastically modify the deterministic scenario. Remember that the unstable point separates the regions leading to one or the other fixed point for given initial conditions larger or smaller than it respectively—see Fig. 2.9. In the parameter region above the separatrix corresponding to $m^- = 1/2$ —solid black line in Fig. 2.10—coexistence is achieved for the deterministic mean field approximation. However, the extinction probability observed in the simulations shows a quite different landscape: mafia dies out for almost all parameters in the same region. The reason for this difference is the proximity of the unstable fixed point m^- to the given initial conditions $m_0 = 1/2$. Small fluctuations may thus drastically change the evolution of the system. Fig. 2.9 illustrates the relative position of the fixed points with respect to the initial conditions for two parameters sets.

Stochasticity does not modify however the deterministic prediction for initial conditions far from the unstable node. This is the case for initial conditions $m_0 = 3/4$, as shown in Fig. 2.11. For comparison purposes, the predicted separatrix by the mean

Figure 2.10: SM: Extinction probability [blue $p_{\text{ext}} = 0$, red $p_{\text{ext}} = 1$] after a time $\tau = 0.01N$ for stochastic mean field simulations with $m_0 = 1/2$ compared to the corresponding $m^- = 1/2$ separatrix predicted for the deterministic thermodynamic limit [solid line]. Note that stochasticity plays a crucial role. Simulations for a system of size $N = 10000$.



field approximation is plotted on top of the extinction probability as obtained by the simulations.

Interestingly, introducing structure in the system qualitatively changes the nature of the stable node in the bistable region. For homogeneous structures, e.g. lattice and networks with large γ , the system reaches the absorbing state, i.e. extinction of the mafia, in regions where coexistence is found under the homogeneous mixing assumption.

The stationary mafia fraction and extinction probability are plotted in Fig. 2.12 for three different structures. In the left side the birth parameter is fixed and the system's behaviour is shown for increasing strength σ . In the right plot the strength is the fixed parameter and the effect of increasing birth rate is investigated. The results for the three structures, regular lattice, $\gamma = 3$, and $\gamma = 2.5$ scale free networks, are compared with the stochastic and deterministic homogeneous mixing cases. The frequency of mafiosi in equilibrium is in good agreement for the deterministic and stochastic mean field approximation. The separatrix delimiting extinction and coexistence are shifted in the different architectures with respect to the homogeneous mixing hypothesis.

We explicitly want to find out whether mafiosi also die out for societies initially populated by the mafia. We want to determine whether the state $m_0 = 1$ is evolutionary stable in homogeneous structures of different sizes. Simulations show that a population of mafiosi is not an evolutionary stable state in those topologies. A few citizens invade the mafiosi population, leading them to extinction.

More heterogeneous networks—smaller γ for scale free graphs—do exhibit coexistence regimes for some areas in the parameters space. Fig. 2.13 shows a phase transition from coexistence to extinction as a function of the network heterogeneity. For the parameter point $\sigma = \beta = 30$ and initial conditions $c_0 = 1/4$, $m_0 = 3/4$ the transition takes place at the critical exponent $\gamma_c \sim 2.7$. These results stress that heterogeneous structures promote coexistence.

How does the coarsening dynamics look like? Starting in the state $m_0 = 1$ the death of mafiosi is the only possible process. Since the characteristic time for mafiosi to death is $\tau_d \sim 1/N$, after a time n/N the first n mafiosi have died leaving empty

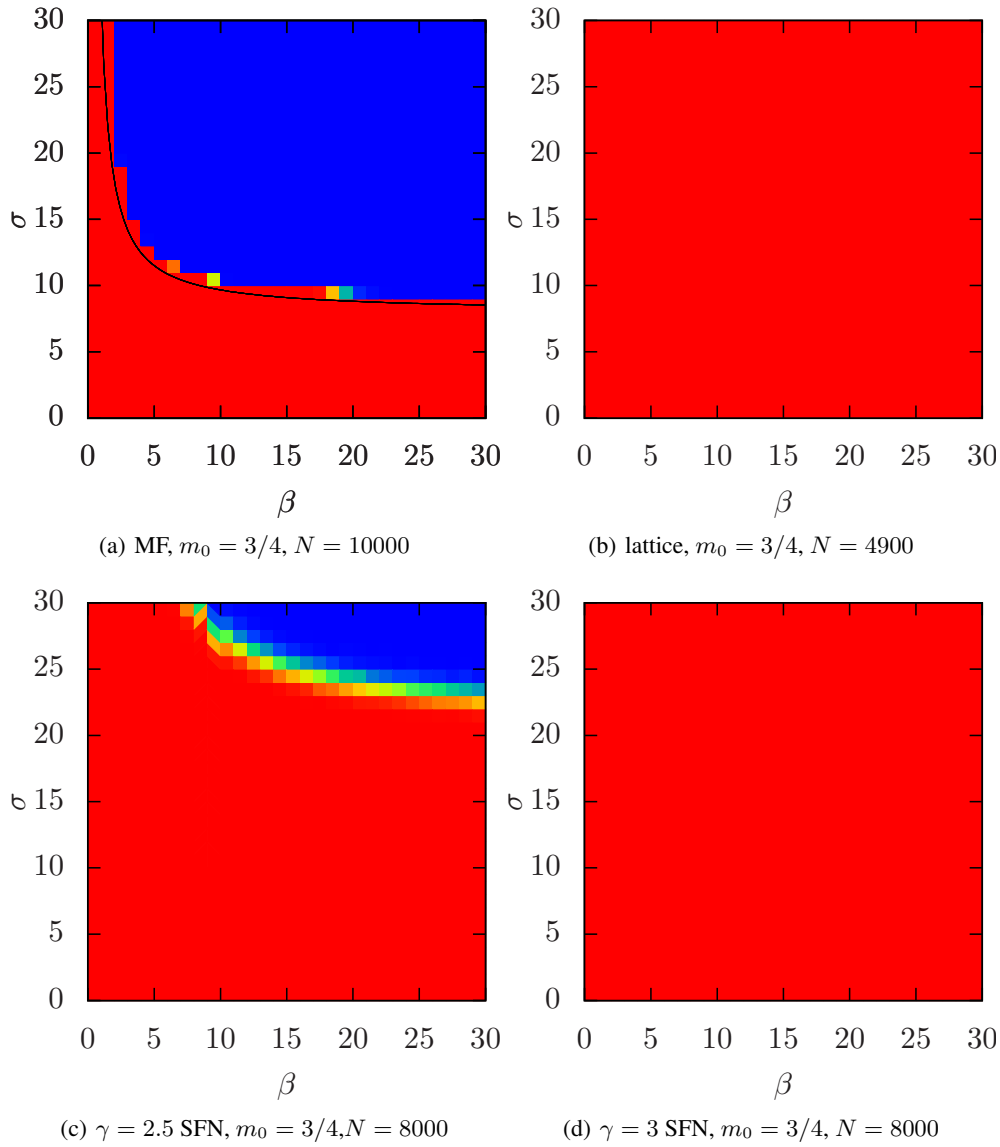


Figure 2.11: SM: Mafia's extinction probability [blue: $p_{\text{ext}} = 0$, coexistence; red: $p_{\text{ext}} = 1$, extinction] in terms of the strength σ and birth rate β . The solid black line represents the corresponding deterministic separatrix. The probabilities are measured after a time $\tau = \lambda N$ with $\lambda = 0.01$. Structures lead the system systematically to extinction, even for an initial population of mafiosi $m_0 = 1$ (not shown).

places⁵. Citizens might be born in those vacant locations with a rate β . After a characteristic time $\tau_b \sim 1/\beta$ there are some isolated citizens in the system. They may either resist the mafia attack or change their strategy. Very rarely citizens induce mafiosi to leave the mafia in these early stages of the dynamics. Despite their minority, citizens survive over a generation often enough to build small clusters of two or three individuals—see Fig. 2.14.

⁵Remember that the death rate was used to define the dimensionless time unit $\tau = td$.

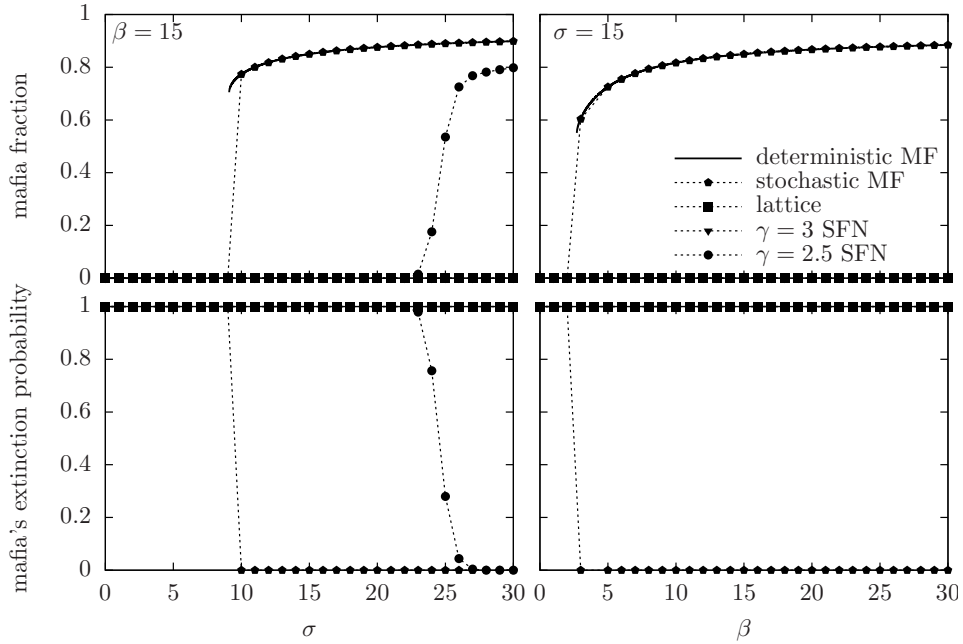


Figure 2.12: SM: Stationary fraction of mafiosi [top] and extinction probability [bottom] for different structures: lattice, $\gamma = 3$, and $\gamma = 2.5$ scale free networks. The deterministic and stochastic mean field results are also displayed. The results for a fixed birth rate $\beta = 15$ and fixed strength parameter $\sigma = 15$ are shown in the left and right side of the figure, respectively. The initial conditions are $m_0 = 3/4$, $c_0 = 1/4$. System sizes: $N_{\text{MF}} = 10000$, $N_{\text{latt}} = 4900$, $N_{\text{SFN}} = 8000$. The extinction probability is measured after a time $\tau = \lambda N$, with $\lambda = 0.01$.

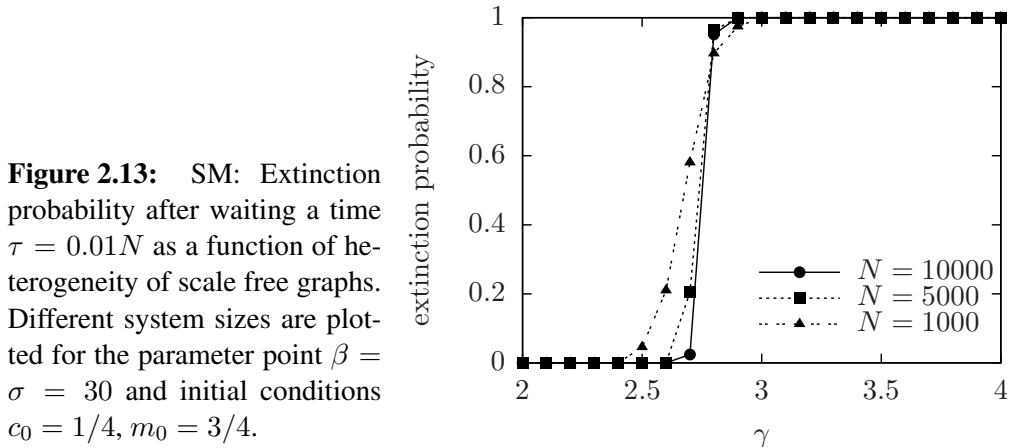


Figure 2.13: SM: Extinction probability after waiting a time $\tau = 0.01N$ as a function of heterogeneity of scale free graphs. Different system sizes are plotted for the parameter point $\beta = \sigma = 30$ and initial conditions $c_0 = 1/4$, $m_0 = 3/4$.

Once small clusters are formed the dominating dynamics takes place at the domain interfaces. In homogeneous structures with small number of neighbours the reaction rates for both species are very similar⁶. In fact, as the population fractions marginally deviate from the values $m \sim c \sim 1/2$ at interfaces, the reaction rates read $\omega_{cm} =$

⁶This holds only in structures for which one may assume a similar fraction of neighbours of every species for all sites at interfaces. And indeed it is in those structures where extinction takes place.

$\sigma m(1 - c) \sim \omega_{mc} = \sigma c(1 - m) \sim \sigma/4$. Consequently, there is a back and forth fight at domain interfaces. Why do mafiosi finally die out? The dynamics is still asymmetric because of the birth of citizens. This process shifts the balance to mafiosi extinction. This dynamics may be visualized for a regular, two dimensional lattice in the Movie 1 of the supplementary CD. The *wall* growth of an initially small citizen population is displayed in the Movie 2.

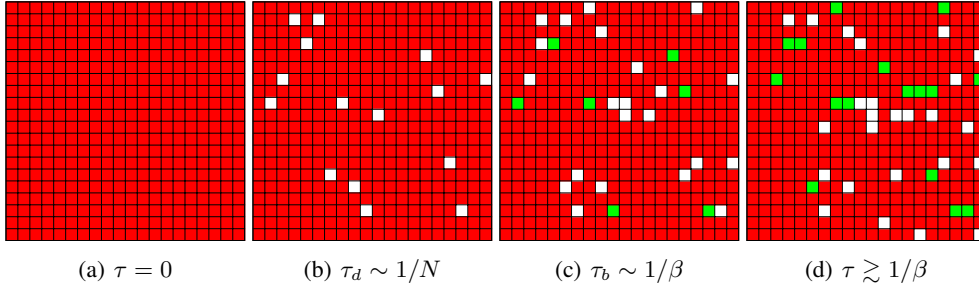


Figure 2.14: SM: First stages of the nucleation process in which small citizens' clusters arise. For an initial population of mafiosi [red] ($\tau = 0$), some empty places [white] appear via death process after a characteristic time $\tau_d \sim 1/N$. In these vacancies citizens [green] are born after a time of the order of $\tau_b \sim 1/\beta$. In the last stage shown, converted mafiosi and adjacent born citizens give rise to the emergence of small citizens' clusters. Thereafter, the death-birth process drives the expansion of citizens' clusters.

Why is extinction not achieved in heterogeneous structures? Extinction is the result of a dynamics driven by the birth-death processes, which become relevant when the reaction rates to change strategy are very similar for both species. The latter happens if the population fractions at interfaces do not show large fluctuations from the average value $c \sim m \sim 1/2$. But fluctuations in the population fractions are negligible only for a very reduced number of possible neighbourhoods, i.e. for a small number of connections. For larger connectivities first the probability to have the particular neighbourhood with species fractions $m \sim c \sim 1/2$ is smaller than for small connectivities and second the population is much more mixed and the system closer to the global mean field description. These might be the reasons why extinction does not emerge for heterogeneous graphs with larger average degrees $\langle k \rangle$ —see Fig. 2.13.

Summarizing, the system behaves very differently on homogeneous structures as in the case of well-mixed populations. The global mean field average performed before is far from capturing the dynamics taking place in small vicinities. A local mean field provides a much better description of the dynamics in structures, as we will see later in this work.

In well-mixed populations the system may reach intermediate, arbitrary population fractions (c^*, m^*) for which the rate at which citizens become mafiosi is large enough to overcome the death-birth effect favouring the formers ($\omega_{cm} \gg \omega_{mc}$). For these states the system enters a stationary regime of coexistence. These global states are however easily undergone in structured architectures because not all population fractions are locally reproducible in a neighbourhood. In homogeneously structured societies, the global composition of the population do not play any role in the dynamics

of single individuals.

How much stronger should mafiosi be to survive?

We have so far simplified the general case to one in which both the citizens and mafia have the same strength. But both strengths, σ_c and σ_m , might be chosen in such a way that stronger mafiosi could overcome the advantage citizens have because of their birth process. A rough calculation suggests that in fact this is possible.

For mafiosi not to die out the number of mafiosi gained at every time step m_g should at least equal that of gained citizens⁷ c_g . The fraction of mafiosi increases via citizen conversion at interfaces, while the fraction of citizens grows via conversion as well as thanks to the birth process. The new born individuals are only safe if they are born close to clusters⁸. Considering the population to be arranged in clusters this balance is achieved if

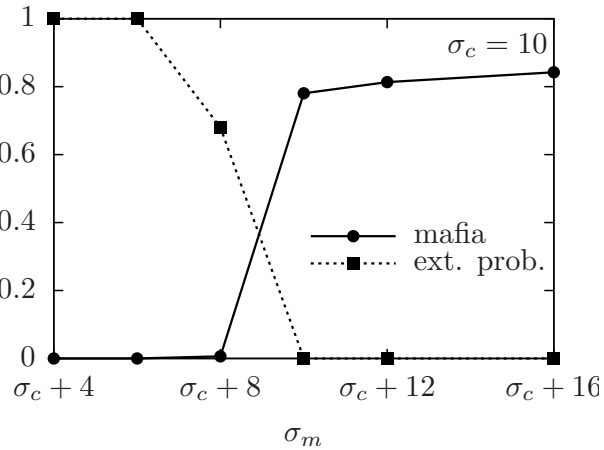
$$m_g \geq c_g \quad (2.41)$$

$$l_{\text{int}} c \omega_{cm} \geq l_{\text{int}} m \omega_{mc} + l_{\text{int}} \phi \beta \quad (2.42)$$

$$c \sigma_m m (1 - c) \geq m \sigma_c c (1 - m) + \phi \beta, \quad (2.43)$$

where l_{int} is the length at the cluster's interface. In homogeneous structures with small vicinities one may assume $m \sim c \sim 1/2$ at interfaces. For this regime there is a threshold value for the mafia strength at which mafiosi do not die out: $\sigma_m \geq \sigma_c + 8\beta\phi = \sigma_c + 8\beta/(1 + \beta)$. For $\sigma_m > \sigma_c + 8$ a transition between extinction and coexistence should be observed in homogeneous structures. Simulations in regular lattices support this heuristic prediction: for $\sigma_c = 10$ the mafia extinction probability reduces already to $p_{\text{ext}} = 0.68$ for a mafia strength $\sigma_m = \sigma_c + 8 = 18$ and coexistence is systematically achieved for larger σ_m —see Fig. 2.15.

Figure 2.15: Transition from mafia's extinction to coexistence for $\sigma_m > \sigma_c + 8$ as heuristically predicted for societies in homogeneous structures without policing elements—see main text. The stationary mafia's fraction and extinction probability are shown for a lattice with size $N = 6400$. In the example $\sigma_c = \beta = 10$.



2.3.2 Fully asymmetric model

The deterministic mean field analysis for the fully asymmetric model predicts three different regimes dependent on the strength and birth rate parameters: coexistence,

⁷We omit the lost individuals since the death rate is the same for both species.

⁸In fact this assumption underestimates the actual number of surviving new born citizens which might also join isolated citizens by chance. But these are very few compared to those joining clusters.

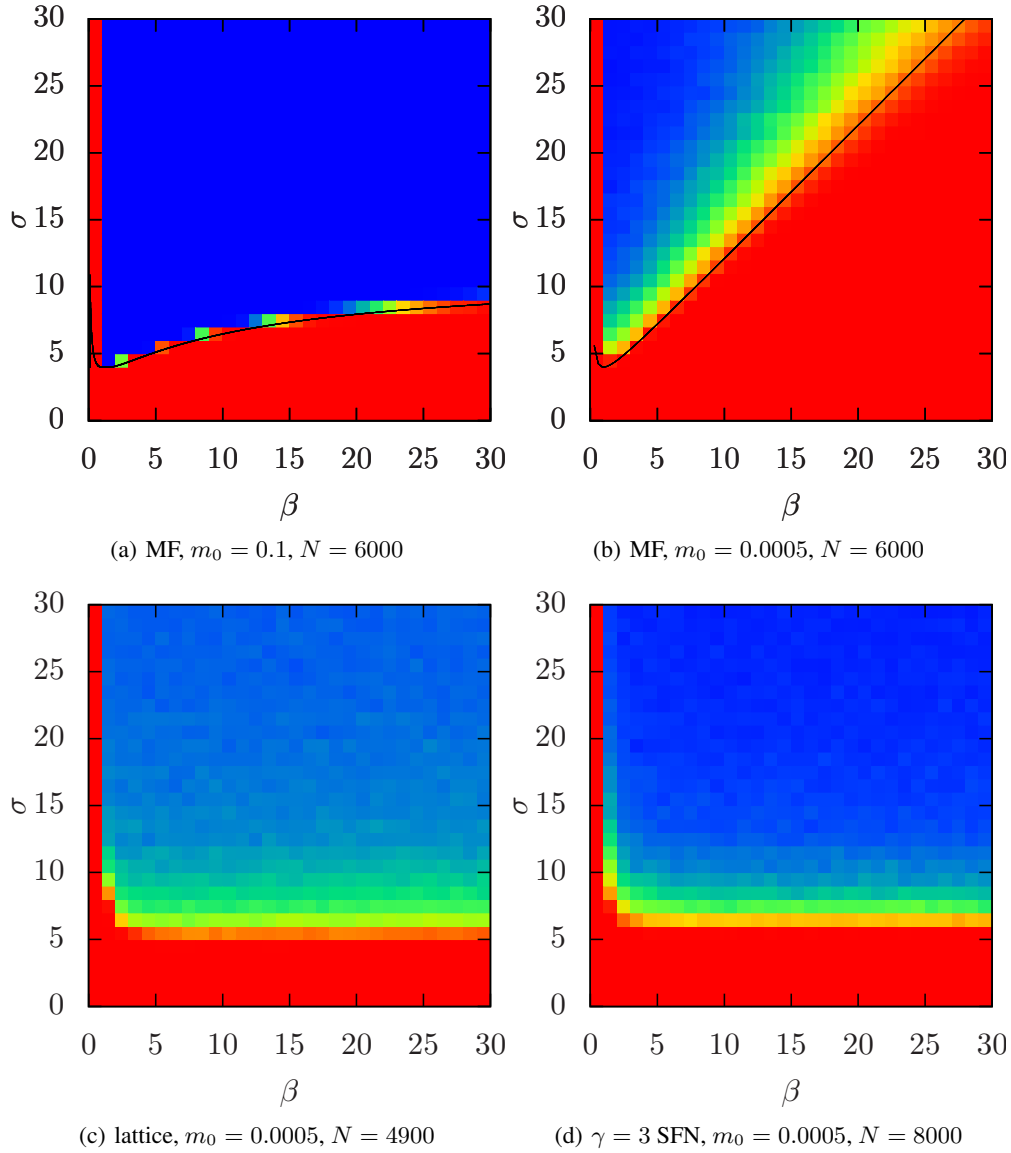


Figure 2.16: FAM: Mafia's extinction probability [blue: $p_{\text{ext}} = 0$, coexistence; red: $p_{\text{ext}} = 1$, extinction] in terms of the strength σ and birth rate β . The solid black lines represent the corresponding deterministic separatrix. The probabilities $p_{\text{ext}}(\tau)$ are measured after a time $\tau = \lambda N$, for $\lambda = 0.01$ for the mean field and the lattice, and $\lambda = 0.015$ for the network. The structures enhance coexistence even for vanishing initial fractions of mafiosi if $\sigma \gtrsim 4$ —see discussion in the main text.

extinction, and bistability. In Fig. 2.16 (top) the extinction probability for the stochastic mean field is compared with the corresponding deterministic separatrix for two different sets of initial conditions. The stationary state resulting from the stochastic simulations is the same as the one predicted by the deterministic calculation. For initial conditions far from the unstable node the specific population fractions in equilibrium are in very good agreement with the solutions of the deterministic mean field equations (not shown).

However, the nature of the stationary state changes qualitatively in structured environments. Topological and spatial arrangements enhance coexistence in the bistable region, as coexistence is found for parameters for which extinction is the stationary state for well-mixed populations. In contrast with the results for the symmetric model, now the absorbing extinction state is the one which is lost in favour of diversity. This phenomenon is shown in the lower part of Fig. 2.16 for the lattice and a $\gamma = 3$ scale free graph, for initial conditions $m = 0.0005$ for which the corresponding results obtained for the well-mixed assumption is displayed in the upper right panel.

Up to which extent is diversity promoted in structured populations? We want to determine whether the absorbing state $m = 0$ is evolutionary stable. In other words, we investigate whether a few mafiosi may invade a population of citizens. For this purpose we simulate the evolution of populations with a few mafiosi on a square lattice and scale free graphs. The results indicate that the absorbing state $m_0 = 0$ is not evolutionary stable, as coexistence is found for $\sigma > 4$.

What is the underlying dynamics which promotes coexistence? To invade the population, the few disperse mafiosi introduced in the society must first survive the drift of the death process. Then they must be able to invade some neighbouring cells and form small clusters able to expand at the expense of citizens. After small clusters are consolidated the dominant dynamics driving the system to coexistence takes place at the domain interfaces until a stationary state is reached. We first discuss under which conditions small mafia clusters emerge and then examine the clusters dynamics leading to the stationary state.

A neighbourhood with an isolated mafioso may evolve in two different directions: either the mafioso dies or he invades some neighbouring site. We are specifically interested in the probability for the isolated mafioso to invade any neighbouring cell instead of dying after one generation⁹. This is required for the successively formation of small clusters. Fig. 2.17 shows a cartoon illustrating this situation.

The probability for an isolated mafioso at site i to die is $p_{\text{ext}} = p_{\text{death}} = \Delta\tau$, while his probability to *invade* a neighbouring node is the sum of the probabilities p_{cm}^j for his k_i citizen neighbours at site j to become mafiosi: $p_{\text{inv}} = \sum_{j=1}^{k_i} p_{cm}^j = k_i p_{cm}^j = k_i \omega_{cm} \Delta\tau = k_i \sigma m (1 - c) \Delta\tau = k_i \sigma \Delta\tau / k_j^2$. In homogeneous structures $k_i \simeq k_j$ and thus $p_{\text{exp}} \simeq \sigma \Delta\tau / k_i$. Hence the expansion probability is larger than the extinction if the mafia's strength is larger than the number of neighbours $\sigma > k_i$. As in the asymmetric model a transition from mafioso to citizen is not possible, but only indirectly through the death-birth process, this reaction is not considered here.

The larger the interaction strength σ , the larger the likelihood for an isolated mafioso to invade any of his neighbouring cells. The extinction probability decreases thus with the mafia's strength. For small strengths and very few mafiosi stochasticity

⁹We refer to a generation as the configuration for every time step.

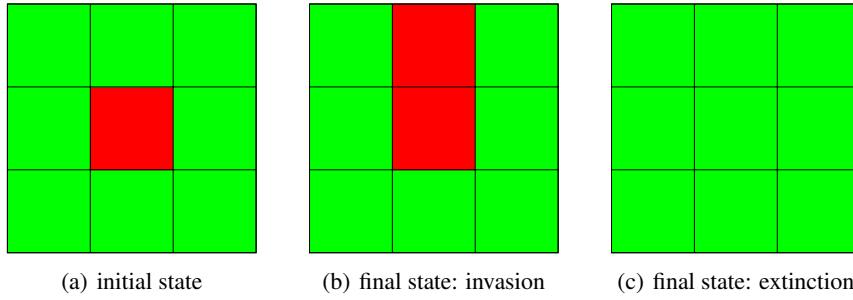


Figure 2.17: FAM: Possible evolutions for an isolated mafioso [red] immersed in a citizen [green] sea [left]. The probability for the mafioso to invade a neighbouring site [middle] is $p_{\text{inv}} = (\sigma/k_i) \Delta\tau$ and to go extinct is $p_{\text{ext}} = \Delta\tau$. Here the lattice neighbourhood consists of four nearest neighbours: north, south, west, and east.

easily drives the system into extinction. This tendency can be observed in Fig. 2.18: the extinction probability is reduced as the mafia strength σ increases. The plots in Fig. 2.18 support these heuristic arguments. As the probability to invade neighbouring cells for the disperse mafiosi increases, the measured extinction probability decreases. The former, proportional to the ratio $\sigma/\langle k \rangle$, increases with the strength σ and decreases with the average degree of the network $\langle k \rangle$. Consequently the extinction probability shows the opposite behaviour. It decreases with the strength and increases with the average degree of the network. In addition, the extinction probability is smaller for a $\gamma = 3$ SFN with $\langle k \rangle = 3.16$ than for a square regular lattice with degree 4. The effect of very large extinction probabilities because of stochasticity, leads in these plots erroneously to smaller population fractions than the actual ones in the stationary state, almost vanishing for some parameters, due to the average process over samples in which mafia has got extinct. However, the interest of these figures resides specifically on the behaviour of the extinction probability for various structures and increasing strengths.

If some mafiosi arrangements arise in the early stages of evolution, what are the conditions for them to grow? In other words, under which conditions do both species coexist in equilibrium? Citizens' clusters shrink due to mafia's attack at their borders and grow thanks to the safely born citizens at their interfaces¹⁰. Therefore, if the number of citizens gained per generation c_g is larger than the number of lost ones c_l , citizens' clusters will grow. This scenario thus would lead to the mafia's extinction. Consequently the absorbing state $m = 0$ would be an evolutionary stable state (ESS). If on the contrary, the number of lost citizens is larger than the number of safely born ones, i.e. $c_g < c_l$, the citizens' clusters will shrink. Fig. 2.19 outlines two possible process taking place within a time step.

To reach a stationary state where species coexist the small arrangements of mafiosi must thus grow, not indefinitely but until a point at which a dynamic stationary state is reached, where the number of lost and gained citizens per unit time are the same. Under these conditions coexistence is the stationary state and extinction turns out to be an evolutionary unstable state.

¹⁰Isolated born citizens die because they cannot fight against the mafia as $\sigma_c = 0$

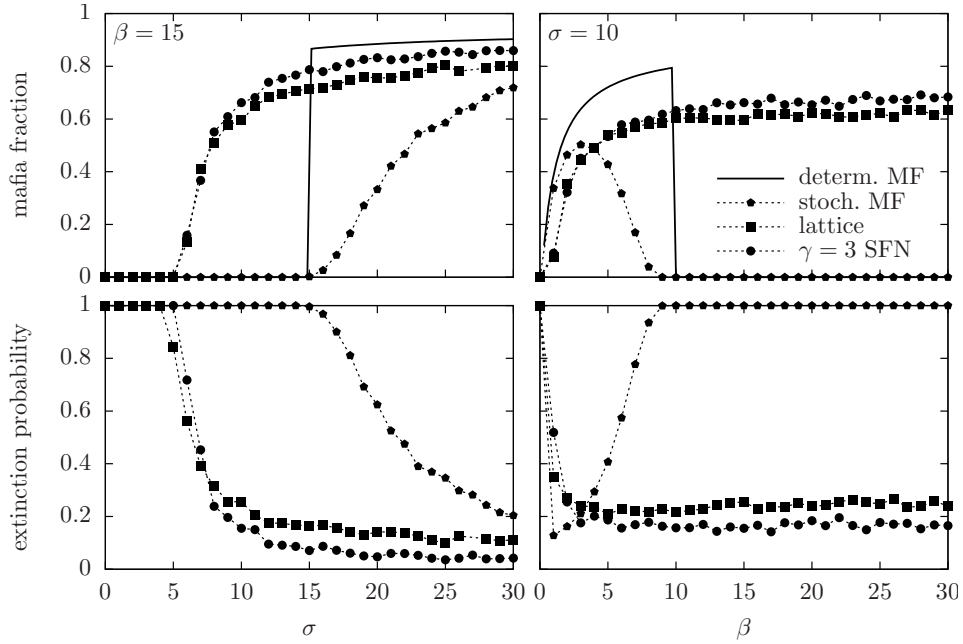


Figure 2.18: FAM: Stationary fraction of mafiosi [top] and extinction probability [bottom] for a square lattice and a $\gamma = 3$ scale free graph. The deterministic and stochastic mean field results are also included for comparison. The initial conditions are close to the absorbing state $m_0 = 0$, with a very small initial mafiosi fraction $m_0 = 0.0005$. In the left plot the birth rate $\beta = 15$ is fixed and the observables are shown as a function of the strength σ . The right figure shows the dependence on the birth rate of population fractions and extinction probability for a fixed strength $\sigma = 10$. System sizes: $N_{\text{MF}} = 6000$, $N_{\text{latt}} = 4900$, $N_{\text{SFN}} = 8000$. The extinction probability is measured after a time $\tau = \lambda N$, $\lambda = 0.01$ for the MF and lattice and $\lambda = 0.015$ for the SFN.

What is the fraction of gained and lost citizens per generation? If one omits the drift of the death process, which is homogeneous for the whole structure and the same for both species, the net number of lost citizens at the clusters' interfaces is $c_l = l_{\text{int}} c \omega_{cm}$, where l_{int} is the interface length. Similarly, the net number of gained citizens is $c_g = l_{\text{int}} \phi \beta$. For large enough birth rates, $\beta \gg 1$, the fraction of empty places is small enough so that one may consider the fraction of citizens at the interface to be one, $c \sim 1$ and thus $c_l \sim l_{\text{int}} \omega_{cm}$. The citizens' clusters will thus shrink if $c_l > c_g$, i.e. if $\omega_{cm} > \phi \beta$. The fraction of both species in the neighbourhood of one site at the interface between domains of different populations are expected to be similar in homogeneous structures: $c \sim m \sim 1/2$. Introducing these values in the previous inequality $\omega_{cm} = \sigma m(1 - c) > \phi \beta$ yields that species coexist if the mafia's strength is larger than the threshold value $\sigma_t > 4 \phi \beta = 4 \beta / (1 + \beta)$. Since $\beta / (1 + \beta) \lesssim 1$, $\sigma_t > 4$ is a sufficient but not necessary condition for the emergence of coexistence, in nice agreement with the simulations results (Fig. 2.18). Note that the initial conditions do not matter for the spatial dynamics given that the process is reproducible for an initial vanishing mafia fraction.

If $\sigma > \sigma_t$ and mafiosi start expanding they do it up to the point at which the number

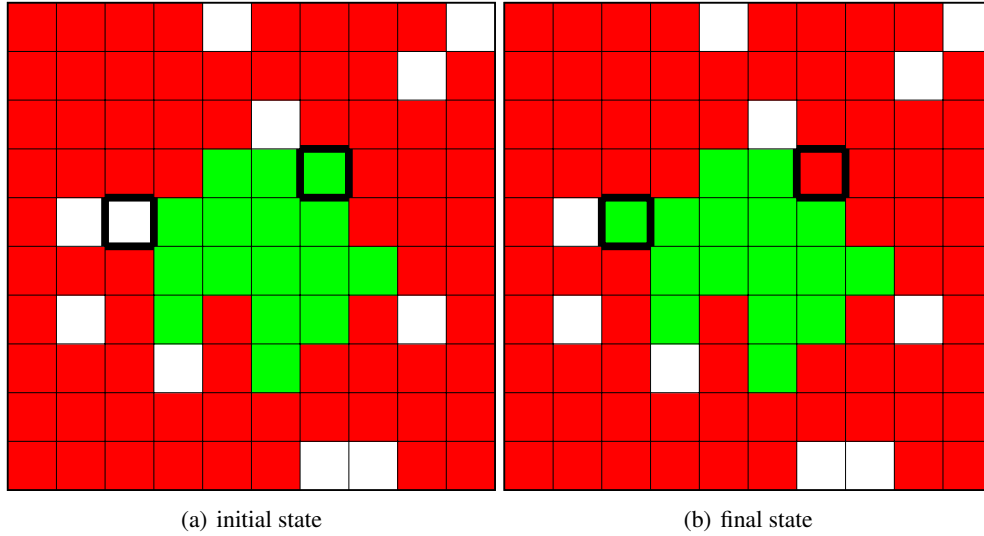


Figure 2.19: FAM: Two possible processes at the interface of a citizens' cluster—the selected cells to undergo a process are marked with a thicker frame. In an empty place [white] a citizen is born with probability $p_{\text{birth}} = \beta\Delta\tau$. A citizen [green] at the border becomes a mafioso [red] with probability $p_{cm} = \sigma m(1 - c)\Delta\tau = \sigma \frac{1}{2} \Delta\tau$ —interactions take place with the four nearest neighbours. If the number of citizens becoming mafiosi at every time step is larger than the number of the new born citizens at the interface, the society evolves towards a coexistence state.

of lost and gained citizens in the clusters are the same. Looking at the simulations for a regular lattice one observes that at this point citizens are either isolated or in small clusters, many of them consisting of two or three individuals. Thus, the approximation $c \sim m \sim 1/2$ for the neighbours fractions of citizens at interfaces is not valid any longer. Rather, the majority or all citizens' neighbours are mafiosi. If one makes a rough approximation for the square lattice and assumes citizens to have on average population fractions of $m_{\text{nn}} \sim 3/4$ and $c_{\text{nn}} \sim 1/4$ in their vicinities, one finds that the fraction of the number of lost $c_l = c\omega_{cm} = c l_{\text{int}} \sigma m_{\text{nn}} (1 - c_{\text{nn}})$ and gained citizens $c_g = \phi l_{\text{int}} \beta$ are equal for $c \simeq \phi \beta / \sigma m_{\text{nn}} (1 - c_{\text{nn}}) \sim 16 \phi \beta / 9 \sigma$. The corresponding fraction of mafiosi in equilibrium is $m = \rho - c \sim 1 - \phi - 16 \phi \beta / 9 \sigma = 1 - \phi(1 + 16 \beta / 9 \sigma)$. This heuristically derived stationary population fraction is in very good agreement with the results of simulations for a constant strength $\sigma = 10$ as a function of the birth rate for a square lattice as displayed in Fig. 2.20.

The equilibrium reached is dynamic. There is a stationary cycle in the population because of the birth-death process: empty places are occupied by citizens, which become mafiosi, some of which die leaving empty places again. The corresponding dynamics for a small number of mafiosi, as well as their wall growth is visualized for a regular lattice in the Movies 3 and 4 of the supplementary material.

In addition, we have found that the fraction of citizens in equilibrium increases in scale free graphs for decreasing heterogeneity, i.e. growing γ , as shown in Fig. 2.21. This is a consequence of the reduction in the average degree. For small connectivities, the ratio of individuals at interfaces and individuals in the core of clusters is smaller

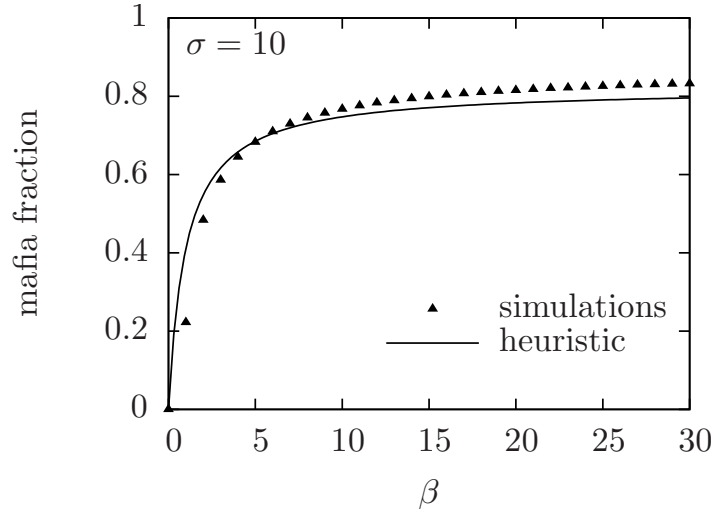


Figure 2.20: Stationary mafia population on a regular lattice as a function of the birth rate β for a constant reaction strength $\sigma = 10$. The results of simulations are displayed together with the heuristic prediction $m \sim 1 - (1 + \beta/c(1 - m)\sigma)/(1 + \beta)$ [solid line]. c and m are here the fraction of citizens and mafiosi in the neighbourhoods of citizens at interfaces, which we assume to be $m \sim 3/4$, $c \sim 1/4$, and thus $m(1 - c) \sim 9/16$ for the square lattice.

than for large ones. Consequently clusters are more resistant against invasions. Given that mafiosi cannot be invaded, because $\omega_{mc} = 0$, only citizens can profit from more defensive structures, thus achieving a better performance in equilibrium.

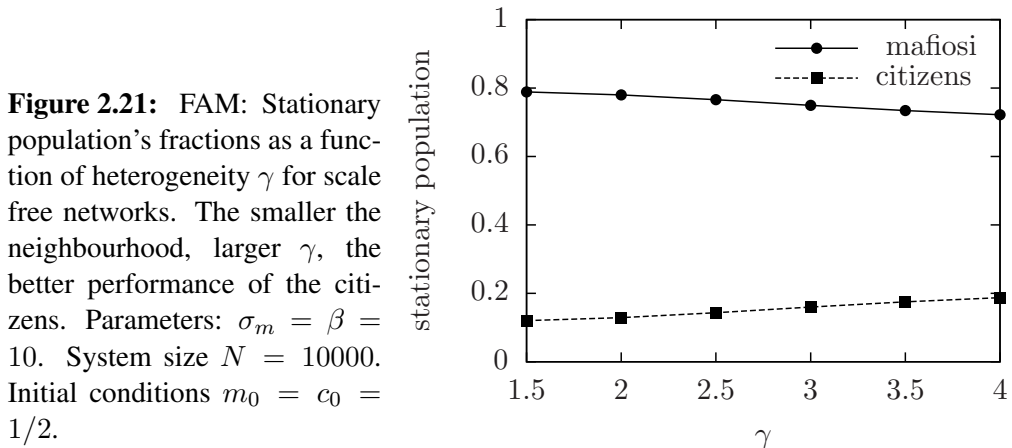


Figure 2.21: FAM: Stationary population's fractions as a function of heterogeneity γ for scale free networks. The smaller the neighbourhood, larger γ , the better performance of the citizens. Parameters: $\sigma_m = \beta = 10$. System size $N = 10000$. Initial conditions $m_0 = c_0 = 1/2$.

Summarizing, we have seen that spatial and topological structures introduce drastic differences with respect to unstructured populations. The few mafiosi immersed in a citizen sea which would have unavoidably died out in a well-mixed scenario are able to invade citizens bringing the system into a coexistence state in networks and lattices. This deviation from the global mean field is a consequence of the local character of the decision process and, ultimately, of the finite number of possible conformations for the neighbourhood of a given node. As we will later see in this work, the system's

behaviour in structures is better captured by a local mean field approximation.

Back to the real society, the lack of global information in spatial structures—the non-validity of the mean field approach in mathematical language—is precisely the reason why mafias succeed. Individuals are not concerned about global situations and act therefore locally under the social pressure of their small universe. No global resistance is offered by societies thus making it very difficult to eradicate mafias.

2.3.3 Fully asymmetric policed model

The mean field analysis of the asymmetric model with control elements provides a stability diagram consisting of a bistable regime for small police fractions and extinction of mafiosi for larger fractions of the control elements. The stochastic simulations for well-mixed populations yield very similar results to those of the deterministic prediction, as illustrated in the top left plot of Fig. 2.22.

The introduction of control elements makes the system behave anomalously: coexistence is found to be stable even for parameter regions where extinction is the only stable fixed point according to the deterministic mean field analysis, shown in the top right part of Fig. 2.22. The reason for this anomalous behaviour resides in the fixation of the control elements. Fixing the control elements to the edges of the lattice and networks is analogous to introducing defects in ordered structures such as crystals. Defects drastically modify the dynamics leading to strong deviations from the mean field behaviour. Whereas citizens and mafiosi are dynamic elements, who are born, die, and change their strategies, the control elements are static, non-interacting objects which destroy the well-mixed assumption. In fact, if the control elements randomly diffuse into neighbouring edges the mean field scenario is recovered: coexistence is only found in regions where the system is bistable under the mean field approach—as shown for the lattice in Fig. 2.23.

We find (Fig. 2.22) that the more homogeneous a structure is, the larger the area in the parameter space displaying coexistence. Why do spatial and topological arrangements strengthen coexistence? By fixing the control elements in a lattice or network the corresponding architecture splits up into many disconnected components, each of which may show a different dynamics. Areas without police presence display a scenario whose dynamics is that of the fully asymmetric model, in which species coexist for mafias' strength $\sigma > 4$. The remaining subregions have an effective police fraction higher than p . Unpoliced areas constitute harmless, friendly habitats for mafiosi, whereas citizens' clusters arise preferentially in policed regions. If the average number of connections of a given structure is small, paths are easily blocked favouring the formations of disconnected islands and enhancing thus the emergence of two different dynamics. Fig. 2.24 shows a typical snapshot of the system on a regular lattice. Its evolution may be visualized in the Movies 5 and 6 of the supplementary material.

In Fig. 2.25 the stationary fraction of mafiosi (left) and extinction probabilities (right) are compared for two police fractions (two upper rows) and for a constant strength (bottom). We observe mafia's fractions very close to null, even there where the extinction probability is no longer one, as in the case of the $\gamma = 2$ SFN for $p = 0.3$. Attending to the extinction probabilities, we observe that for a fixed police fraction (upper and middle plots), the strength needed for mafiosi to survive increases with the heterogeneity of the structure. While a given fraction of control elements suffice to

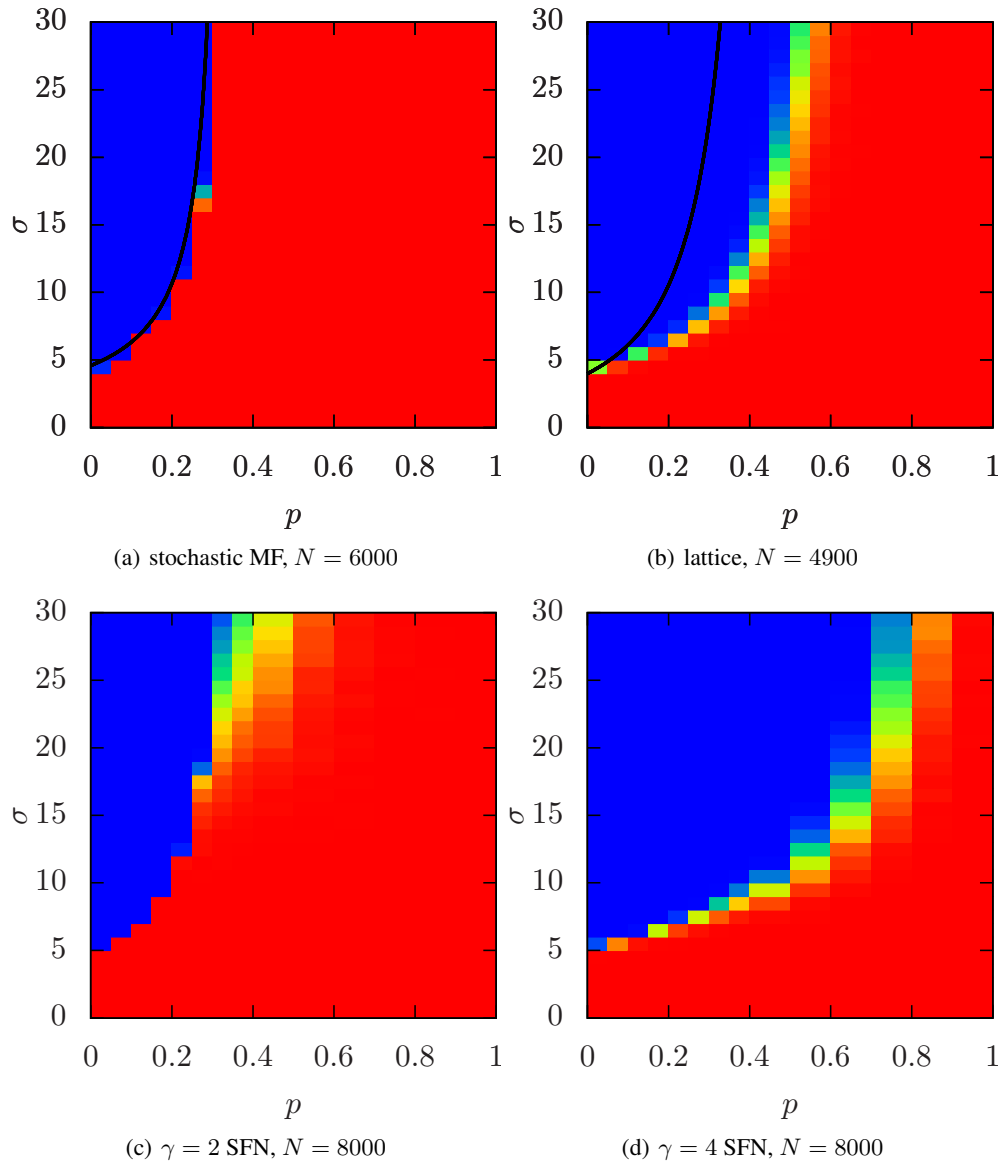


Figure 2.22: FAPM: Mafia's extinction probability as a function of the police fraction p and the strength σ [red: $p_{\text{ext}} = 1$, extinction; blue: $p_{\text{ext}} = 0$, coexistence]. Diversity in a regular lattice, $\gamma = 2$, and $\gamma = 4$ scale free networks and the unstructured mean field approximation are compared. The $m^- = 1/2$ separatrix is plotted on top of the MF results [top left] and the saddle-node bifurcation curve separating the bistable and monostable regimes predicted by the deterministic mean field is plotted on top of the lattice results [top right]. The initial population is homogeneously distributed, $m_0 = c_0 = 1/2$.

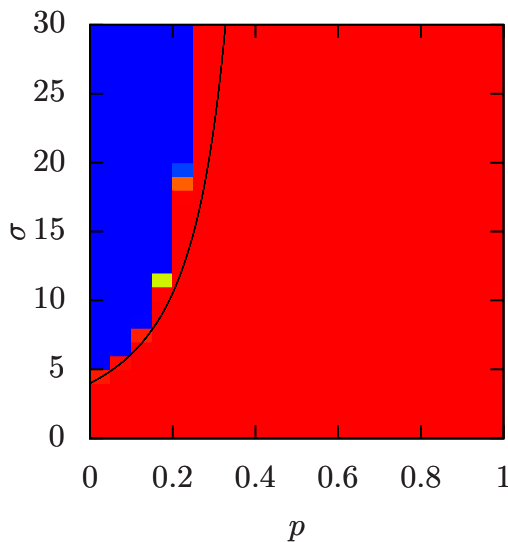


Figure 2.23: FAPM: Extinction probability for a lattice where the control elements randomly diffuse among edges. The mean field prediction for the stability is recovered. Coexistence does not take place—as in a lattice including *defects*—over the bifurcation [black line] predicted by the deterministic MF which separates the bistable region and the monostable region where extinction is the only stable state.

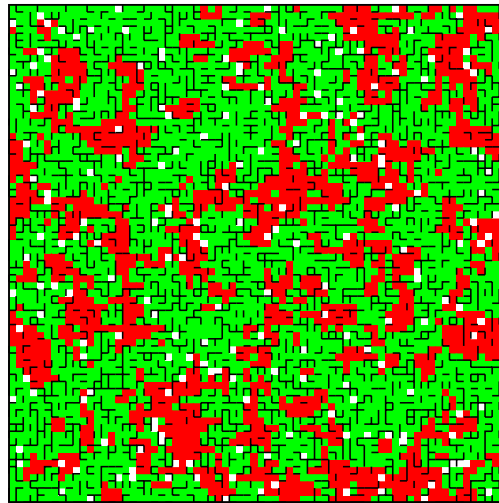


Figure 2.24: FAPM: Snapshot of the population structure after a time $\tau = 10$ for strength and birth rate $\sigma = \beta = 25$ and police fraction $p = 0.3$. Note that citizens and mafiosi clusters arrange mostly in policed, respectively unpoliced areas creating substructures with different regimes. Lattice size $N = 4900$. [Green stands for citizens, red for mafiosi, and white for empty places. The black segments between cells represent control elements].

end with the mafia in a well-mixed population, a homogeneous structure allow mafiosi to find protection in areas with a low density of control elements. Therefore, the more homogeneous a structure is, the better it promotes coexistence. Similarly, for a fixed strength the fraction of control elements required to finish with the mafia increases in regular structures with smaller connectivity.

However, the promotion of coexistence does not necessarily imply that the mafia fraction in equilibrium is systematically increased. Indeed, homogeneous structures as the lattice and $\gamma = 4$ scale free graph lessen the fraction of mafiosi with respect to the well-mixed case for parameters where the coexistence regime emerges both in

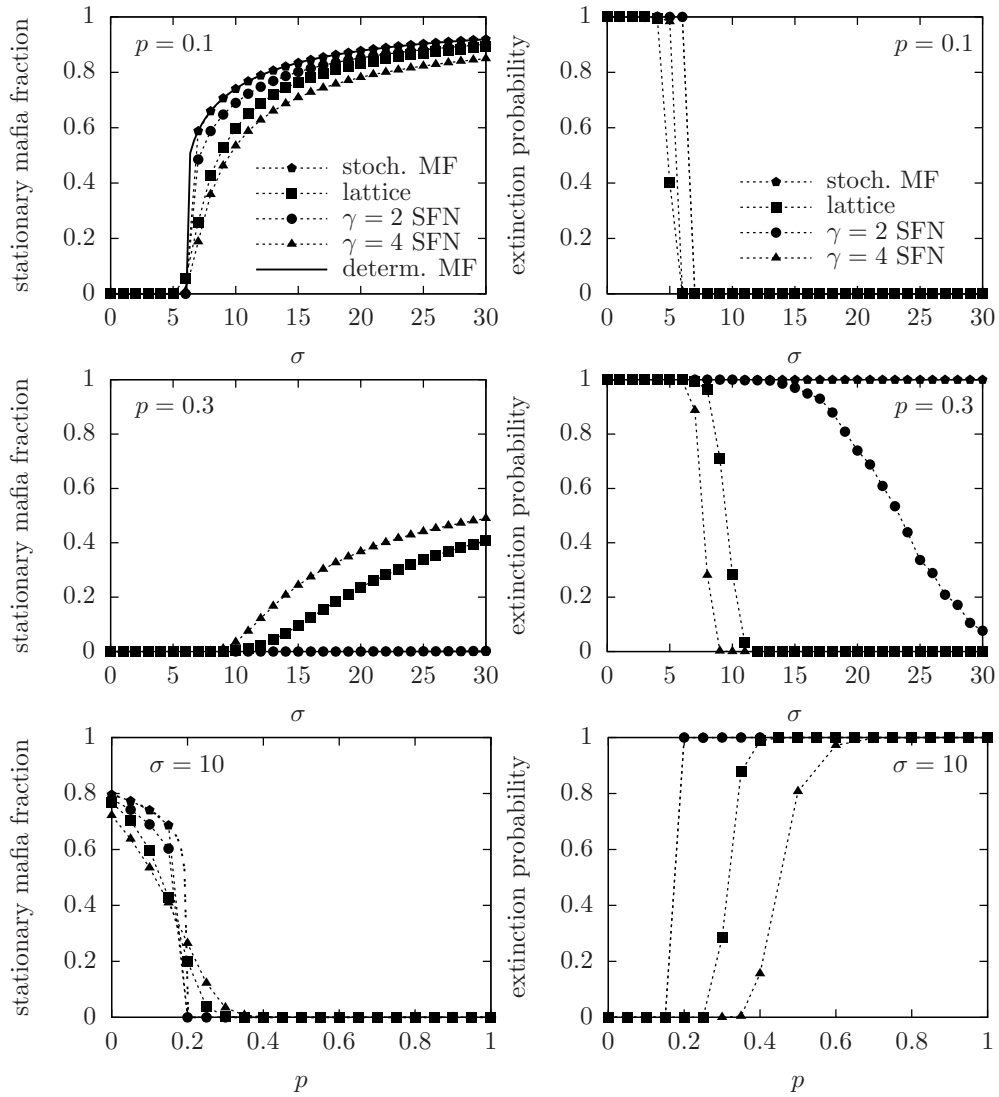


Figure 2.25: FAPM: Stationary mafiosi fraction [left] and extinction probability [right] for the mean field approximation and different structures [same legend code]. In the two upper rows the mafiosi population is plotted as a function of σ for different constant fractions of police, $p = 0.1, 0.3$; whereas in the bottom row the stationary population and extinction probability are plotted against the police fraction for a fixed value of the strength parameter $\sigma = 10$.

unstructured societies and in organized ones—as is the case for $p = 0.1$ in Fig. 2.25. This is also a consequence of the fixed attachment of the control elements. Whichever population is in minority is strengthened due to the subregimes dynamics induced in the structure. The most clear evidence for it is the transition from extinction to coexistence, but not the only one, as one also observes that the fraction of citizens in equilibrium grows with respect to that in unstructured societies when citizens represent a minority. In disconnected networks, both citizens and mafiosi may find subregimes which benefit their interests.

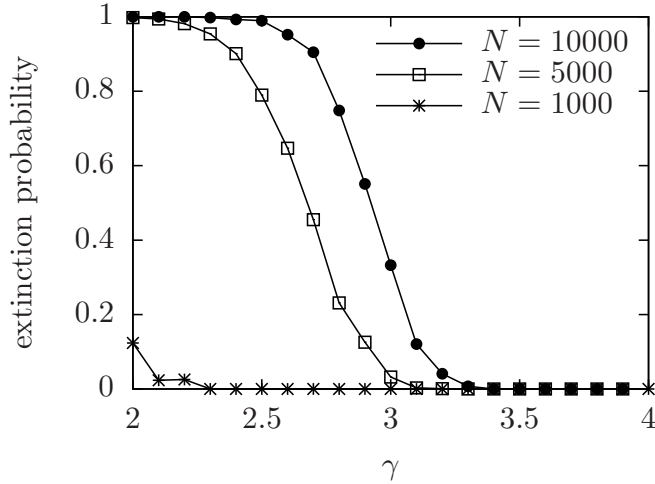


Figure 2.26: FAPM: Extinction probability as a function of heterogeneity in scale free graphs. A transition from extinction to coexistence takes place for some γ between 3 and 3.5 for different system sizes. The parameter point reads $\beta = \sigma_m = \sigma_p = 10$, $p = 0.3$ and initial conditions are $c_0 = m_0 = 1/2$.

In addition, one finds a transition from extinction to coexistence in scale free graphs with increasing homogeneity. In fact, for fixed parameters coexistence emerges for some value between $\gamma = 3$ and $\gamma = 3.5$ depending on the network size—Fig. 2.26 illustrates the transition. This result confirms the thesis that homogeneity promotes coexistence.

To summarize, in asymmetric policed systems the more homogeneous an architecture is, the better it promotes diversity, either avoiding extinction—Figs. 2.25 and 2.26—or bringing stationary population fractions closer to each other—Fig. 2.27.

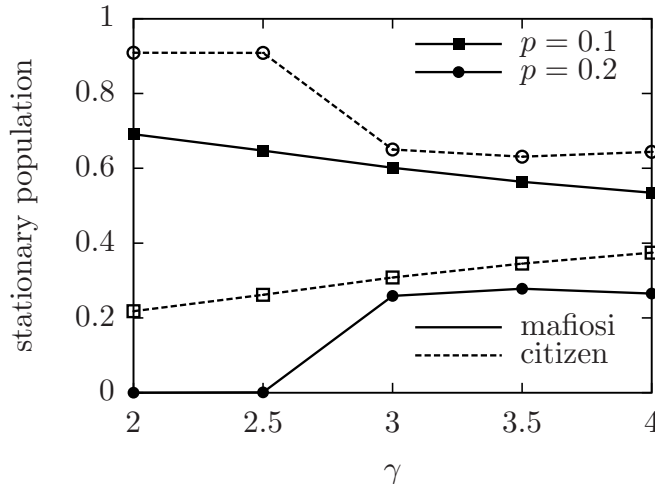


Figure 2.27: FAPM: Dependence of the stationary population fractions on the heterogeneity, γ , of scale free networks for two different police fractions $p = 0.1$, $p = 0.2$. Network size $N = 10000$. Initial conditions $m_0 = c_0 = 1/2$. Parameters: $\beta = \sigma_m = \sigma_p = 10$, $\sigma_c = 0$.

Targeted police distribution

In the same way that vaccination in infection processes is more effective if targeted to highly connected nodes or hubs [107], the distribution of control elements might matter in the eradication of mafias. We study the effect of preferential attachment of the control elements in scale free networks. In particular, we investigate two specific

distributions of control elements:

$$p_1(e_{ij}) = \frac{d_i d_j}{\sum_{ij} d_i d_j}, \quad (2.44)$$

$$p_2(e_{ij}) = \frac{(d_i d_j)^{-1}}{\sum_{ij} (d_i d_j)^{-1}}. \quad (2.45)$$

The probability for a control element to *sit* on an edge e_{ij} for the distribution p_1 (p_2) is directly (inversely) proportional to the product of the degrees of the nodes connected by the edge, i.e. $d_i d_j$. The first distribution, p_1 , favours the police attachment around highly connected nodes, whereas the second, p_2 , promotes control elements to surround sparsely connected nodes.

One expects the network topology to be the key in understanding the relevance of a specific police distribution. The relation between the fraction of edges accommodating control elements and the fraction of nodes which are connected with those plays a substantial role in the analysis of the problem. Indeed, a fraction p of control elements protects a larger or smaller effective fraction p' of nodes depending on the police distribution. The number of edges connected to the n nodes with the lowest degree k is much smaller than those connected to the same number of nodes with the highest degree. Consequently a given fraction of policed edges p protects a larger (smaller) fraction p' of nodes if they are lowly (highly) connected. The normalized degree N_k/N and cumulated degree $\sum_k N_k/N$ distributions together with the fraction of total edges required to connect the nodes up to a given degree k_i , $\sum_{k=0}^{k_i} k N_k / (N \langle k \rangle)$ illustrates this topological feature—Fig. 2.28. The cumulated fraction of edges grows more slowly than the cumulated fraction of nodes.

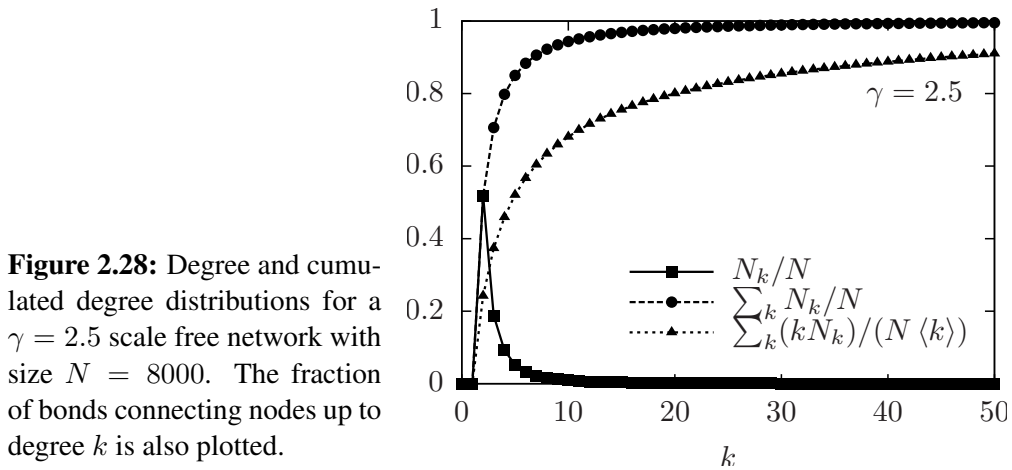


Figure 2.28: Degree and cumulated degree distributions for a $\gamma = 2.5$ scale free network with size $N = 8000$. The fraction of bonds connecting nodes up to degree k is also plotted.

One can introduce an *effective* police fraction p' which is the fraction of protected nodes—sites with the majority of their edges policed. If the control elements were randomly distributed, the effective fraction should be the same as the actual fraction of control elements p , which is certainly not the case for preferential attachment. If control elements attach around hubs (p_1 distribution), $p' < p$ and vice versa $p' > p$ if small nodes are preferentially policed (p_2 distribution).

In addition, for both distributions the more homogeneous a structure is, i.e. larger γ , the larger the effective police fraction p' . Scale free networks with large exponent γ

have large fractions of lowly connected nodes and small fractions of highly connected nodes, as well as a smaller maximal degree. Hence, for a given fraction p if hubs are the favourite targets a larger fraction is protected because they have less connections. As for the small nodes counterpart, also a larger fraction of them are protected as more nodes show small connectivities.

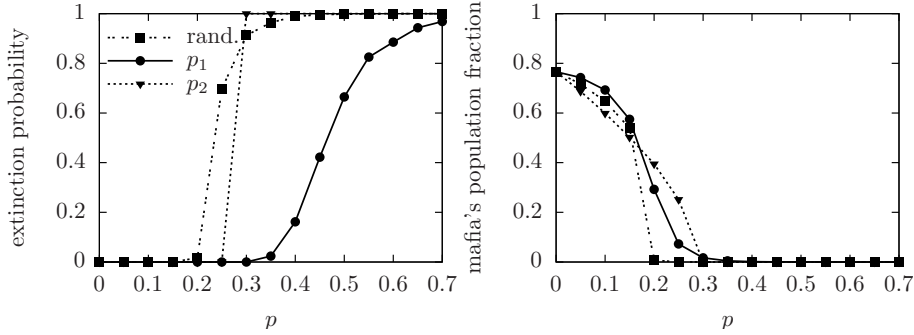


Figure 2.29: Extinction probability [left] and stationary mafia's fraction [right] for a $\gamma = 2.5$ network with size $N = 10000$ for the random police attachment and the targeted distributions p_1 and p_2 . [Same legend code]. Parameters: $\sigma = \sigma_m = 10$. Initial conditions: $m_0 = c_0 = 1/2$.

Simulations reveal that locating the police around large hubs benefits mafiosi performance. Although counter intuitive at first glance, this is an understandable behaviour. The police distribution originates two subregimes in the system. First, citizens establish in a policed fraction $p' < p$ corresponding to the largest nodes, which stay in a stationary state from the very first stages of the dynamics. The remaining $1 - p'$ network fraction is a more homogeneous unpoliced architecture with effective $\gamma' > \gamma$. The dynamics taking place here is the same as that of a fully asymmetric model without policing elements in homogeneous structures. Coexistence is found even for almost vanishing mafiosi fractions for this case. The interplay between both subregimes, extinction in hubs and coexistence elsewhere, yields the stationary configuration of the system. To reach extinction the unpoliced subregime must be so small, that the control elements at its border succeed in fighting the mafia. To conclude, a larger fraction of control elements is required to extinguish the mafia when they target hubs than when they are randomly distributed. The results of simulations in figure 2.29 illustrate this statement. While a fraction of control elements $p = 0.3$ suffices to achieve the mafia's extinction for a random distribution, a fraction close to $p = 0.7$ is required for the preferential distribution p_1 .

The results displayed in Fig. 2.30 for the exemplary parameters set $p = 0.2$, $\gamma = 2.5$, $\sigma = 10$ support the previous analysis. Despite the decrease of citizens in the early stages, the average degree of nodes occupied by citizens $\langle k_c \rangle$ increases in these initial times. It indicates that citizens overtake policed regions very fast. These nodes are *blocked* and may only influence decisions on neighbouring sites. Subsequent variations in the population fractions only take place in unpoliced areas as can be observed in the bottom left figure: policed neighbourhoods show an almost constant population. A rearrangement of the population in the unpoliced regions slightly decreases the average degrees of nodes allocating citizens $\langle k_c \rangle$ and mafiosi $\langle k_m \rangle$, as those are

nodes with small degree (top right figure). The degree distribution of nodes allocating citizens and mafiosi in equilibrium are shifted with respect to the network degree distribution. If they would follow the same distribution as the network, the fractions C_k/N_k and M_k/N_k (displayed in the bottom right part of Fig. 2.30) should be those of the populations in equilibrium for all degrees k , i.e. c and m , respectively. However, C_k/N_k is significantly greater than c for hubs, while M_k/N_k is much smaller than m there. This result substantiates the hypothesis of the network's division in subregimes.

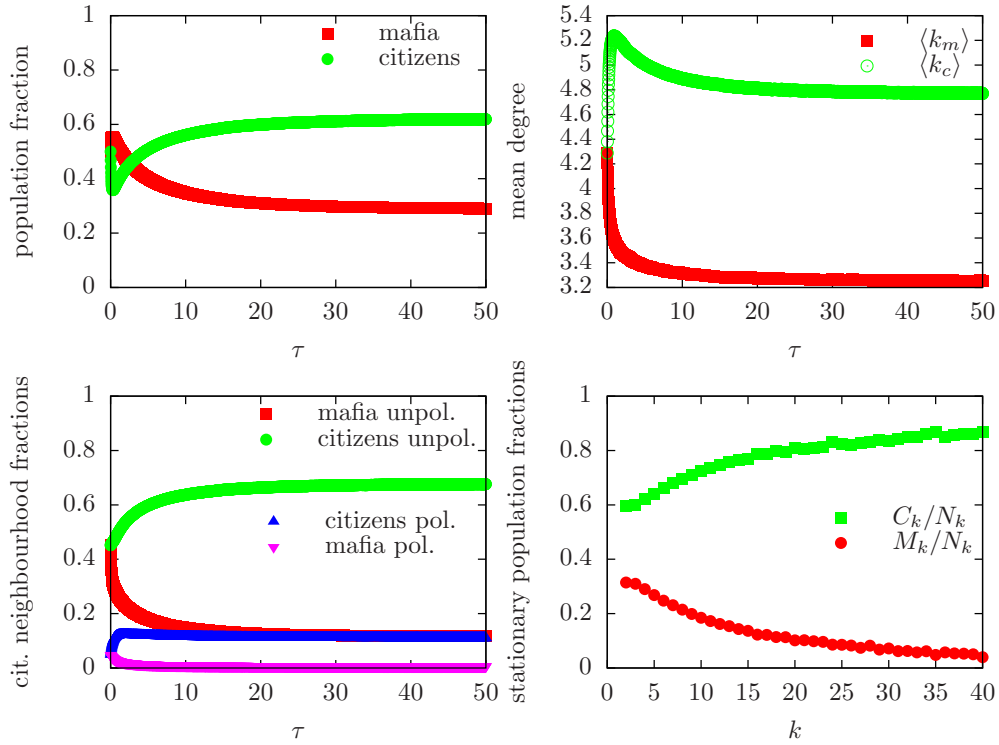


Figure 2.30: Police in hubs: population's fraction [top left], average degree of nodes with both species $\langle k_c \rangle$ and $\langle k_m \rangle$ [top right], citizen neighbourhood—(un)policed refer to the number of citizens' neighbours of a given type with (un)policed bonds—[bottom left], and fraction of citizens and mafia in nodes with degree k [bottom right]. Parameters $\sigma = 10$, $p = 0.2$, $\gamma = 2.5$, $N = 8000$.

Targeting the control elements to small nodes also yields very interesting results. The preferential attachment of a fraction p of control elements to lowly connected nodes effectively protects a fraction $p' > p$ of nodes. These lowly connected nodes are fast populated with citizens. The region is almost inactive with no other reactions than those of the birth-death process. This dynamics may be understood as if the *extremities* of the initial network were blocked. The remaining structure, the skeleton of the network, has highly connected, unprotected nodes. The dynamics taking place there is close to that of the well-mixed population for the unpoliced fully asymmetric model. For this case, the stationary state depends on the parameters and initial conditions, but shows large regions of coexistence even for small initial fractions of mafiosi. In particular, for the parameters used here $\sigma = \beta = 10$ coexistence was already achieved for

an initial mafia's fraction¹¹ $m_0 = 0.1$.

The resulting stationary population is thus a combination of a fraction $p' > p$ of citizens and a fraction $1 - p'$ of a coexistence state as in the mean field case. For a certain threshold police fraction the size of the region showing mean field behaviour is no longer large enough to compensate the effect of citizens at its border. In particular, for a police fraction $p = 0.3$ —for which a fraction larger than $p' = 0.5$ of nodes are protected and hence populated by citizens—the extinction probability becomes abruptly one in a step-wise function. Furthermore, in Fig. 2.31 one observes that this transition between coexistence and extinction does not depend on the system's size, unlike to the transitions for the other distributions. The fact that, for the p_2 distribution, slightly larger fractions p generate drastic increments in the effective fraction of protected nodes p' could be the origin of the sharpness in the transition from coexistence to extinction. Additionally, one could explain the independence of the system's size as the result of the effective block of extremities of the network, which could switch off possible size effects.

Fig. 2.32 displays the stationary population's fractions as a function of heterogeneity in scale free graphs for both police's distributions compared to the random case. It shows that strategies favouring police attachment to highly and lowly connected nodes have a larger impact in networks with larger degree fluctuations, i.e. heterogeneous scale free networks with small γ .

For the distribution p_1 , the citizen's fractions slowly increase¹² with homogeneity, very similarly as they do in the unpoliced asymmetric model—see Fig. 2.21 for comparison. For the distribution p_2 , the population's fractions of stationary coexistence states are almost constant in heterogeneous structures (small γ) as a result of the mean field like behaviour. For homogeneous structures (large γ) the unpoliced fraction of the network is rather homogeneous for both distributions, as the network itself is. Therefore the results of both strategies are not far from each other.

2.4 Individuals may move

Individuals in societies, bacteria in cultures, animals in ecological systems are all mobile agents which do not stay in fixed positions. The role of mobility, be it directly aimed at achieving a goal or undirected, is an important feature when modelling social dynamics. Despite its importance, there is not much research done on the role of mobility in the most common models describing evolutionary systems. Nevertheless, the few works dealing with this topic reveal very interesting results.

This is the case of the work of Reichenbach et al. [111] which proves that mobility jeopardizes coexistence in the spatial rock-paper-scissors game. Helbing et al. [60, 59] examined how success-driven migration promotes cooperation and makes it robust against different types of noise in the spatial prisoner dilemma game. Other authors have analysed the role of random mobility in the prisoner dilemma and, even though their results are not conclusive, they have observed modifications with respect to the immobile case [40, 136]—see section 1.2.1 for a more extensive discussion.

¹¹In the subregime dynamics we are considering the initial mafia fraction is understood as the resulting mafia in the highly connected region once the influence of the neighbouring citizens has been taken into account.

¹²If coexistence is a starting point.

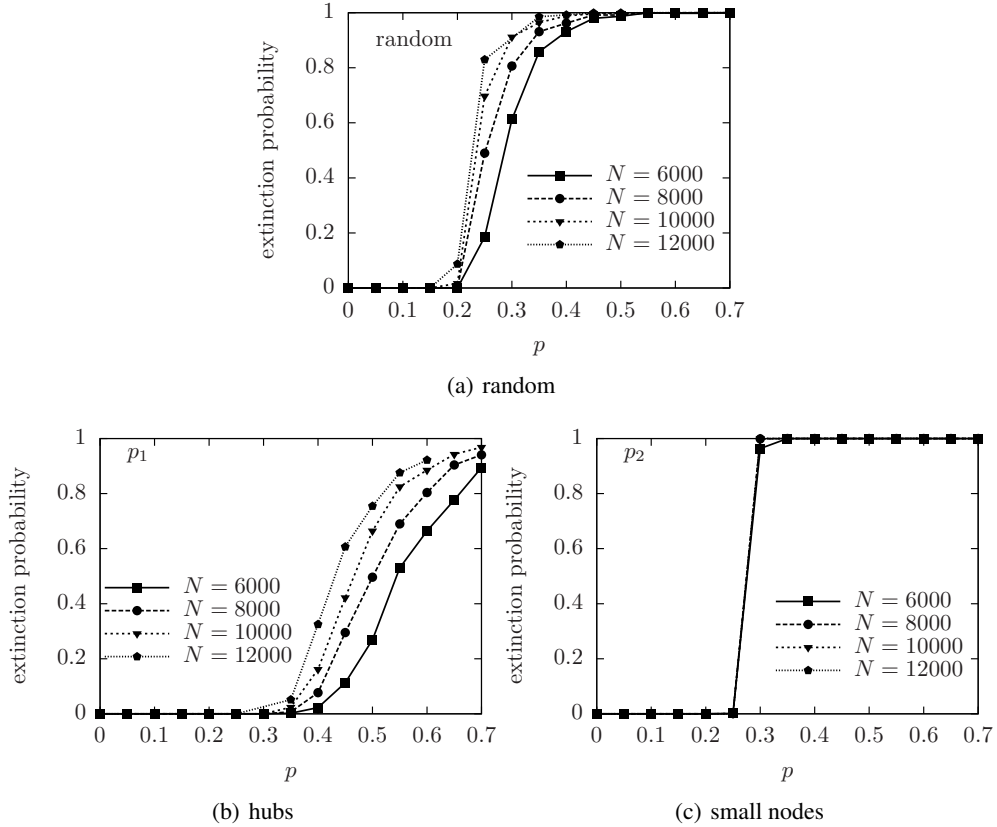


Figure 2.31: Extinction probability as a function of the police fraction for several system sizes in a $\gamma = 2.5$ scale free network. Police distributions p_1 and p_2 are compared to random attachment. Parameters: $\sigma = \sigma_m = 10$. Initial conditions: $m_0 = c_0 = 1/2$.

We now investigate the role of mobility for the mafia model. That is, we analyse whether allowing individuals to displace into neighbouring nodes modifies the system's behaviour and to what extent this is so. We distinguish between two types of mobility or *migration*: In the first one individuals may only migrate to empty places in their neighbourhood, whereas in the second type they can also swap their position with other actors. We also compare two strategies: *directed* (or intelligent) and *undirected* (or random) mobilities. If agents move intelligently they rationally select the neighbouring site where they have the largest probability to keep their strategy unchanged, whereas if individuals move in an undirected way they simply move to a random site in their neighbourhood, without making any further considerations. Since the undirected migration with possible interchanges of sites among individuals is nothing but random diffusion, we will refer to diffusion—extending its usual meaning—when speaking of mobility in which individuals are allowed to change their locations, even if they do it in a directed way, in contrast with migration to empty places. We restrict the sites they can access within one displacement to their nearest neighbours for any type of mobility considered. We investigate the scenario in which only one species may migrate, citizens or mafiosi, as well as that in which both species are able to move.

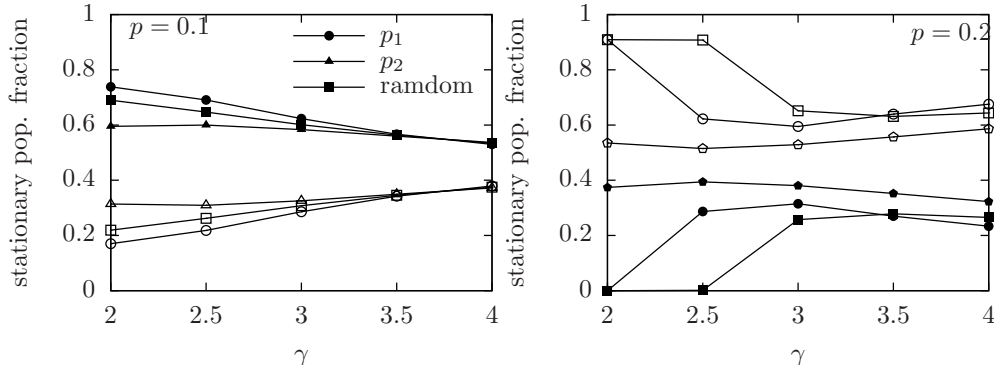


Figure 2.32: Comparison of the stationary population's fraction between random, p_1 , and p_2 , police distributions as a function of heterogeneity (γ) in scale free networks. Full and empty symbols represent the mafia and citizens populations respectively. Police fractions: $p = 0.1$ [left] and $p = 0.2$ [right, same legend]. System size $N = 8000$. Parameters: $\sigma_c = \sigma_p = \beta = 10$.

Directed mobility works as follows: a randomly chosen individual explores the fictitious probability that he would have in all of his nearest neighbouring sites so as to keep his strategy unchanged and moves there where this probability is the largest, i.e. where the corresponding reaction rate ω_{cm} or ω_{mc} is the smallest. However, if the probability to not change strategy is not improved by moving, then he stays at his original site. Otherwise he swaps his location with the empty place or individual allocated in the chosen destination. Individuals follow paths with a *negative gradient*: the gradient of the reaction rate to change their strategy must be negative in all displacements, i.e. $\nabla\omega < 0$. Directed mobility represents mainly a defensive strategy. The individual who moves looks for safer locations but does not search positions where he could induce changes in the strategy of the opponents.

When both species move (randomly) fast enough, so that the rate of displacements is much larger than the rate to change strategy, the population is well-mixed and one would expect to recover the dynamics of well-mixed populations. However, as we will see in this section, the mean field behaviour for well-mixed populations is not recovered suggesting that a local mean field approximation might much better describe the behaviour on spatial and social structures.

To have a richer spectrum of outcome events we choose points in the parameter space for which the stationary equilibrium on lattices or graphs differs from that predicted by the mean field theory.

Active versus passive diffusion

The concepts of *active* and *passive* diffusion are crucial to understand the system's dynamics analyzed in the following sections. Within the migration mechanism agents cannot be passively displaced, as the target locations for the migrating agents are empty places. Every time an agent changes its location, be it rationally or randomly, a second agent is involved in this displacement, namely the one located at the selected final destination. This one will move to the location the first agent came from. The latter

displacement is what we refer to as a passive displacement, whereas the former one is an active displacement.

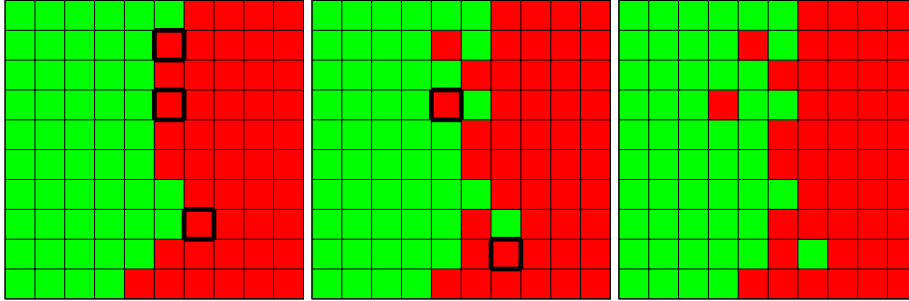


Figure 2.33: Active and passive diffusion at cluster interfaces. In these cartoons mafiosi [red] actively diffuse, while citizens [green] diffuse passively. The steps represented here are only examples to illustrate the concept of passive diffusion; they are not real time steps in the evolution of the system. In the first step the three selected mafiosi diffuse to the left. In the second step the selected mafioso at (5, 7) diffuses to the left and the other at (7, 2) upwards—coordinates are given with respect to the bottom left corner. In all these movements citizens have been passively displaced as shown in the cartoons.

Passive mobility plays a very important role, especially when only one species is allowed to move. Passively displaced agents cannot choose their final location and are often displaced to sites which are less favourable for them than their initial positions. This is often the case for agents at interfaces. Since these passively displaced individuals have no mobility themselves, they cannot move further seeking safer positions, but have to stay where they were displaced until they die or are forced to change strategy. These individuals immersed in the opponent field are mostly forced to finally change their strategies, which represents an indirect growth mechanism for the actively diffusing species. Fig.2.33 shows an example of active and passive diffusion.

2.4.1 Symmetric model

The symmetric model yields extinction of mafiosi in structures that are sufficiently homogeneous for immobile agents. The process which dominates the dynamics in the immobile case, i.e. the change of strategy at clusters interfaces, is symmetric for both species. The symmetry is only broken by the birth process—see discussion in section 2.3.1. Is this result stable if agents move? To gain some understanding of how the different mobility strategies alter the system's dynamics, we carry out an inspection of the exemplary parameter point $\sigma_c = \sigma_m = \beta = 15$. For this parameter point, which lies in the bistable region, species coexist within the mean field approximation, but extinction is stable in homogeneous architectures for initial conditions $c_0 = 1/4$, $m_0 = 3/4$. We investigate mobility in a $\gamma = 3$ scale free graph for which extinction is observed in the case of immobile agents.

Table 2.1 displays the results of different mobility strategies¹³. The four strategies

¹³ddiff and udiff standing for directed and undirected diffusion and dmig and umig for directed and undirected migration.

studied are arranged in different columns, while the rows correspond to the moving agents. The results for the immobile scenario for the same network are shown in the top of the table. We specify the extinction probability p_{ext} and the stationary population fractions (c, m) . The displayed data correspond to a mobility rate $\mu = 100$, i.e. the rate at which displacements to neighbouring nodes are tried or performed in the case of directed, respectively undirected mobility.

SM for a $\gamma = 3$ SFN				
$\mu = 0$	$p_{\text{ext}} = 1, (c, m) = (0.94, 0)$			
$\mu = 100$	ddiff	udiff	dmig	umig
citizens	$p_{\text{ext}} = 1$ (0.94, 0)	$p_{\text{ext}} = 1$ (0.94, 0)	$p_{\text{ext}} = 1$ (0.94, 0)	$p_{\text{ext}} = 1$ (0.94, 0)
mafia	$p_{\text{ext}} = 0$ (0.87, 0.07)	$p_{\text{ext}} = 0$ (0.15, 0.78)	$p_{\text{ext}} = 1$ (0.94, 0)	$p_{\text{ext}} = 1$ (0.94, 0)
both	$p_{\text{ext}} = 0.08$ (0.92, 0.02)	$p_{\text{ext}} = 1$ (0.94, 0)	$p_{\text{ext}} = 1$ (0.94, 0)	$p_{\text{ext}} = 1$ (0.94, 0)

Table 2.1: SM: Results of applying different mobility strategies to a symmetric model system in a $\gamma = 3$ scale free network, $N = 8000$. The mean field approximation yields $p_{\text{ext}} = 0, (c, m) = (0.09, 0.85)$. Parameters: $\sigma_c = \sigma_m = \beta = 15$ for initial conditions $c_0 = 0.25, m_0 = 0.75$.

One realizes that migration for $\mu = 100$ does not change the steady state of the system with respect to the case $\mu = 0$. The fraction of places available to move in $\phi = 1/(1 + \beta) \sim 0.05$ is too small to induce qualitative changes in the dynamics.

In the rest of the section, we discuss in detail the characteristics of directed and undirected diffusion for the symmetric model.

Directed diffusion

Rational or directed diffusion is a defensive strategy in which individuals move to less risky sites. Within the cluster dynamics in the symmetric model a species may profit from directed diffusion either if isolated individuals reach clusters or building smoother cluster borders weaken the opponent's attack. Species are stronger against invasions if their clusters have smooth interfaces, as the fraction of adjacent cells occupied by the opponent is lowered for smooth interfaces. The directed mobility effectively acts as a surface tension to create smooth interfaces by reallocating individuals. The smoother the interfaces, the better the protection for the cluster. If only one species is rationally moving its performance is improved through this mechanism with respect to the other. The cartoon in Fig. 2.34 and the corresponding caption illustrate this strategy.

When both species are moving the extinction probability is significantly reduced, though the mafiosi fraction in equilibrium is very small. Why should mafiosi get an advantage through the mechanism if the defensive strategy is available to both species? The citizens' advantage against mafiosi, if agents are immobile, relies on the asymmetric birth of citizens joining clusters. However, if clusters interfaces are very smooth,

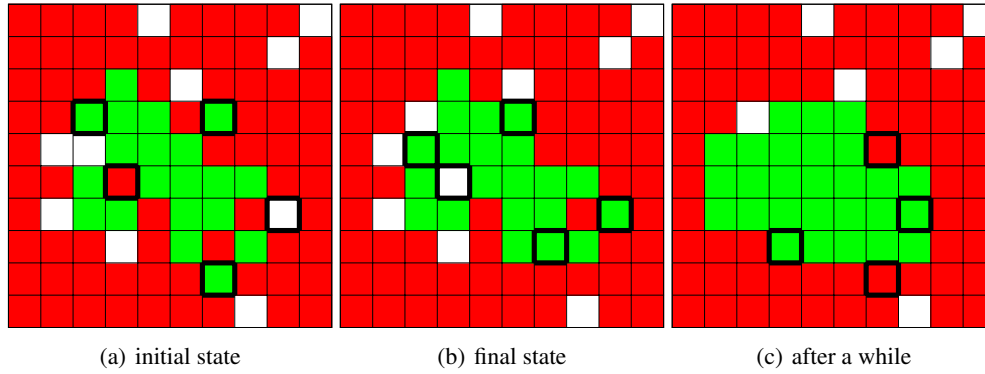


Figure 2.34: SM: Directed citizen diffusion in a symmetric model. Three kind of processes are represented in the transition from the initial state [left] to the final one [middle] after a time step. Coordinates (x, y) have their origin at the bottom left corner. First, three citizens at sites $(3, 7)$, $(7, 2)$, and $(7, 7)$ [displayed with thicker frames] lessen their probability to become mafiosi by diffusing to neighbouring sites. For example, the one at $(7, 7)$ reduces his transition rate from $\omega_{cm}^0 = \sigma$ to $\omega_{cm}^f = \sigma/8$. The mafioso at $(4, 5)$, who dies, leaves an empty place where a potential born citizen will survive. And last, a citizen born in $(9, 4)$, who would become mafioso with reaction rate $\omega_{cm} = \sigma$ at this site, is very likely to survive fleeing to the neighbouring site $(8, 4)$. After a while the cluster has adopted a more compact shape with a smoother interface; hence directed mobility acts as an effective surface tension [right cartoon]. Interfaces become more stable, as the reaction rates are smaller. Citizens in corners, e.g. $(4, 3)$, have a transition rate $\omega_{cm} = \sigma/4$ and in edges, e.g. $(8, 4)$, $\omega_{cm} = \sigma/16$. Mafiosi may become citizens with a rate $\omega_{mc} = \sigma/4$ in inner corners, e.g. $(7, 6)$ and $\omega_{mc} = \sigma/16$ at edges, e.g. $(7, 2)$.

the new born citizens outside the clusters do not find the same protection at the domain borders as they found for rougher interfaces without mobility.

The stationary mafia's fraction and extinction probability for diffusion of mafiosi and both species as a function of the mobility rate μ are plotted in figure 2.35.

Undirected diffusion

Surprisingly, the performance's improvement of the mafia thanks to undirected diffusion is much better than the improvement resulting from directed, rational mobility. Directed mobility only allows displacements along a path with negative gradient of the reaction rate of the diffusing species, i.e. $\nabla\omega < 0$. Therefore, movements in which a mafioso enters a citizen's cluster are strictly forbidden. Directed mobility provides a better defensive position, but does not care about striking the contrary. But interestingly, positions which, for instance, represent a slight disadvantage for the mafia, i.e. $\nabla\omega_{mc} > 0$, may yet introduce a much larger damage for passively displaced citizens: $\nabla\omega_{cm} \gg \nabla\omega_{mc}$. When a randomly diffusing individual, independent of his identity, hops a cluster interface he actively enters an adversary's domain. But in addition an individual of the opponent species passively diffuses into the enemy's field as well. Both displaced agents are in danger. The difference between them is that the active

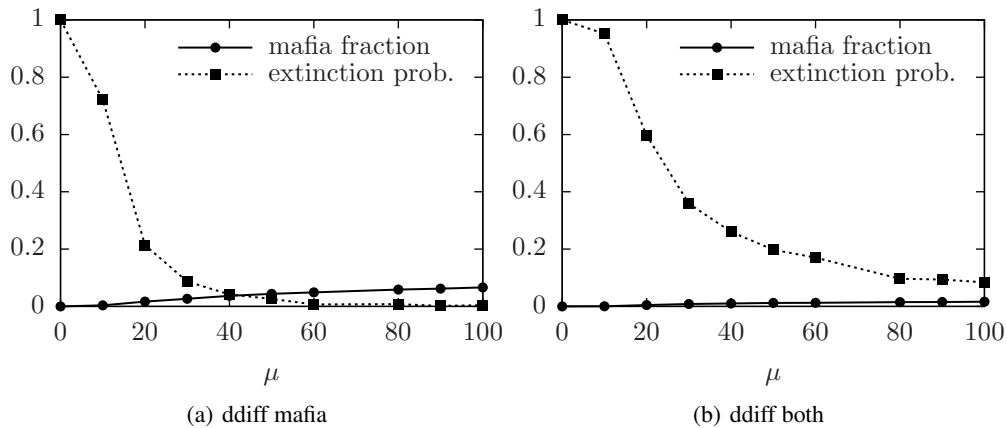


Figure 2.35: SM: Directed diffusion of mafia [left] and of both species [right] in the symmetric model for a $\gamma = 3$ SFN with size $N = 8000$. Stationary mafia's fraction and extinction probability after a time $\tau = \lambda N$ with $\lambda = 0.01$ are plotted. Parameters: $\sigma = \beta = 15$, initial conditions $c_0 = 1/4$, $m_0 = 3/4$.

agent continues his random walk, whereas the passive one must stay in the enemy field. The next time they update their strategies the first has a large probability to be far away, whereas the second is with almost absolute certainty where he was passively displaced. Moreover, the larger the mobility rate is, the higher the probability for the actively diffusing individual to have fled and avoid a strategy change. See the mafia's fraction and extinction probability as a function of the mobility rate μ in Fig. 2.36 for the case in which mafiosi diffuse.

If only mafiosi diffuse, they continuously weaken citizens resistance by breaking their clusters. As a result, they improve their performance and coexistence is found in equilibrium. The stationary state is thus qualitatively changed with respect to that of immobile agents. If both species randomly diffuse, both have the same opportunity to escape before having to take a decision. Mobility does not induce differentiating advantages for any species and extinction is reached as in the case without mobility.

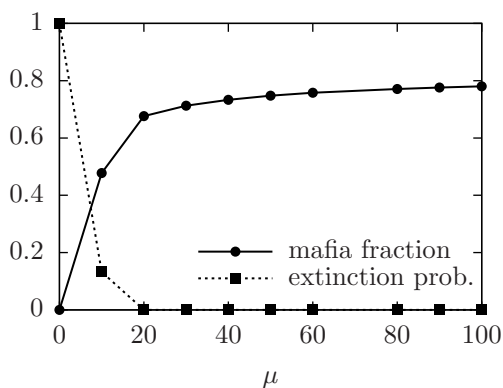


Figure 2.36: SM: undirected diffusion of mafia. Random diffusion of mafiosi in the symmetric model for a $\gamma = 3$ SFN with size $N = 8000$. Stationary mafia's fraction and extinction probability after a time $\tau = \lambda N$, $\lambda = 0.01$, are plotted. Parameters: $\sigma = \beta = 15$, initial conditions $c_0 = 1/4$, $m_0 = 3/4$.

2.4.2 Fully asymmetric model

We focus now our attention on the role of mobility in the fully asymmetric model. We choose a parameter point in the bistable regime $\beta = 20$, $\sigma = 7$. For initial conditions $c_0 = 0.8$, $m_0 = 0.1$, the mean field approximation predicts extinction but homogeneous structures, in particular the $\gamma = 3$ network which we take as an example, promote coexistence.

Table 2.2 displays the mafia's extinction probability and the stationary population's fractions for diffusion and migration. As before we compare the directed and undirected strategies for a mobility rate $\mu = 100$ in a $\gamma = 3$ scale free network with size $N = 8000$.

FAM for a $\gamma = 3$ SFN				
$\mu = 0$	$p_{\text{ext}} = 0, (c, m) = (0.26, 0.69)$			
$\mu = 100$	ddiff	udiff	dmig	umig
citizens	$p_{\text{ext}} = 0$ (0.92, 0.04)	$p_{\text{ext}} = 0$ (0.20, 0.75)	$p_{\text{ext}} = 0$ (0.28, 0.67)	$p_{\text{ext}} = 0$ (0.24, 0.7)
mafia	$p_{\text{ext}} = 0$ (0.26, 0.69)	$p_{\text{ext}} = 0$ (0.15, 0.80)	$p_{\text{ext}} = 0$ (0.26, 0.69)	$p_{\text{ext}} = 0$ (0.20, 0.75)
both	$p_{\text{ext}} = 0.001$ (0.92, 0.03)	$p_{\text{ext}} = 0$ (0.16, 0.79)	$p_{\text{ext}} = 0$ (0.28, 0.67)	$p_{\text{ext}} = 0$ (0.21, 0.74)

Table 2.2: FAM: Results of different mobility strategies for $\mu = 100$ and $\sigma_c = 0$, $\sigma_m = 7$, $\beta = 20$, $p = 0$ in a $\gamma = 3$ scale free network whose size is $N = 8000$. The mean field yields $p_{\text{ext}} = 1$, $(c, m) = (0.95, 0)$. Initial conditions are $c_0 = 0.8$, $m_0 = 0.1$.

The dynamics of the asymmetric case in structures is also dominated by the growth of clusters which emerge in the first stages of evolution. Citizens become mafiosi through strategy updating with reaction rate $\omega_{cm} \neq 0$, while mafiosi become citizens via the death-birth process as $\omega_{mc} = 0$. Mafia's clusters grow at the expense of citizens at the rough interfaces between domains. Citizens' clusters only grow via birth process at a rate β in empty places. In the asymmetric model, new citizens only survive if they are born in a citizen cluster or at its border. Otherwise the mafia environment forces them to become mafiosi.

The results of the simulations including mobility reveal the same tendencies for diffusion and migration, although much stronger for the diffusive case due to the larger number of possible displacements.

Directed mobility

Directed mobility is a defensive strategy from which mafia do not benefit as mafiosi cannot be beaten by citizens, $\omega_{mc} = 0$. All sites are equally safe for mafiosi because the death process, which is the only action affecting them, is homogeneous in space and therefore independent of the site. Directed mobility is thus not an option for mafiosi to improve their performance.

On the contrary, citizens largely profit from directed mobility thanks to two mechanisms: the surface tension shaping the domains' interfaces and the migration of the citizens born at isolated sites.

This improvement in citizens' performance is not particularly significant when they migrate. In the migration scenario citizens may only move to empty places. Although they lessen their probability to change strategy, they also passively displace potential future citizens—empty places—to the unsafer position they come from. Effectively the system remains unchanged. If citizens may also swap their positions with mafiosi, i.e. if they diffuse, they first have a larger number of available destinations, but more important, the global final configuration benefits them as empty places are not systematically displaced into unsafer locations.

Fig. 2.37 shows the stationary population's fraction and the fraction of both species in citizens' neighbourhoods when the latter diffuse in a directed way¹⁴. The fraction of neighbours of type b in the vicinity of an a agent, n_b^a , with the constraint $\sum_b n_b^a = 1$ for $b = c, m, \phi$, is defined as follows:

$$n_b^a = \frac{1}{N_a} \sum_{x_i \in a} \frac{1}{k_i} \sum_{j=0}^{k_i} \delta_{x_j b}, \quad (2.46)$$

where N_a is the number of individuals of species a , k_i the degree of site i , and x_i is the strategy of the individual located at site i . The citizens neighbourhood shown in the figure confirms that the search of stable positions translates into a net growth of the citizens clusters, n_c^c fraction, in the stationary state. The equilibrium configuration is independent of the initial conditions (not shown).

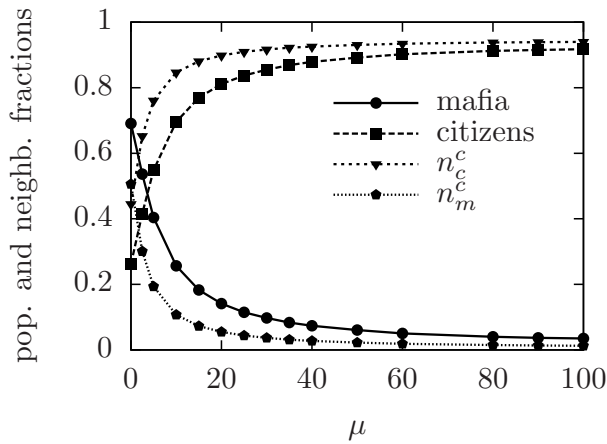


Figure 2.37: FAM: directed diffusion of citizens. Stationary fraction of species and citizens' neighbourhood as a function of mobility for citizens intelligently diffusing in a $\gamma = 3$ SFN. n_c^c and n_m^c stand for the citizen, respectively mafia fractions in the citizen vicinity—defined in the main text. Network size $N = 8000$. Parameters: $\sigma_m = 7$, $\beta = 20$, $\sigma_c = 0$. Initial conditions $m_0 = 0.1$, $c_0 = 0.8$.

The stationary citizens' fraction grows monotonically with the mobility rate. However, the most significant variation takes place for mobility rates similar to the strength $\mu \sim \sigma = 7$. Mobility allows born citizens to move along a path with $\nabla \omega_{cm} < 0$. As intelligent displacement is a *ballistic* or directed movement, the number of newly

¹⁴The results for both species diffusing in a rational way are the same, as mafiosi do not perform any displacement since $\omega_{mc} = 0$ in all sites.

born citizens in isolated areas who finally reach a citizens' cluster per unit time is directly proportional to the mobility rate and inversely proportional to the distance d they have to travel. Provided they find a path of decreasing gradient the number of citizens joining the clusters per unit time is:

$$\# \text{ born citizens } \frac{\mu}{d} = \beta \phi N \Delta\tau \frac{\mu}{d}. \quad (2.47)$$

The faster they move, the more of them survive and therefore the better the global performance of the species. However, as the number of born citizens per unit time is limited by those born in a time step, $\beta \phi N \Delta\tau$, a structural limit in the citizen's growth is achieved when they all have joined the clusters of citizens. This saturation should occur for mobility rates similar to the maximal path length d_m . For larger mobilities the improvement in citizens' performance is only due to the surface tension effect that make clusters more stable against mafia invasion.

In Fig. 2.38 we analyse the interdependence between the heterogeneity of structures and the directed mobility strategy in the fully asymmetric model when both species can diffuse. It turns out that the more heterogeneous a structure is, the smaller the critical mobility rate required to reach a crossing point of the population fractions.

This is indeed an expected result. As we have argued above, the number of citizens reaching safe positions per unit time should be proportional to the ratio of the mobility rate to the distance which must be covered to reach safer locations μ/d . We have learned in section 1.1.4 that scale free networks show small-world behaviour, with an average path length depending on their exponent γ . It scales as the double logarithm of the network size for $2 < \gamma < 3$, as $\log N / \log \log N$ for $\gamma = 3$, and as the simple logarithm for $\gamma > 3$. Thus the average path length for a network with $N = 10000$ nodes becomes $l_{\gamma < 3} \sim 2.2$, $l_{\gamma = 3} \sim 4.2$, $l_{\gamma > 3} \sim 9.2$. For a square lattice, the average path length scales as \sqrt{N} giving $l_l \sim 80$ for $N = 6400$. We expect thus, that the larger the average path length of a structure is, the higher the mobility rate needed to observe a crossover in the stationary fractions of both species. The critical mobility in which all isolated citizens have reached safe locations is expected to be proportional to the average path length $\mu_c \propto l$. The mobility rates at which the crossover takes place in the simulated results seem to agree with these heuristic arguments.

The difference observed in the mobility rate at the crossover point for the $\gamma = 2$ and $\gamma = 2.5$ networks could arise from the large difference in their average degrees, $\langle k \rangle_{\gamma=2} = 7.45$ and $\langle k \rangle_{\gamma=2.5} = 4.29$. A network with a larger number of connections $N_E = \langle k \rangle N$ offers more paths for mobile agents to find safer locations. Therefore, the mobility rate needed for the $\gamma = 2$ scale free graph to reach the crossover point between population's fractions is smaller than for $\gamma = 2.5$.

Undirected mobility

Undirected or random mobility favours the mafia's performance independent of who is moving. Both, migration and diffusion show similar tendencies although diffusion effects are more prominent. Again mobility plays a determinant role at the border between clusters of different species.

A diffusing mafioso hops over domain interfaces entering citizens' clusters. Accordingly, a citizen passively performs the opposite displacement. The mafioso in a

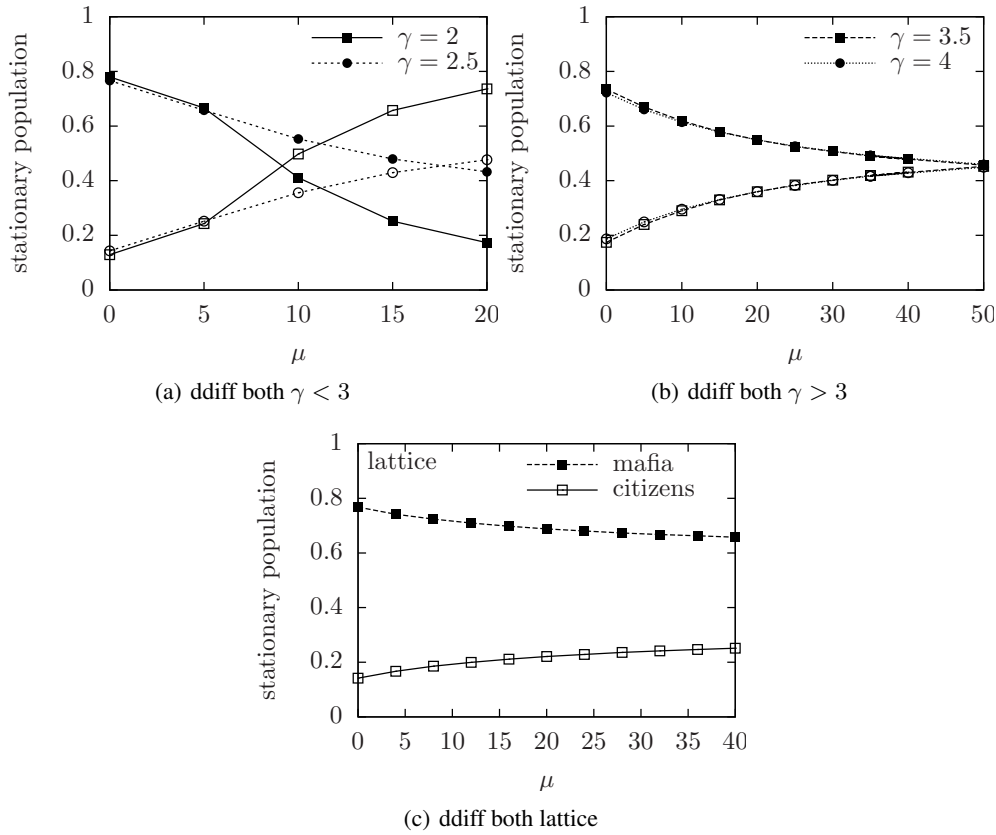


Figure 2.38: FAM: directed diffusion of both species. Stationary fraction of species as a function of mobility in different structures with increasing homogeneity: SFN with $\gamma < 3$ and $\gamma > 3$ in the top row, and the regular lattice in the bottom. The data confirm that citizens profit largely from mobility in more heterogeneous architectures and that mobility effects are identical in scale free networks with $\gamma > 3$. Full and empty symbols represent the mafia and citizen population respectively. Systems size: $N_{\text{SFN}} = 10000$, $N_{\text{latt}} = 6400$. The parameter point considered is $\sigma_m = \beta = 10$, $\sigma_c = 0$.

citizen cluster may induce strategy changes in citizens during his erratic random walk there. But the mafioso himself cannot change his strategy independent of his location. At the other side of the interface, the displaced citizen, now in a mafia sea, is very likely to become a mafioso because he cannot run away.

If a citizen diffuses he may enter a mafia's cluster. He has a good chance to avoid conversion by further diffusing. But with the diffusion process a mafioso is also passively introduced in the citizen cluster. This individual may invade the cluster before he dies. The asymmetric character of the model, in which mafiosi do not change strategy $\omega_{mc} = 0$, is the reason why mafiosi also profit from citizens' mobility. Actually citizens do not get any advantage from random diffusion.

Of course, if both species diffuse in an erratic way simultaneously mafiosi are again better off. The crucial process favouring mafiosi is the invasion of citizens' clusters by passively or actively diffusing mafiosi. More generally, undirected diffusion makes

interfaces rougher and allows individuals entering adversary's clusters. Rougher interfaces imply larger perimeters and thus a larger fraction of citizens exposed to mafia's strikes, while the invasion of clusters damages the defensive strategy of citizens to avoid the mafia attack.

2.4.3 Local mean field approximation in square lattices

In the limit of large diffusion $\mu \rightarrow \infty$ when both species randomly diffuse, the population of the structured systems is well-mixed. One would expect that the mean field approximation for the well-mixed assumption discussed in section 2.2 properly captures the dynamics of this regime. Surprisingly, this is not the case for the mafia model. The reason lies in the local character of the interactions and in particular in the discreteness of the available neighbourhoods in homogeneous structures. The frequencies c , m , and ϕ for a lattice or network's node may only take some values among a discrete set. The mean field behaviour we described at the beginning of the chapter may only emerge in models where the possible local conformations are not restricted.

For simplicity we illustrate the nature of this local dynamics on square regular lattices. In the mafia model, a given actor interacts with its four nearest neighbours simultaneously. The reaction rates ω_{cm} and ω_{mc} , which are functions of the population frequencies, cannot assume any value for structured populations. The reason is that the fractions m , c , and ϕ cannot take arbitrary values in the neighbourhood of a cell for square lattices. The available fraction of agents of every species—citizens, mafiosi, and empty places—in a cell neighbourhood are $0, 1/4, 2/4, 3/4, 1$, with the constraint $c + m + \phi = 1$. Every site has thus fifteen possible neighbourhoods, $nn_\alpha = (C_\alpha, M_\alpha, \Phi_\alpha) = (4, 0, 0), (3, 1, 0), \dots, (0, 0, 4)$, with C_α , M_α , and Φ_α the total number of individuals of each species, between 0 and 4, which fulfill $C_\alpha + M_\alpha + \Phi_\alpha = 4$ —see two possible neighbourhoods in Fig. 2.39.

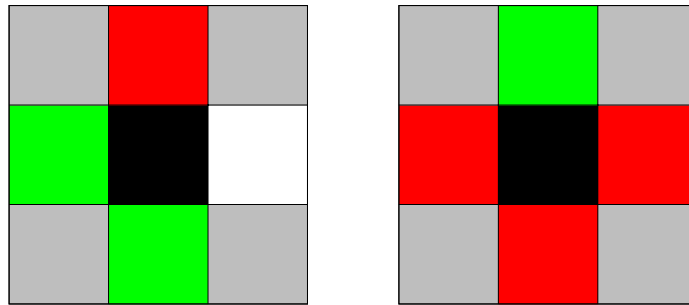


Figure 2.39: Two possible neighbourhood conformations on a square lattice of the black cell in the middle. Only the four neighbours in colour form the von Neumann neighbourhood. The specific conformations shown in these cartoons give rise to the population fractions $(c, m, \phi) = (1/2, 1/4, 1/4)$ for the left and $(c, m, \phi) = (1/4, 3/4, 0)$ for the right cartoon. These are the population fractions entering the reaction rates ω_{cm} and ω_{mc} . The colour code is: green for citizens, red for mafiosi, and white for empty places.

The interaction mechanisms of some evolutionary models as the voter or the rock-paper-scissors models effectively preserve the global fractions c , m , and ϕ . The agents

do not feel the effect of the restricted neighbourhoods in their interactions, because interactions are one-to-one. In this case the average fractions of the randomly drawn interacting pairs in a square lattice with high mobility are the same as for a well-mixed unstructured population. But since in the mafia model one agent evolves according to all its neighbours—interactions are one-to-four in the square lattice—the discrete population fractions in the neighbourhood play a crucial role.

To include the limitation imposed by the finite number of possible vicinities one substitutes the expressions for the reaction rates ω_{cm} and ω_{mc} in the differential equation (2.25). In particular, one replaces the well-mixed mean field value by a weighted expression which accounts for the fact that in a lattice one has to average over a finite set of possible local neighbourhoods:

$$\omega_{cm} = \sigma m(1 - c) \longrightarrow \sum_{\alpha} p_{\alpha} \sigma \frac{M_{\alpha}}{4} \left(1 - \frac{C_{\alpha}}{4}\right), \quad (2.48)$$

$$\omega_{mc} = \sigma c(1 - m) \longrightarrow \sum_{\alpha} p_{\alpha} \sigma \frac{C_{\alpha}}{4} \left(1 - \frac{M_{\alpha}}{4}\right). \quad (2.49)$$

The summation runs over all possible neighbourhoods α , where the probability of every neighbourhood $(C_{\alpha}, M_{\alpha}, \Phi_{\alpha})$ is given by p_{α} . As the population is well-mixed, one may assume that there are no site correlations. Therefore, the probability to have C_{α} citizens, M_{α} mafiosi, and Φ_{α} empty places is that of drawing the specific combination out of a mixed sample of different objects—typically coloured balls in the urn model without return. However, as the system size is much larger than the vicinity, $N \gg 4$, one may assume a constant probability for a selected individual to be of type i —the frequencies c , m , and ϕ —as if the process were with return. The corresponding probability for a given neighbourhood is given by the *multinomial distribution*:

$$p_{\alpha} = p(C_{\alpha}, M_{\alpha}, \Phi_{\alpha}) = \frac{(C_{\alpha} + M_{\alpha} + \Phi_{\alpha})!}{C_{\alpha}! M_{\alpha}! \Phi_{\alpha}!} c^{C_{\alpha}} m^{M_{\alpha}} \phi^{\Phi_{\alpha}}. \quad (2.50)$$

Note that in the lattice $C_{\alpha} + M_{\alpha} + \Phi_{\alpha}$ is identically 4.

For simplicity, from here on we will restrict ourselves to the fully asymmetric model to analyze in detail the lattice approximation. Introducing the neighbourhood probability in the discretized expression for the reaction rates (2.48) and this in the evolution equation for mafiosi, $\dot{m} = -m + c\omega_{cm}$, one gets a differential equation for the system dynamics on a well-mixed lattice:

$$\dot{m} = -m + c\omega_{cm} = -m + c\sigma \sum_{\alpha=1}^{15} p_{\alpha} \frac{M_{\alpha}}{4} \left(1 - \frac{C_{\alpha}}{4}\right) \quad (2.51)$$

$$= -m + c\sigma \left(\frac{1}{4}c^3m + \frac{3}{2}c^2m^2 + \frac{9}{4}cm^3 + m^4 + \frac{3}{2}c^2m\phi + \frac{9}{2}cm^2\phi + 3m^3\phi + \frac{9}{4}cm\phi^2 + 3m^2\phi^2 + m\phi^3 \right). \quad (2.52)$$

We have used the constraint $c + m + \phi = 1$ and the solution for empty places in a stationary state $\phi = 1/(1 + \beta)$. The previous equation has three solutions:

$$m^0 = 0, \quad (2.53)$$

$$m^{\pm} = \frac{(-2 - \beta - \beta^2)\sigma \pm \sqrt{(1 + \beta)^4 \sigma (\sigma - 3)}}{3\sigma(1 + \beta)^2}, \quad \in \mathbb{R} \text{ if } \sigma \geq 3. \quad (2.54)$$

At the parameter point $\sigma_{\text{sn}}^* = 3$ a saddle-node bifurcation occurs, where the number of solutions is reduced from three to one. Furthermore, a transcritical bifurcation, occurs for $\sigma_{\text{tc}}^* = 4(1 + \beta)^2 / (4\beta + \beta^2)$, where m^0 becomes unstable.

The extinction fixed point m^0 is stable for $\beta = 0$ or $\beta > 0$ and $0 \leq \sigma < \sigma_{\text{tc}}$, while the coexistence node m^+ is stable for $0 < \beta \leq 2$ and $\sigma > \sigma_{\text{tc}}$ or $\beta > 2$ and $\sigma > 3$. The third solution, the coexistence node m^- is unstable for the physically meaningful values $m^- > 0$.

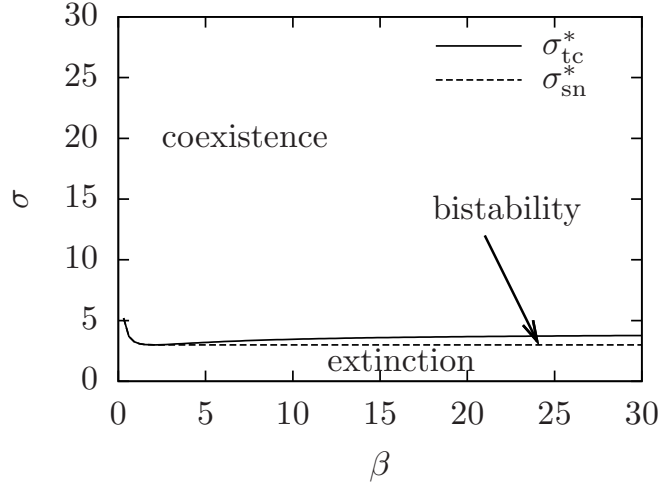


Figure 2.40: FAM: Stability diagram for the fully asymmetric model within a local mean field approximation in regular lattices. Three regimes are observed—extinction, coexistence, and bistability—as in the well-mixed mean field approach. However, the bistability region is drastically reduced with respect to the well-mixed case.

The stability diagram in Fig. 2.40 shows the stable states for a well-mixed lattice. It reveals that the bistable region is drastically reduced in favour of the coexistence regime compared to the output of the well-mixed mean field approach—see diagram 2.4. In particular, the investigated parameter point $\sigma = 7, \beta = 20$, within the bistable region in the global mean field approach, lies now in a region where coexistence is the only stable outcome. This modification of the stability landscape perfectly explains the simulated results for the lattice¹⁵ and large random diffusion ($\mu = 100$). The fixed point predicted by the lattice approximation (2.54) $(c^+, m^+) = (0.163, 0.790)$ and the one obtained with the stochastic simulations $(c, m) = (0.165, 0.787)$ are in excellent agreement.

The general solutions for the symmetric model are much complexer than those of the asymmetric model. However, the specific solutions analogous to (2.52) for the investigated parameter point $\sigma = \beta = 15$ reveal that the only stable fixed point is the extinction one $m^0 = 0, c^0 = \rho$ as confirmed by the simulations—both in a lattice and a $\gamma = 3$ network. Note that within the mean field approach this parameter point lies in a bistable region—see the stability diagram in Fig. 2.2.

¹⁵The result was also reached for a $\gamma = 3$ scale free network.

2.4.4 Fully asymmetric policed model

Finally we investigate the role of mobility in the fully asymmetric policed model. A fraction p of control elements both fight mafia and protect citizens by effectively lessening the mafia's strength $\sigma \rightarrow \sigma(1 - p)$. Citizens cannot strike the mafia back as their strength vanishes, $\sigma_c = 0$. To gain some insight in the dynamics of the policed model with mobile agents, we examine the exemplary parameter point $\sigma = \beta = 20$, $p = 0.3$. For a homogeneous initial population, $c_0 = m_0 = 1/2$, the mean field approximation predicts mafia's extinction, while the system evolves into coexistence for a $\gamma = 3$ scale free network with immobile agents.

The essential element characterizing the dynamics of the policed model on lattices and graphs is the police's attachment to the edges. It splits up the network in subregimes with two genuinely different dynamics—see discussion in section 2.3.3. Unpoliced regions exhibit the dynamics of the unpoliced asymmetric model, ruled by the growth of mafia's clusters via $\omega_{cm} = \sigma m(1 - c)$, where citizens resist only via the asymmetric birth process. In policed areas mafiosi do have a finite probability to leave the mafia proportional to the reaction rate $\omega_{mc} = \sigma p(1 - m)$ while citizens experience a smaller strength from the mafia. As a result mafiosi and citizens phase separate into unpoliced and policed areas, respectively.

In addition, the presence of control elements is innocuous for mafiosi arranged in clusters due to their self-protection, since ω_{mc} vanishes if the mafia fraction in the vicinity is $m = 1$. However, mafia's clusters in policed regions were not observed for immobile populations, because for this structures to emerge the system must undergo intermediate states with isolated mafiosi in policed areas which are rather adverse for mafiosi. Therefore, mafia has not been observed to establish in policed areas when agents are immobile.

Table 2.3 shows the characteristics of the stationary state when agents diffuse accordingly to different strategies at a rate $\mu = 100$ in a scale free graph with $\gamma = 3$. In the rest of the section we extensively discuss the mechanisms leading to these results.

FAPM for a $\gamma = 3$ SFN				
$\mu = 0$	$p_{\text{ext}} = 0, (c, m) = (0.61, 0.34)$			
$\mu = 100$	ddiff	udiff	dmig	umig
citizens	$p_{\text{ext}} = 0$ (0.82, 0.14)	$p_{\text{ext}} = 0$ (0.85, 0.11)	$p_{\text{ext}} = 0$ (0.57, 0.38)	$p_{\text{ext}} = 0$ (0.73, 0.22)
mafia	$p_{\text{ext}} = 0$ (0.47, 0.49)	$p_{\text{ext}} = 0$ (0.22, 0.74)	$p_{\text{ext}} = 0$ (0.48, 0.47)	$p_{\text{ext}} = 0$ (0.53, 0.42)
both	$p_{\text{ext}} = 0$ (0.73, 0.23)	$p_{\text{ext}} = 0$ (0.25, 0.71)	$p_{\text{ext}} = 0$ (0.50, 0.45)	$p_{\text{ext}} = 0$ (0.57, 0.38)

Table 2.3: FAPM: Results of applying different mobility strategies to a policed asymmetric model system in a $\gamma = 3$ scale free network, $N = 8000$. The mean field approximation yields extinction: $p_{\text{ext}} = 1, (c, m) = (0.95, 0)$. Parameters: $\sigma_c = 0$, $\sigma_m = \sigma_p = \beta = 20$, $p = 0.3$ for initial conditions $c_0 = 0.5, m_0 = 0.5$.

Directed mobility

Individuals profit from directed mobility in several ways: building smoother interfaces at their domains to be less susceptible to the external influence, migrating towards areas with a higher or smaller police density according to their interests, and joining clusters in unpoliced areas in the case of isolated citizens. The shape of interfaces matters for the mafia dynamics only in policed areas since otherwise $\omega_{mc} = 0$. Although both species are expected to improve their performance thanks to intelligent mobility, citizens should do in a more significant way because they profit from it in policed and unpoliced regions and unlike mafiosi by protecting born isolated citizens.

The simulations performed for systems including mobility in a scale free network support the intuition outlined above. If only one population is moving its fraction in equilibrium increases, independent of its strategy. In this case migration and diffusion yield similar results, though enhanced for the latter due to the larger number of target locations available. As expected, the profit of intelligent mobility is larger for citizens. As citizens already governed policed regions in systems with immobile agents the net consequence of mobility is that their clusters grow in unpoliced areas. Mafiosi moving intelligently cluster in policed areas to protect themselves from the police presence. On the contrary, clustering in unpoliced regions does not benefit their strategy, in spite of which, mafia's clusters also grow indirectly there due to the mafiosi fleeing from policed regimes. This turns out to be the most prominent and intriguing effect of intelligent mobility for mafiosi because the mafiosi escaping from police strike citizens in the unpoliced regions where they arrive, even though this was not the pursued goal.

These features are quantified in the top (citizens' diffusion) and middle (mafia's diffusion) graphs of Fig. 2.41 for the diffusive strategy. The left column shows the total fraction of both species and the right one some relevant neighbouring fractions for both policed and unpoliced neighbourhoods. Somebody's neighbour belongs to the first or the second fraction, respectively, depending on whether the connection between neighbours allocates or not a control element.

If both species diffuse in a directed manner, citizens often achieve a net better performance compared to the reference case without mobility¹⁶, although the stationary state subtly depends on the interplay between the parameters: strength, birth rate, and police fraction. Nevertheless, citizens are in general better off because first they profit from directed diffusion through more mechanisms and second they do both in policed and unpoliced areas—mafiosi only get advantage of intelligent diffusion actively in policed areas. Since the asymmetry of the benefit takes place in unpoliced areas, the net effect observed when both species displace intelligently is the enlargement of citizens' clusters in unpoliced regions as shown in the bottom plots of Fig. 2.41.

This scenario might be slightly altered when dealing with migration. Citizens only may access empty places, i.e. potential future citizens, and therefore migrating there leaves the global configuration unchanged. Consequently, the net benefit of migration for citizens is considerably smaller than that of diffusion.

¹⁶Other parameter points, not shown, have been checked. Although a citizen improvement is observed in the majority of the cases, some exceptions were found.

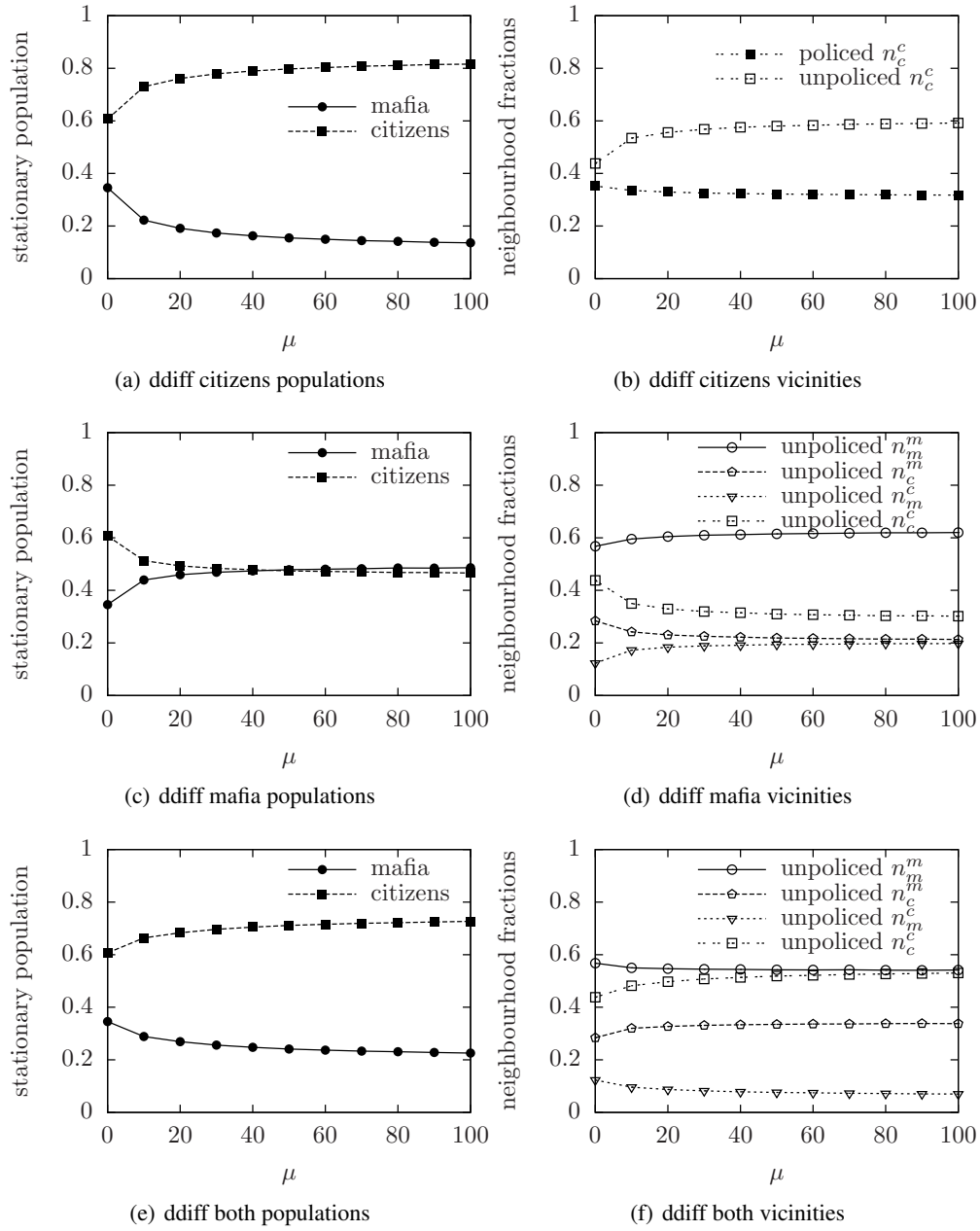


Figure 2.41: FAPM: Directed diffusion for a $\gamma = 3$ scale free network with citizens [top], mafia [middle], and both species [bottom] moving. The stationary population fractions of both species are shown in the left. The plot in the right side shows the interesting fractions n_j^i in the neighbourhood of a species i as a function of increasing mobility rates μ . These fractions are separated for the cases in which the link between two neighbours contains a control element (policed) or not (unpoliced). The investigated parameter point is $\sigma = 20$, $p = 0.3$. Initial conditions $m_0 = c_0 = 1/2$ and system size $N = 8000$.

Undirected mobility

Undirected diffusion turns out to be an unexpected brilliant offensive strategy for the mafia when they freely diffuse. The crucial scenario to modify the game lies again at clusters interfaces. Active and passive diffusion play an important role in the performance of both species as in the previous models. Remember that the principal difference between both displacements relies on the fact that passively displaced individuals must stay at new locations, where they are usually forced to change their strategy. A mafioso actively entering unpoliced clusters of citizens may invade them before he diffuses further. But even more, the passively displaced citizen will not survive in the mafia environment. When mafiosi enter policed areas they do not induce strategy changes but do not change theirs either because they very likely move further before having to take any decision about their strategy. However, still the net effect of the displaced citizens into the mafia domains makes mafia profit from the strategy.

All in all, the most surprising achievement of undirected diffusing mafiosi is that they do settle in policed areas. If they diffuse faster than they take decisions, they can hop over police walls and access citizens domains with a low concentration of control elements, but which were nevertheless inaccessible for immobile agents due to the police barrier they have to go through. Even more, if the fraction of mafiosi entering policed regions simultaneously is high enough to protect themselves from the control elements influence, they can invade policed areas which were completely forbidden for them. This behaviour has been observed in the simulations whose results are displayed in Fig. 2.42. For mobile mafiosi one observes how in unpoliced regions (central column, middle row) citizen clusters are broken, smaller n_c^c fraction, while mafia population increases as reflected by the fraction of mafiosi in citizens' vicinities, n_m^c . In policed areas (central column, bottom row) citizens' clusters also shrink, but here both mafiosi in citizens' neighbourhood n_m^c and mafia's clusters themselves n_m^m grow due to the dynamics exposed.

Unlike to the dynamics in the unpoliced asymmetric model, citizens do profit now from undirected diffusion if they are the only species diffusing. Whereas in the unpoliced model, the passively displaced mafiosi fell in innocuous unpoliced citizen domains invading them, in the policed case the displaced mafiosi may enter policed areas, where they have a big probability to change their strategy. Therefore, mafia's fraction (n_m^m) reduces in unpoliced regions while citizens' frequency increases (n_c^c, n_c^m). The active and passive random displacement of both species explicitly results in a rather mixed population in policed areas which is adverse for mafia. Consequently the fraction of citizens increases, although their clusters (n_c^c) shrink. This reduction is greatly compensated with a larger fraction of citizens around mafiosi n_c^m .

When both species diffuse in an undirected way mafia gets a larger advantage as it benefits from active and passive diffusion both in policed and unpoliced regions. As in the case of mafia's diffusion the result is a highly mixed population in unpoliced regions, which benefits invulnerable mafiosi, and the enhancement of mafia settlements in policed regions. The evolution with the mobility rate for both populations, as well as the interesting neighbouring fractions are plotted in the right column of Fig. 2.42.

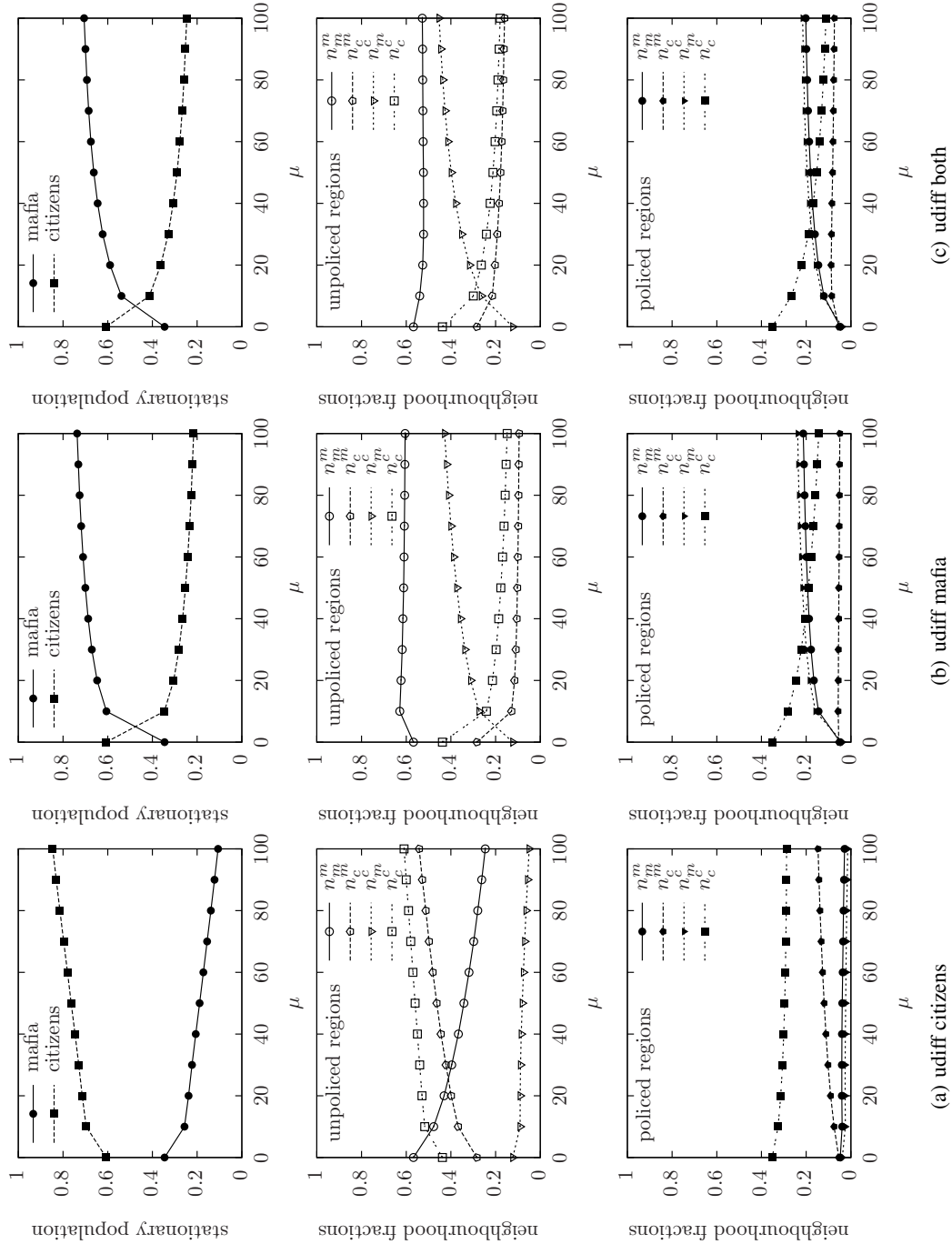


Figure 2.42: FAPM: undirected diffusion. Stationary population fraction [top], unpoliced [middle] and policed [bottom] neighbourhoods for citizens [left], mafiosi [center], and both species [right] randomly diffusing in a $\gamma = 3$ scale free network as a function of the mobility rate μ . Parameter point: $\sigma = 20$, $p = 0.3$. Initial conditions: $m_0 = c_0 = 1/2$. System size: $N = 8000$.

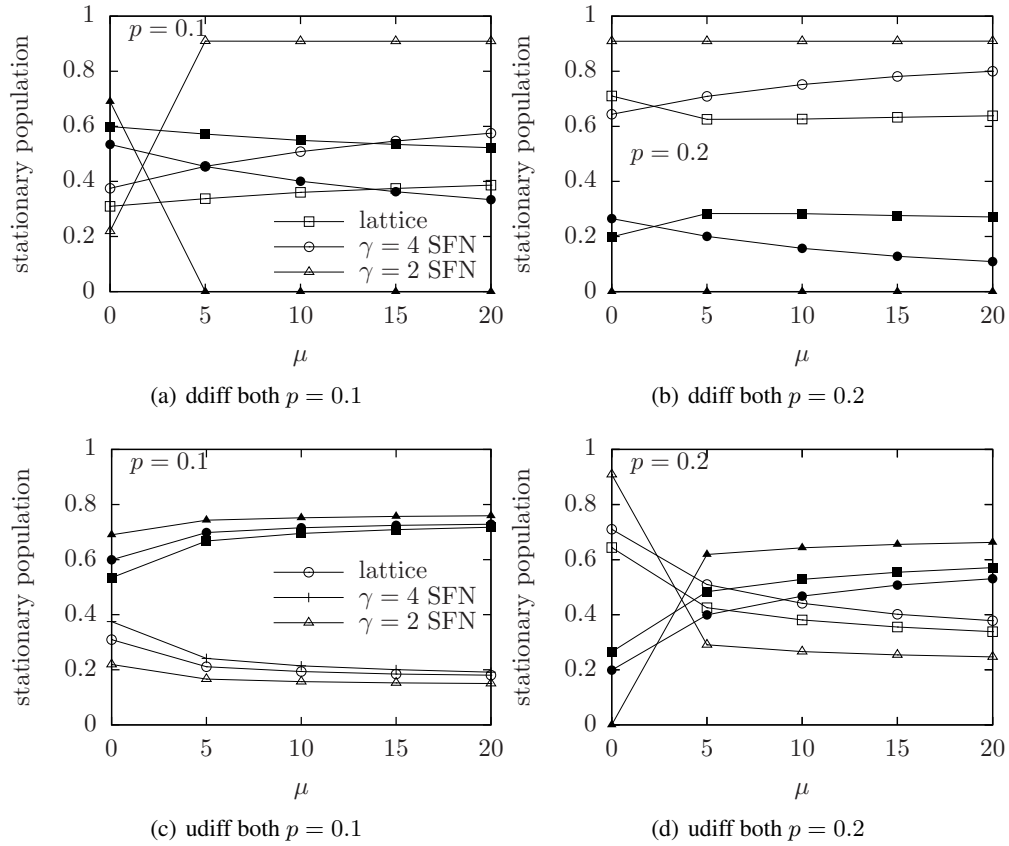


Figure 2.43: FAPM: stationary fraction of species as a function of the mobility rate for directed [top] and undirected [bottom] diffusion on a regular lattice, $\gamma = 2$ and $\gamma = 4$ scale free graphs. The more heterogeneous the structure, the larger its influence on the directed diffusion. Simulations were performed for a lattice with $N = 6400$ and networks with $N = 8000$. Two parameter points are shown $p = 0.1$ [left] and $p = 0.2$ [right] for $\sigma = \beta = 10$. Full and empty symbols represent the mafia and citizen population respectively. Initial conditions $m_0 = c_0 = 1/2$.

Finally, Fig. 2.43 displays the stationary population fractions for directed (top) and undirected (bottom) diffusion of both species in different structures. Two parameter points $p = 0.1$ and $p = 0.2$ for $\sigma = 10$ are investigated. The results of both strategies match the general highlights discussed above: citizens profit mostly from directed and mafia from undirected diffusion. Again, heterogeneous structures stress the effects of mobility. In particular, for the directed strategy, as this is a targeting displacement, the enormous difference in the average path lengths of the three structures considered demands very different mobility rates to invert the behaviour of the system.

Surprisingly, the strategy pursuing safer locations, rational, directed mobility, leads to a global worse performance for the species diffusing than undirected mobility, which turns out to be a very efficient offensive strategy.

2.5 Conclusion and outlook

In this chapter we have presented a social model for mafias ruled by a set of non-linear equations which, in spite of its apparent simplicity, gives rise to a rich phase diagram and adequately describes a great variety of plausible situations in social dilemmas. We have identified the attenuation of the persuasiveness of the adversary as the key element in providing the model with a simple regulating mechanism. Such attenuation is due to the support offered by alike individuals and the external control elements proportional to their fractions. In addition, we have shown that coexistence of both social groups or extinction of the mafia critically depends on the parameters' regime (birth rate and strength of the groups). In particular, we have investigated three instances of the model: the symmetric model, in which mafiosi and citizens have the same strength; the asymmetric model, in which citizens have no strength to persuade mafiosi to leave the mafia; and the policed asymmetric model, in which control elements persuade mafiosi to become citizens and protect simultaneously citizens from the mafia pressure. We have explicitly identified threshold strengths and critical initial conditions leading to both extinction of the mafia and coexistence of species for the three cases.

The dynamics of the model in spatially and topologically structured societies drastically differs from that predicted by a well-mixed assumption, in which individuals interact all-to-all. This is a consequence of the local character of interactions. Indeed, we have shown how the emergent phase diagrams in structured societies present a radically different picture. In general terms, the more homogeneous the underlying structure is—the extreme case being the regular lattice—the larger is the deviation with respect to the well-mixed mean field approximation. Special mechanisms emerge in lattices and networks since each individual's behaviour is determined by the composition of the population in its immediate vicinity. This is made up of the von Neumann neighbourhood in square lattices and of the k sites connected to each node in networks. This locality of interactions allows even small fractions of a given species to survive in structured societies by clustering. In addition, the presence of control elements may split up the social structure in unconnected subnetworks ruled by different dynamics. We have presented explicit cases of transitions from coexistence to extinction as a function of the heterogeneity of the underlying scale free network.

Our investigation on the role of mobility fills an important gap in the literature on social modelling by enabling a clearer interpretation of its influence in the description of social conflicts. We have found that while simple migration to empty places has an almost negligible influence, diffusion—which also takes into account interchanges of locations among individuals—may strongly affect the system's behaviour. If only one species diffuses, directed diffusion allows mobile agents to seek safer positions and increases their population's fraction in equilibrium. This enhancement strongly depends on the heterogeneity of the underlying network, in particular on its average path length, which in turn is determined by the structure's topology. The most surprising implications of mobility, however, arise in the case of undirected diffusion. Undirected diffusion enables individuals to enter areas of the network which would be otherwise forbidden in rational scenarios. It turns out to be an excellent strategy in the quest for domination. If only one species is actively diffusing, the role of passive diffusion is decisive: defenseless immobile agents passively swap their locations with actively diffusing individuals. Since the immobile species enter domains which are usually

adverse to them and from which they cannot escape, the mobile agents dominate the local environment thanks to this indirect mechanism.

To the best of our knowledge the social models reported in the literature have dealt with well-mixed populations in topological and spatial structures under the mean field assumption of agents interacting all-to-all. However, such an approach is unsuited to capture crucial aspects of the dynamics of social systems. In our work, we have learned that even for high mobilities in which the resulting population is well mixed, the equilibrium state differs from the mean field prediction. The discreteness of the possible neighbourhoods forces population fractions to take discrete values among a finite set of available configurations. This constraint invalidates the all-to-all interaction assumption. To overcome this limitation in the case of square lattices, we introduce a local mean field theory which accounts for the discrete set of available neighbourhoods and their corresponding probabilities. The characterization of the system resulting from this local approach is in excellent agreement with the agent-based simulations performed in two-dimensional lattices. This success does not depend on particular properties of the mafia model explored here but portrays a fundamental understanding of the constraints which spatial and topological structures impose on the dynamics of evolutionary systems where interactions of many agents are present. Our approach has a broad range of applications. For example, it may lead to a better understanding of paradigmatic models in game theory such as the prisoner dilemma.

One possible direction for further work is to ask whether locating one of the species at hubs, be it via an initial distribution or target mobility, qualitatively modifies the stationary state of the system. As another interesting feature of actual social systems one could think of studying the effect of a tunable interaction, e.g. in a (geometrical) distance-dependent manner. In our view, however, the most compelling extension consists in considering adaptive networks. In fact, in real societies the network of contacts of every individual updates in the course of time. One could consider several possible mechanisms to account for this fact: networks with a fixed number of nodes and edges, where edges may be rewired; graphs with a fixed number of nodes, but a variable number of edges which may additionally be rewired; or even networks which may grow by attaching new nodes.

Chapter 3

Pattern diversity in self-assembled monolayers

La perfection est atteinte, non pas
lorsqu'il n'y a plus rien à ajouter,
mais lorsqu'il n'y a plus rien à retirer.

ANTOINE DE SAINT-EXUPÉRY

Molecular building blocks have been observed to self-assemble in supralayers¹ displaying intriguing patterns which may be engineered to pursue specific functionalities. In particular, these systems open promising routes in the manufacture of patterned nano-devices. However, the principles leading to self-assembly which enable better control of these systems have not been yet fully understood. Motivated by this fact, we investigate in this chapter the mechanism of self-assembly from a theoretical point of view. The goal of this work is to provide generalized means to model self-organization of supramolecular constituents based on very few universal principles. By designing suitable models one should gain sufficient predictive power which facilitates the engineering of experimental systems.

The chapter is structured as follows: First, we summarize the well-known features which give rise to the emergence of monolayers from the perspective of supramolecular chemistry and describe the specific characteristics of Fréchet dendrons as constituents. We then review the theoretical studies with the focus on understanding order in two dimensional systems. After that, we describe the experiments carried out by Bianca Hermann's group at the LMU München for a model system with Fréchet dendrons as building blocks. Then, we introduce a simplified interaction-site model which aims to condense the salient features to understand the self-assembly process for this particular experimental setup. We discuss in detail the predictions obtained by Monte Carlo simulations within our theoretical approach and compare them with the experimental findings.

¹Throughout this chapter we speak interchangeably of monolayers or supralayers, as they assembled following the principles of supramolecular chemistry, referring both terms to the films obtained by the organization of single building blocks.

3.1 Self-assembly and order in two dimensional systems

3.1.1 The principles of self-assembly of monolayers

The constant improvement in techniques to produce smaller and smaller functional nanodevices is reaching fundamental limits [14]. Most of them used a so-called *top-down* approach, where very precise external techniques are used to shape and pattern materials mostly within the framework of photolithography. In the past years, however, much cheaper *bottom-up* methods arise as a very good alternative to manufacture nanotechnology. They are based on built-up assemblies from individual constituents, be they atoms or molecules, which arrange on top of atomic substrates.

In particular, the fabrication of artificial nanosystems mimicking the principles of self-organization in biology such as the assembly of virus capsules [145] or DNA [3, 121] is a promising route to go beyond lithography. Self-organization and assembly of molecules or atoms offer a powerful mechanism to get an ample diversity of ordered systems in the nanoscale regime [14]. They provide not only access to smaller length scales than other methods, but also facilitate the fabrication.

Supramolecular chemistry is the field which describes the chemistry of the non-covalent bond. It includes the assembly of supramolecular structures thanks to the recognition of molecular building blocks via weak interactions. The most common interactions involved in supramolecular processes are hydrogen bonding, metal coordination, hydrophobic and van der Waals forces, π and electrostatic interactions. They operate in the nanometer scale suitable to engineer nanotechnology. This field, which emerged in the last years of the 19th century, is essential to understand the origin of life as it describes the assembly of proteins, DNA, or viruses among others. But it also greatly contributed in the last decades to the development of functional nano systems.

Self-organization of macromolecules might thus represent the future of nanoelectronic devices production because it offers important advantages with respect to other methods. First, patterns with very small length scales may be accomplished. Second, it does not demand the use of expensive techniques and instruments in the manufacturing process, since it is based on self-organization growth phenomena which take place spontaneously at room temperature. Last and even more important, the power of chemical synthesis ensures access to a vast functional and structural diversity of building blocks which may be steered to forge any desired suprastructure.

Many organic molecules on top of well-defined atomic structures—more generally decorated substrates—have been observed to self-organize or self-assemble in two-dimensional supralayers which display regular ordered patterns. The gain in internal energy after the ordering process must compensate the loss of entropy in the ordered phases. By self-assembly one understands the spontaneous formation of perfectly ordered patterns with a fixed attachment to the substrate, which are stable in equilibrium. The emergent supralayers may also be self-organized. In this case ordered structures emerge temporally, far from thermodynamic equilibrium, as the result of the interplay between molecular interactions and diffusion processes. The monolayers then exhibit dynamic patterns that change in time into one another [13].

The self-assembly of supramolecular monolayers is based on the adsorption, mobility, and lateral interactions of the macromolecular units [13]. First, the building blocks couple to the atomic decorated surface of the underlying substrate. They can

then diffuse to adjacent sites, rarely even hop, and rotate to search favourable configurations. Finally, the lateral interactions, be they direct through molecular recognition among groups or indirect via substrate-mediated interactions, guarantee the final conformation of the ordered supralayer.

In order to let the molecules have enough time to explore the potential energy of the adsorbing surface and achieve a growth close to equilibrium conditions the ratio between the diffusion and deposition rates of molecules must be rather large. Slow deposition leads mostly to stable structures because the system reaches configurations which are minima of the free energy. On the contrary, a fast deposition does not leave molecules enough time to explore all possibilities. The growth is mainly kinetically driven yielding metastable structures [80].

The building blocks used in the assembly are rather malleable structures whose cores, predominantly made of aromatic elements, display regular polygonal shapes. Chains or functional groups are attached to the cores giving the molecule a highly ramified structure. The branched character promotes interdigitation of the blocks to enhance the stability of the emerging structures. Additionally, the shape of the molecular core must fit the decoration of the underlying substrate, which strongly conditions the packing fraction and the ordering motifs. Planar molecules exhibiting extended π -systems are specially suitable to build up functional monolayers, because they bond to the atomic surface in a flat-lying structure and let their periphery free to interact with each other.

The molecular units should exhibit good solubility and synthetic versatility. They preferably have well-differentiated regions responsible for the interactions and functions involved in the assembly. Functional groups and even external molecules can be attached to many organic macromolecules or included in the cavities they form. Blocks showing this adaptability are suitable units to address functionalization issues.

When molecules in solution are casted on top of substrates such as gold, copper, or graphite, which exhibit regular lattice arrangements, they organize in peculiar long-range ordered patterns. Four interactions are involved in the dynamical self-assembly: molecule-molecule, molecule-substrate, molecule-solvent, and solvent-substrate. The intermolecular interactions are mainly due to hydrogen bonds [120], van der Waals interactions [116], or metal coordination [77, 108]. The stronger bonds built by metal coordination give rise to more robust patterns at the same time as tailoring the metallic groups might increase the scope of possible applications of the assembled supralayer.

Van der Waals interactions with the chains of the building units or π -interactions with their cores are the key factors for the molecule-substrate interaction. Lengthening the molecular chains strengthens these interactions [116]. The molecular conformations, the mobility of the building blocks, and the supramolecular coordination are restricted due to the coupling with the substrate [77]. In some experiments the substrate-molecule interaction is even thought to induce a long-range repulsion between molecules—though not fully understood yet—which gives rise to unusual large voids or pores in the ordered patterns, much larger than the length scales of the molecule [108]. A brief overview over the energy and length scales for the various interactions is shown in table 3.1.

Solvents could play an important role in self-organizing systems. First, they may directly interact with the molecules or partially screen some of the other interactions. Strong interactions of the solvent with the substrate or the formation of layers are in

interaction	energy scale [eV]	interaction range
adsorption	0.5-10	1.5-3 Å
substrate mediated	0.001-0.1	nm
hydrogen bonds	0.05 -0.7	1.5-3.5 Å
van der Waals	0.02-0.1	< 1 nm
electrostatic ionic	0.05-2.5	long range
metal ligands	0.5-2	1.5-2.5 Å

Table 3.1: Energy scale and interaction range for some interactions involved in the assembly of monolayers [13].

general excluded. However, it could be coadsorbed in the voids of some patterns and restrict the mobility of the supramolecules during their dynamical organization.

Transitions between different patterns have been observed in many experimental settings. Several arguments might explain this phenomenon depending on the specific nature of model system investigated. First, as the emerging supralayers are often local minima of the internal energy, transitions between metastable states are easily driven with thermal activation energy. The heat due to the interaction with the measurement devices might be enough to overcome small potential barriers. Second, in systems which self-organize—as opposed to self-assembled systems—initial patterns are thought to be kinetically favourable, while the final phases are supposed to be thermodynamically stable [116]. Last but not least, the evaporation or readsorption of the solvent is thought to play a role in possible reorganizations of the system as it might vary the local interactions.

3.1.2 Fréchet dendrons as building blocks

Fréchet dendrons or dendrimers belong to a group of dendritic molecules whose name comes from the greek $\delta\epsilon\nu\delta\rho\nu$ which means tree, as they are very ramified and highly symmetric molecules. Dendrons were first synthesized by Tomalia [134] and Newkome [97] in the 1980's. Molecules were built via divergent synthesis in these first attempts, i.e. starting at the core and radially adding monomers to the exterior. Fréchet in 1990 was the first who synthesized dendrons via convergent synthesis [57, 58], i.e. from the external layers into the core, which is supposed to be more efficient. Dendrons have since attracted much interest because of their special properties to produce many functional structures [47].

Dendrimers are globular, monodisperse molecules—the constituent monomers are a collection of objects with similar masses—in which branches made of repeated units stemming from a central point conform regular patterns. They are very versatile molecules with a high degree of adaptability: variable volume in solution, multivalent periphery, controlled size, or tailored intramolecular dynamics—and consequently conformation—among others. Dendrons may be prepared in energetically stable conformations which exhibit the required features to accomplish specific goals.

Fréchet dendrons constitute suitable building blocks to assemble supralayers as they show all the aspects desired to supply appealing model systems. Their branched

and regular shape promotes the formation of many different ordered motifs. In addition, as they are easily adaptable they offer promising perspectives to look for new and specific patterns. Their symmetric cores made of aromatic rings, polygonal objects which are responsible for the basic unit of the ordered motif, firmly attach to the substrate via π -interactions. This guarantees planar conformations of the molecule which favours the formation of stable monolayers. It is thought that dendrons which optimize self-organization are rich in aromatic rings [61]. Arbitrary long carbonated chains strengthen the interaction with the substrate and account for the intermolecular interactions. Furthermore, as they are very flexible, an ample landscape of interdigitated patterns is available. Functional groups are easily attachable to the rings of dendrons. Supralayers may thus be prepared to serve specific goals at the same time as interactions between functional groups guarantee more stable structures. Since specific parts of the dendrons are responsible for various tasks, the building units are especially suitable for the target they are designed for.

Because they are very flexible, floppy objects dendrons may form cavities in solution. Possible solvent particles may then easily penetrate them, though dendrimers usually rearrange and lose their volume when the solvent evaporates.

3.1.3 Understanding order in two dimensional systems

Not much theoretical work has been reported to model self-assembly in macromolecular systems. Heuristic arguments have been given in terms of the shape of the building blocks [83] or the energy of the adsorbed molecules. Many studies have successfully computed energies and conformations of the assembled structures with the help of molecular mechanics (MM) and density functional theory (DFT) software [144, 109, 119, 67, 52, 123]. The minimization methods used for this purpose require the experimental observations as inputs. Given that these methods take into account all chemical and physical details involved in the investigated systems, one cannot identify the salient features in the assembly process. Some recent studies have combined Monte Carlo methods with input coming from MM or DFT simulations to explain concrete aspects of assembly processes such as the multilayer growth of molecules with a fixed conformation [56] or the formation of ordered domains in monolayers [132, 124].

However, order in two dimensions has been thoroughly investigated for systems of different nature. These studies focus on the characterization of melting transitions taking place in colloidal suspensions subject to external fields—see [1] for a review. These model systems resemble particularly good atomic systems on top of decorated substrates such as graphite layers, for instance. The patterns of atomic layers are well reproduced among other mechanisms with laser beams, a method which was pioneered by Chowdhury et al. in 1985 [31]. Ordering processes are the result of the interplay between the interactions amongst the colloids and those with the external field.

In colloidal systems one can modify the potential by changing the angle, intensity, or number of lasers. The interactions among colloids may be easily screened by tuning the salt concentration of the solvent. The filling factor may also be adjusted controlling the number of colloidal particles in the sample. In this way one can artificially build more complex objects, as dimers or trimers, which show a collective dynamics in laser fields [19, 23]. Many experiments have been performed to investigate the ordering transitions taking place in two dimensional systems [112, 113, 114].

Semi phenomenological models have been developed to gain some understanding in these phenomena. They consider colloids as single particles or composite objects, in the case of dimers and trimers, which interact amongst them in a potential accounting for the external laser field. Composites are located at the sites of lattices with different geometries and the colloidal interactions are accounted for by suitable hamiltonians. Monte Carlo simulations and analytical solutions yield a full characterization of the ordered phases and their melting transitions [142, 141].

Another approach to predict the ordered phases observed in colloidal systems has been addressed by Kahl et al. in which genetic algorithms explore the ground states of colloidal systems [53, 44]. This algorithm computes the most energetically favourable configuration for unit cells with various numbers of colloids which interact with each other under the influence of an external potential. Although the method successfully predicts an ample variety of ground states, it is not able to provide any analysis of the stability of the phases nor to identify possible transitions and their nature.

Our goal is thus to lay out a theoretical model which provides some insight in understanding the crucial features of self-assembly. The model must be able to predict emergent ordered structures independently of the experimental observations and to identify the stability regimes as well as the corresponding transitions.

3.2 Experimental observations

Bianca Hermann and her coworkers at the LMU München have imaged a model system by scanning tunneling microscopy (STM) in which Fréchet dendrons on top of graphite substrates self-assemble in complex supralayers which exhibit various ordered patterns [61, 34]. The second generation Fréchet dendrons used in this experiment are flexible building blocks, which consist of three phenyl-rings symmetrically disposed in the vertices of a triangle with two alcoxichains attached at the lateral rings. The alcoxichains are made of carbon units exhibiting van der Waals and hydrogen bonds. The length of these chains is easily adjustable and has been systematically varied at one side of the molecule from four, to eight, to twelve carbon atoms, while the other side remains with chains of eight carbon units—see the structural formula in Fig. 3.1.

Monolayers have been prepared by casting small droplets of a dilute solution of dendrons in various solvents—ethanol, hexane, or heptadecane—on top of decorated substrates, namely highly oriented pyrolytic graphite surfaces at room temperature. The monolayers are assembled in a dry environment after a quickly evaporation of the solvent². The graphite substrate shows a honey-comb like decoration which displays a six-fold rotational symmetry.

Hermann and collaborators have observed up to eight general ordering motifs for the three molecules investigated. The sawtooth, honeycomb, jigsaw, and tiretrack motifs displayed in Fig. 3.2 dominate the emerging monolayers for the 8/8 and 8/12 molecules. In particular for 8/12 dendrons in the hexane solution, the honeycomb pattern emerges minutes after casting the sample. Half an hour later the four main motifs coexist with ratios 1%:15%:25%:20% for sawtooth:honeycomb:jigsaw:tiretrack in

²The sample is slightly cooled down because of the evaporation and then heated up due to the STM measurements. These differences in the temperature are thought to be responsible for the observed dynamic reconfiguration between the patterns.

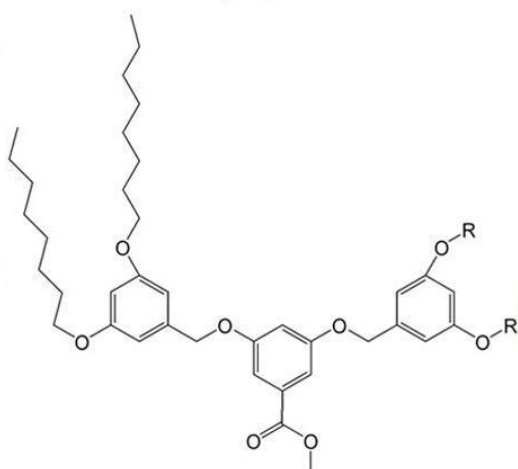


Figure 3.1: Chemical configuration of the Fréchet dendrons used in Hermann's experiment. Three possible radicals have been systematically attached to the right side with four ($R = C_4H_9$), eight ($R = C_8H_{17}$), and twelve ($R = C_{12}H_{25}$) carbon units which represent what we call the 4/8, 8/8, and 8/12 molecules. The chains of the other side have eight carbon atoms in all cases. Image courtesy of Hermann.

domains of typically $20 \text{ nm} \times 20 \text{ nm}$, leaving 39% of the surface covered with other patterns and domain boundaries. Finally, after some hours the system evolves to a configuration in which 60% of the graphite surface is covered with the tiretrack pattern, which has been identified to be thermodynamically stable by slowly heating.

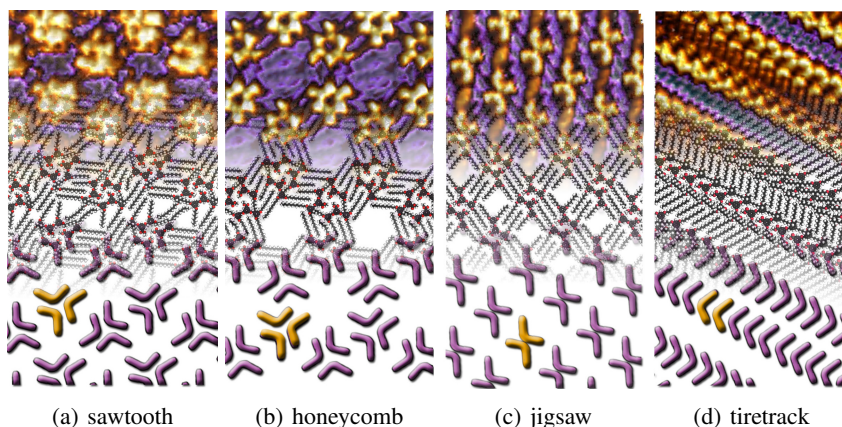


Figure 3.2: Four main experimental patterns observed in the assembled monolayers for the 8/8 and 8/12 Fréchet dendrons. STM images on the top, MM energy-minimized configurations in the middle, and schematic main motif in the bottom. Courtesy of Hermann.

Both chiralities of the molecule have been found to coexist giving rise to domains with different orientations.

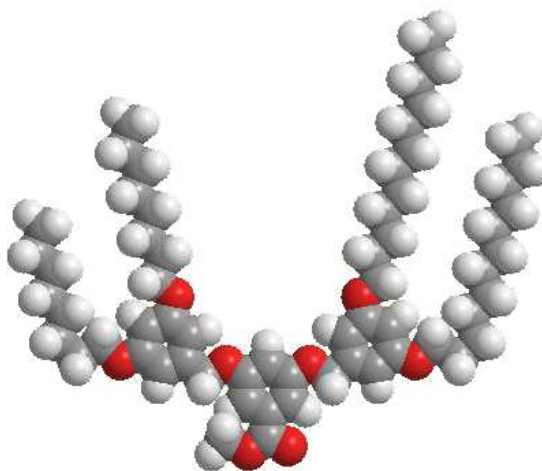
Because of the weak character of the interactions involved in the self organization, be they intermolecular or substrate-molecule π -interactions, the ordered motifs represent local minima with similar values of the internal energy. Low activation energies—believed to be of thermal origin—suffice to overcome the potential barriers between the rather similar minima of the energy. This explains the dynamic reconfiguration of

the pattern in the assembled monolayers as have been observed in the experiments.

The aromatic rings of the dendrons used in this experiment are able to follow the graphite structure exceptionally well providing robust, energetically favourable substrate-molecule π -interactions. They determine the long-range order and the basic motif of the pattern. The coupling to the substrate is enhanced by van der Waals interactions of the carbonated chains with the graphite surface. In addition, the intermolecular interactions of the lateral arms of adjacent molecules are responsible for the formation of interdigitated patterns which stabilize the emergent structures. The interplay between the commensurability of the molecular rings with the graphite substrate and the chain interdigitation determines, ultimately, the optimal regular motif for the assembled supralayer.

A detailed analysis of the STM images provides suitable initial configurations for the molecular mechanics (MM) simulations carried out by Hermann's group. These simulations reveal the exact positions of the individual molecules and their conformations, as well as the interaction energies involved via energy minimization of the initial patterns on a double layer of graphite substrate—for the atomistic picture see Fig. 3.3. We will use the molecular conformations yielded by this minimization to construct the inputs for our theoretical *interaction-site* model. In addition, the energy-minimized geometries also serve as input for density functional theory (DFT) computations to derive the local density of states of free single molecules.

Figure 3.3: Molecular conformation in an atomistic picture of a 8/12 Fréchet dendron given by the energy minimization of the molecular mechanics simulation. Two chains of eight and twelve carbons are attached to the left and right aromatic ring respectively. Functional groups are represented in red. Image courtesy of Hermann.



The MM minimization provides information about the dominant parts of the internal energy due to van der Waals interactions. It allows the computation of the adsorption energy per unit cell or area by evaluating the energies of a monolayer on top of the graphite substrate i_{sup} , of a gas phase net³ i_{gn} with n molecules per unit cell, and of an isolated molecule i_{iso} . The subtraction $I_{c-n-c} = i_{\text{gn}}/n - i_{\text{iso}}$ gives the energy between neighbouring chains per molecule while $I_{m-s} = (i_{\text{gn}} - i_{\text{sup}})/n$ is the molecule-substrate interaction per molecule. The pattern which emerges at the early stages of the experiment, the honeycomb motif, minimizes the van der Waals part of the energy per molecule in a phase where the building blocks are mainly found isolated. In the

³A gas phase net is a monolayer showing long-range order but without any underlying structure. The intermolecular interactions are essentially the same, while the molecular-substrate interactions are switched off.

course of time, the system evolves according to the *Kitaigorodskii principle* [66] of avoiding free space to the tiretrack pattern which minimizes the energy per area. In this later stage the majority of the surface is covered with ordered domains. The tiretrack pattern is also the phase which has been found to be thermodynamically stable.

pattern	molecules/unit cell	I_{m-s} /molecule	I_{c-n-c} /molecule
sawtooth	6	-674	-147
honeycomb	6	-691	-163
jigsaw	2	-653	-117
tiretrack	2	-528	-222
pattern	unit cell size [nm ²]	I_{m-s} /nm ²	I_{c-n-c} /nm ²
sawtooth	24.5	-167	-38
honeycomb	26.5	-155	-38
jigsaw	8.4	-151	-25
tiretrack	6.1	-172	-75

Table 3.2: Van der Waals part of the molecule-substrate and interchain energies given by the MM minimization per molecule and per area. Energies are given in kJ/mol.

3.3 Theoretical model

In this section we introduce an interaction-site model to investigate the pattern formation in self-organized monolayers. The model is based on very few universal principles of self-assembly. We study the system's behaviour with Monte Carlo simulated annealing and investigate the stability of the phases found. In particular, we outline a stability diagram for the various ordering motifs as a function of the density of the sample and the temperature and study the zero temperature energy of the stable phases. Finally, we compare the results of our model with the experimental observations carried out by Hermann and coworkers and discuss the validity of our model.

3.3.1 The interaction-site model

Interaction-site models are simplified abstractions of real physical processes. They aim to isolate the minimal number of salient features needed to understand and reproduce the physics behind specific phenomena. The numerous microscopic forces are drastically reduced to the interactions between some selected *interaction points*. The complexity to conceive an interaction-site model lies precisely in the recognition of appropriate points where the interactions take place and the identification of the forces relevant for the dynamics and those which are negligible.

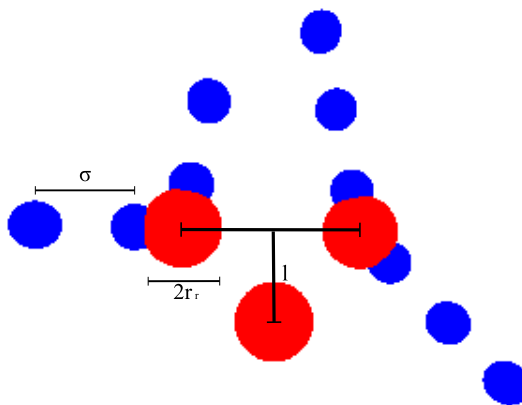
In this section we outline the design of a suitable interaction-site model to describe the assembly of Fréchet dendrons monolayers. Fréchet dendrons are very flexible structures with many degrees of freedom. The number of possible conformations between pairs of interacting atoms is hence so large that an atomistic description is almost impossible. This limitation explains the lack of theoretical models to understand such macromolecular processes.

According to the experimental observations the crucial features leading the self-assembly are the steric repulsion between the molecular rings, the weak interactions of the carbonated chains, and the coupling of the building blocks with the substrate.

The symmetric molecular core in our model consists of three *hard spheres* located at the vertices of a flattened isosceles triangle—red spheres in the cartoon of Fig. 3.4. At the center of the longer, unequal side of the triangle resides what we refer to as the *molecular centre*—though it is not the centre of mass due to the arm’s asymmetry—around which the molecule is allowed to rotate. The centers of the three spheres are at a distance $l = 6.1 \text{ \AA}$ from the molecular centre. The spheres of radius $r_r = 2.6 \text{ \AA}$ represent the aromatic rings of the Fréchet dendrons. They interact as hard spheres with the rings of other molecules.

The carbonated chains of the real molecules are modelled as a reduced number of inter-penetrable beads. Every four CH_2 units of the actual alcoxychain are coarse-grained as one bead with diameter $\sigma = 6 \text{ \AA}$ —small, blue spheres⁴ in Fig. 3.4. Although this simplification does not allow to model chains of arbitrary lengths, still enough tuning is possible for the purposes of this work. Every bead in a molecular chain interacts with all other beads in the chains of other molecules. The spheres are disposed in straight, rigid arms where their centers are separated a distance σ —contiguous beads are adjacent. They do not have any degree of freedom other than the orientation of the straight segment with respect to the molecular core.

Figure 3.4: Interaction-site model—the cartoon represents a 8/12 Fréchet dendron. Red spheres account for aromatic rings and blue beads represent subunits in the carbonated chains. Every sphere stands for four CH_2 units in the arms of the dendrons.



All the geometrical features of the coarse-grained molecule are extracted from the conformations yielded by the molecular mechanics simulations performed in Hermann’s group, Fig. 3.3. The relevant length scales of the Fréchet dendrons range approximately from 15 \AA of the skeleton to 50 \AA for the spanned molecule. The tunable parameters of the molecule, i.e. the radii of the hard spheres and beads, the relative positions of the hard spheres, and the lengths (number of beads) and orientations of the arms take fixed values in our simulations. We will explore various conformations of the molecules, varying the lengths of the arms and their orientations.

To account for the actual non-covalent microscopic forces leading to self-assembly the model considers a subset of essential interactions between the key points defined

⁴ A particularity affects the representation of the beads in the arms in the cartoon of Fig. 3.4: to better identify global patterns they are displayed smaller as they actually are. But of course the size of the beads entering the interactions in our simulations is that coming from the molecular mechanics simulations.

above, lying in the centers of hard spheres and beads. The strength and shape of these *coarse-grained* interactions are accordingly modified.

We encode the strong steric repulsion between the aromatic rings as hard spheres repulsion between the three central spheres of different molecules. This prevents the cores of the molecules from overlapping. The steric repulsion is also the major responsible for the long range order in the structure, as it determines together with the lattice constant the local motif, i.e. the repeated basic subunit. Finally, the weak, short-ranged van der Waals attraction of the lateral chains is described by a Lennard–Jones potential: $V(r) = 4\epsilon \left((\sigma/r)^{12} - (\sigma/r)^6 \right)$. The diameter of the beads in the chains σ is the relevant length scale of the interaction. When the distance between two beads in different molecules r is smaller than σ the potential becomes repulsive. Only chains in different molecules interact with each other.

The atomically flat graphite surface with its six-fold rotational symmetry constitutes a template for the pattern formation. It enables six energetically equivalent orientations of the molecule on its surface. The molecule-substrate attraction is mainly mediated by π -interactions between the phenyl-rings and the graphite surface. This interaction is about ten times larger than the intermolecular one, so that considering the molecules to be attached to the lattice sites is a reasonable assumption. In addition, the size of the spanned molecule of around 45 Å is up to six times larger than the lattice constant of a few Å. Therefore, only the symmetry of the underlying substrate plays a role in the monolayer assembly. We consider then molecules whose centres are attached to the vertices of a coarse-grained, fully occupied triangular lattice whose lattice constant a is comparable to the size of the building blocks and which shows the same symmetry as the original graphite honey-comb structure.

Molecules may discretely rotate as rigid bodies around their centers and adopt one of the six preferred orientations given by the six-fold symmetry of the underlying graphite.

To summarize, the interaction-site model accomplishes a significant reduction of degrees of freedom setting the flexibility of the molecule aside. While the molecular mechanics model contains about hundreds of atoms per molecule able to independently displace and rotate, the coarse-grained interaction-site model consists of a rigid object with no others degrees of freedom than the rotation around its center.

We investigate the system from a starting point in which one considers individual molecules as rigid entities and focus on the intermolecular interactions, relevant for the assembly of stable supralayers. We are not interested in the intramolecular forces which determine the configuration of individual molecules. Instead we assume the molecular conformations entering our model to already be energetically favourable. We can proceed in this way because we are considering conformations resulting from the energy minimization carried out in the molecular mechanics simulations.

3.3.2 Theoretically predicted ordered motifs

The final purpose of our investigation is to gain predictive power for the regular patterns emerging in the spontaneously assembled supralayers. In particular, we want to determine the stability of the long-range ordered assemblies, as well as the temperature regime at which they melt into a disordered phase.

To address this issue we use the simplified interaction-site model introduced above. Dendrons with fixed molecular conformations, i.e. rings' positions, arms' lengths, and arms' orientations α_i (see Fig. 3.5) are disposed in the vertices of a triangular lattice whose lattice constant a adopts values similar to the typical length scales of the molecules—the dimensionless lattice constant a/σ ranges from 2.8 to 4.2. Given that there are two molecules per triangular cell of side a the density of the sample in terms of the lattice constant reads $\rho = 2/\sqrt{3}a^2$. The systems we study contain from some hundreds to a few thousands molecules, sizes similar to those investigated in the experiments—a molecule covers a surface of approximately 4 nm^2 and the samples observed occupy some hundred nm^2 .

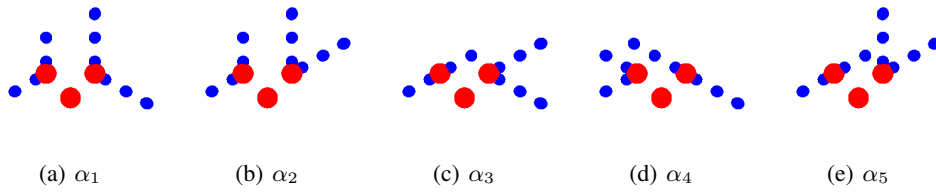


Figure 3.5: Molecular conformations showing different orientations of the lateral straight arms. The angles of the arms with respect to the positive x -axis are given clockwise from the left to the right: $\alpha_1 = (-5\pi/6, \pi/2, \pi/2, -\pi/6)$, $\alpha_2 = (-5\pi/6, \pi/2, \pi/2, \pi/6)$, $\alpha_3 = (-5\pi/6, \pi/6, \pi/6, -\pi/6)$, $\alpha_4 = (-5\pi/6, 5\pi/6, 5\pi/6, -\pi/6)$, $\alpha_5 = (-5\pi/6, \pi/6, \pi/2, \pi/6)$.

The molecular blocks in our model interact via Lennard-Jones potentials through which their carbonated chains are attracted to each other while their centers are fixed to the lattice sites to emulate the strong substrate-molecule interaction.

To investigate the system behaviour we carry out Monte Carlo simulations [48, 76, 18]. Monte Carlo is a well-known method which consists of approaching equilibrium by means which do not correspond to the actual temporal evolution of the system. Instead, Monte Carlo methods effectively sample the important points of the configuration space so that the system successively evolves through a set of states by accepting or rejecting new configurations. From a given state the system may access neighbouring configurations, meaning, that they can be obtained by introducing some allowed changes in the old configuration. The power of Monte Carlo resides in the fact that all configuration changes are possible, as it does not care for the dynamics in the system's evolution through the configuration space. New configurations which lower the internal energy of the system are systematically accepted, but also those with a larger energy may be accepted with a probability given by the Boltzmann factor—see App. C for more details. This algorithm has been proved to be efficient to reproduce equilibrium states for systems of very different natures.

In our problem, neighbouring configurations are generated by modifying the orientations of single molecules. More concretely, a Monte Carlo trial consists of a $\pm \pi/3$ rotation for a randomly selected dendron. Beyond Monte Carlo we perform simulated annealing to search the possible ground states of the system. We prepare a disordered initial configuration for a given density, where molecules with identical conformations take a random orientation among the six possible directions. Starting at a given temper-

ature the system evolves through Monte Carlo trials until the equilibrium is reached⁵. Then the temperature is lowered and the process repeated. The system is cooled down to temperatures around 170 K. They are enough for our investigation, as the experiments were performed at room temperature. For some molecular conformations and densities long range ordered patterns are observed in the stationary state.

We have investigated five molecular conformations α_i of the 8/8 and 8/12 Fréchet dendrons shown in Fig. 3.5. They differ from each other in the orientations of the arms. The molecular configurations used as input in our simulations are the outputs of the molecular mechanics energy minimizations performed by Hermann and coworkers.

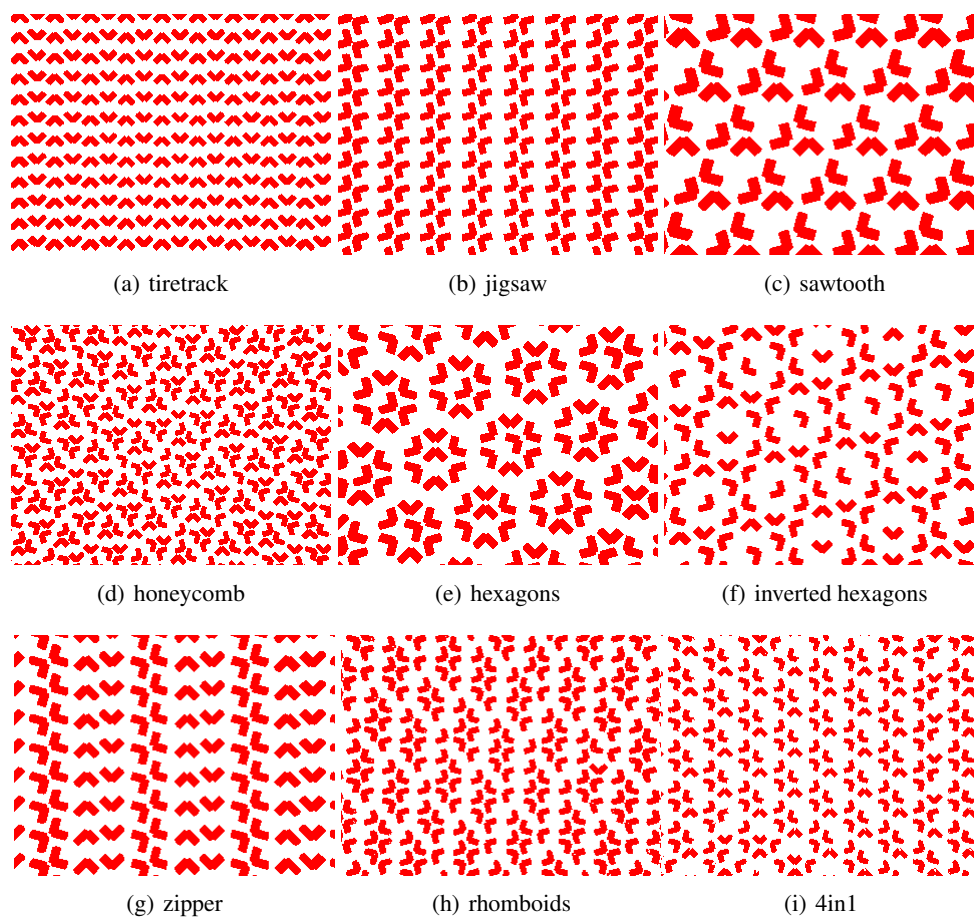


Figure 3.6: Ordered motifs found for the supralayers assembled from 8/8 and 8/12 Fréchet dendrons with different conformations within the interaction-site model. Molecules are represented as boomerangs matching their three aromatic rings to better identify the long range order. The carbonated arms are not shown in these cartoons.

An ample variety of ordered patterns arises by cooling samples of the 8/8 and 8/12 molecules in all conformations, which are displayed in Fig. 3.6. The emerging

⁵In every Monte Carlo (MC) step each molecule updates on average once. After running 500 MC steps to equilibrate the sample, the energy and order parameters have been sampled during other 1000 Monte Carlo steps before lowering or raising the temperature.

motifs have two, three or six-fold symmetry, matching the possible symmetries of the honeycomb lattice of the graphite substrate. In all the patterns, except for the sawtooth and the 4in1, opposite orientations of molecules appear in pairs. In the tiretrack and jigsaw patterns only two possible orientations of the molecules are present, three in the sawtooth, four in the zipper, rhomboids⁶, and 4in1 phases, and six in the honeycomb, hexagons⁷, and inverted hexagons.

Some basic units as the tetramer found in the 4in1 phase may arrange in several domains, giving rise to slightly different long range configurations as the zigzag pattern found for the 8/8 molecule and displayed in Fig. 3.7.

Changing the chirality of the asymmetric molecule 8/12, i.e. interchanging the length of the lateral chains, modifies the relative orientation of the main subunits in patterns as the sawtooth or zipper.

Table 3.3 specifies the patterns found in the cooling process for every building-block and conformation, together with the reduced⁸ lattice constant a/σ at which they have been observed. Symmetric configurations, i.e. the 8/8 molecule in general and the α_1 conformation in particular, assemble into a larger variety of ordered patterns.

To what extent are the emergent motifs stable? To address this question we carry out the reverse process. We prepare perfectly ordered configurations of the system at low temperatures with the phases yielded by the cooling process and then we slowly heat them up. We monitor the energy and suitable order parameters for each pattern to characterize the melting transition and identify the critical temperatures at which the entropic forces induce disorder in the sample.

The order parameters are defined to take values which range from one when the pattern is perfectly ordered to zero in the disordered phase. Every pattern displays various sublattices, defined as the set of lattice's sites at which the molecules points in the same direction—for instance alternative rows in the tiretrack pattern represent two different sublattices. The order parameter measures the fraction of molecules in a sublattice orientated in the preferred direction of the sublattice they belong to. The order parameter for a sublattice A with N_A molecules and preferred orientation σ^A is

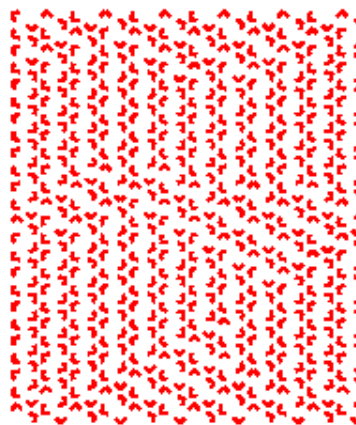


Figure 3.7: Zig-zag pattern.

⁶The rhomboid pattern has been observed for a configuration of the 8/8 molecule which is not included in the α_i conformations shown here.

⁷The same order has been found for colloids in a laser field in the so-called 6in1 phase [141].

⁸Both energies and lengths are dimensionless magnitudes: lengths are *reduced* with the characteristic length scale of the chains σ and energies with the corresponding energy scale ϵ of the van der Waals potential.



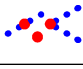

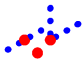
	8/8	8/12
α_1	 tiretrack (2.8, 3.6, 4, 4.2) inverted hexagons (3.4)	tiretrack (3.8, 4, 4.2) inverted hexagons (3,4) hexagons (3, 3.2)
α_2	 jigsaw (4.2) hexagons (3) zigzag (3.4)	jigsaw (4.1, 4.2) honeycomb (2.8, 2.9) stripes (3.2)
α_3	 jigsaw (4.2) zipper (4.2)	tiretrack (4.2) zipper (4.1)
α_4	 zipper (4.1) sawtooth (2.8, 3.4, 3.6, 3.8) jigsaw (4.2)	tiretrack (4.1, 4.2) sawtooth (3.6, 3.8, 4)
α_5	 honeycomb (2.8, 3) stripes (3.2) hexagons (3.6)	honeycomb (2.8, 3)

Table 3.3: Emerging ordered phases by cooling down samples with $N = 576$ Fréchet dendrons—for different chains' lengths and orientations α_i . In parenthesis the dimensionless constant lattice a/σ for which they were observed and in bold font the stable phases under heating.

defined as:

$$m_A = \frac{N_A^{\sigma_A}}{N_A} - \frac{1}{5} \sum_{\sigma_i \neq \sigma_A} \frac{N_A^{\sigma_i}}{N_A}. \quad (3.1)$$

The factor $1/5$ is introduced to assure that $m_A = 0$ in a disorder phase where all orientations are equiprobable. The order parameter we monitor is just the average of the order parameters of all sublattices i :

$$m = \sum_{i=1}^{n_s} \frac{m_i}{n_s}. \quad (3.2)$$

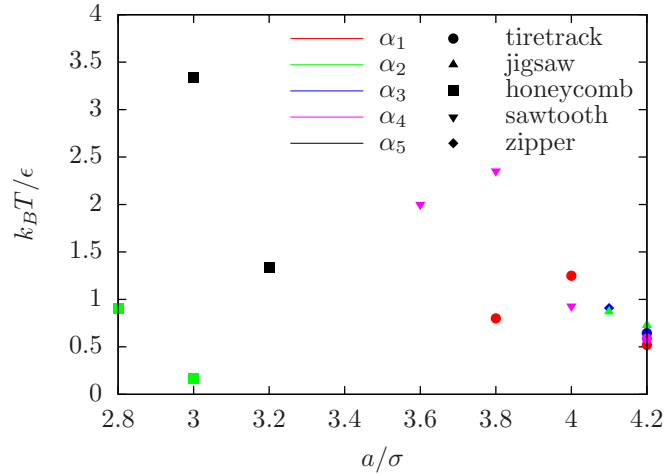
Fig. 3.8 shows the stability diagram, i.e. the temperature regimes for which different monolayers are stable before melting into the disordered phase as a function of density for the 8/12 Fréchet dendron⁹. For some regimes, specially at low densities, i.e. large lattice constant a , many phases are stable and might be thus theoretically observed or even coexist in equilibrium. To build this diagram a phase has been considered to be ordered if 90% of the molecules follow the preferred direction of their sublattices, i.e. $m > 0.9$.

The dependence of the energy and order parameter as well as their variances, i.e. specific heat

$$c_N = \frac{N}{k_B T^2} \left(\langle u^2 \rangle - \langle u \rangle^2 \right) \quad (3.3)$$

⁹The stable phases are also marked in a bold font in table 3.3 for the 8/8 and 8/12 molecules.

Figure 3.8: Stability diagram for the 8/12 molecule. Points represent the highest reduced temperature $k_B T/\epsilon$ for a given dimensionless lattice constant a/σ at which the corresponding patterns are stable— α_i refers to the molecular conformation [colour code] in the order motifs.



and susceptibility

$$\chi_m = \frac{1}{k_B T} \left(\langle m^2 \rangle - \langle m \rangle^2 \right), \quad (3.4)$$

with the increasing temperature allows one to identify the nature of the melting transition.

Exemplary, Fig. 3.9 shows the energy per molecule u/ϵ and the order parameter m as a function of the reduced temperature $k_B T/\epsilon$ for the melting transition of the sawtooth phase for the 8/12 dendron. The data suggest the transition to be discontinuous because of the jump in the order parameter.

What are the internal energies of the emergent patterns? Can one draw conclusions about the dominant phases comparing their energies? Fig. 3.10 displays the energy of all the stable patterns as a function of the reduced lattice constant a/σ for the 8/12 molecule. For small distances between molecules the honeycomb pattern shows the lowest energy, the sawtooth is the most favourable motif at intermediates densities, and the tiretrack phase minimizes the energy for lower densities. All the phases which minimize the energy for a given regime of the density are stable under heating in greater or lessen extent, so that no pattern should be excluded of being observed in equilibrium.

3.3.3 Theory versus experiment

The interaction-site model succeeds in reproducing many of the general features observed in supramolecular systems, such as the ample diversity of patterns, the role of chirality, the local ordering, the global symmetries, as well as the specific motifs of the patterns.

All the patterns observed in the experiment for the 8/8 and 8/12 dendrons have also been found by the interaction-site model, namely the tiretrack, jigsaw, honeycomb, and sawtooth pattern. Although the latter shows the same long range order in the theoretical and experimental results, it only contains one type of trimers in the theoretical predictions with molecules pointing in three of the six orientations available. In the experiments, however, two kinds of trimers are present, one rotated $\pi/3$ with respect to the other, showing thus the whole pattern all possible orientations. The conformations of the molecules giving rise to a specific pattern agree to a great extent with

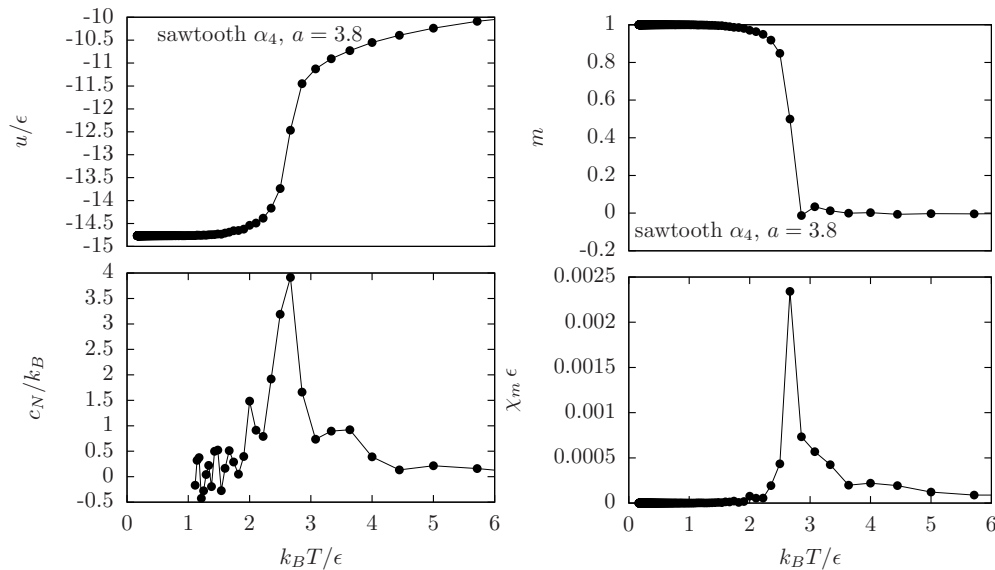


Figure 3.9: Melting transition for the sawtooth phase. Energy per molecule [top left] and order parameter [top right] are shown as a function of the dimensionless temperature. The corresponding susceptibilities are shown in the bottom. The jump in the order parameter m suggests a discontinuous transition. This simulation was performed for $N = 576$ 8/12 Fréchet dendrons in the α_4 conformation on a lattice with constant $a/\sigma = 3.8$.

those observed in the experiments. In addition five new phases were predicted by the simulated cooling process: hexagons, inverted hexagons, zipper, rhomboids, and 4in1.

Both in the experiment and the simulations a change in the chirality of the molecule results in a variation of the relative orientations in the local ordering motif, although the long range order remains unchanged.

According to the Monte Carlo simulations the long-range ordered patterns are stable up to dimensionless temperatures $k_B T / \epsilon$ ranging from half to three approximately. A rough computation with the energies provided by the molecular mechanics simulation allows to estimate the order of the energy scale ϵ in the Lennard-Jones potential. From the MM minimization we learned, that the weak interaction between the alkylchains contribute around 18kJ/mol in fully interdigitated chains for every four CH_2 units. If one assumes that the full overlap corresponds to the minimum of the Lennard-Jones potential, $r_{\min} = 2^{1/6}\sigma$, one gets $\epsilon \sim 1.5 \cdot 10^{-20}$ J yielding a ratio $\epsilon/k_B \sim 10^3$ K. For the experimental model system we are interested in, the melting temperatures predicted by our theoretical model range from 500 K to 3000 K. One may hence consider the experimental patterns assembled at room temperature as the ground states of the system.

The densities observed in the experimental findings, from 0.328 molecules/ nm^2 in the tiretrack pattern to 0.226 molecules/ nm^2 in the honeycomb, correspond to lattice constants from $a \sim 3.2\sigma$ to $a \sim 3.8\sigma$ respectively.

In the interaction-site model the phase with the lowest energy sensitively depends on the lattice constant. Because the character of the main interactions is rather weak, the fully interdigitation of the carbonated chains plays a crucial role to get low en-

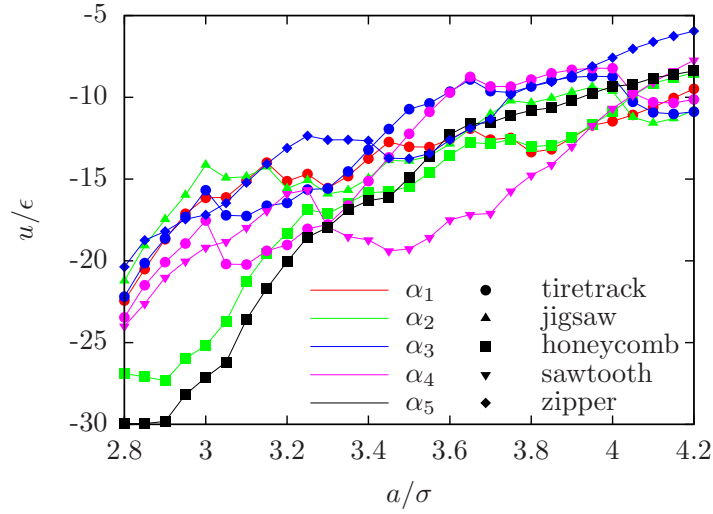


Figure 3.10: Zero temperature energies for several patterns and molecular configurations α_i [colour code] of the Fréchet dendron 8/12 as a function of the lattice constant. Energies and lengths are given in dimensionless units, i.e. reduced by the characteristic energy scale ϵ and length scale σ of the Lennard-Jones potential respectively.

ergy configurations. The fraction of the arms which overlap depends on the molecular conformation, the distance between the molecular centres, i.e. lattice constant, and the relative order of molecules in the local motif.

According to the theoretical results the honeycomb, the sawtooth, and the tiretrack patterns represent the ground state of the system for different regimes of the lattice constant. So is the honeycomb the preferred phase for high densities or small lattice constants, the sawtooth for intermediates, and the tiretrack for low densities. Since all of them are stable in the regimes where they minimize the energy, one would expect to find them interchangeably or coexisting when the system reaches the thermodynamical equilibrium in the laboratory. However, although all of them coexist at the very early stages of the experiment, only the tiretrack pattern is stable in hexane solvent after waiting enough time. What could be the reasons for this discrepancy?

- i. First of all, the continuous arbitrary value of the lattice constant in the theoretical predictions is an artificial resort of the interaction-site model. In the experiments the molecules must couple to the underlying lattice and the distances between their centers are restricted to some multiples of the actual lattice constant of the graphite.
- ii. The interaction-site model does not prevent the aromatic rings and the carbonated chains of different molecules from possible overlapping. In the experiments, however, such overlapping does not take place. The honeycomb phase, ground state for large densities according to the simulations, cannot be observed in the experiment. In the model, the distance between molecules is $a \sim 3\sigma$, while the length of the arms is either 2σ or 3σ , so that centers and chains might overlap and the phase cannot be considered to be stable. Such high densities are not observed in the experiment because of the lack of space to accommodate the

molecules.

- iii. The theoretical model does not account for the effect of the solvent. It is thought that some solvents tend to interact via hydrogen-bonds with the OH groups of Fréchet dendrons—the red coloured part in the atomistic model of Fig. 3.3. The configuration of the tiretrack pattern is believed to favour the formation of such bonds, while the conformation of the sawtooth and honeycomb phases could hinder such interaction. This might be the main reason why the tiretrack pattern is the only stable phase in some solutions, in spite of the theoretical prediction which foresees a larger diversity of stable patterns. In particular in the case of the hexane solvent, which is supposed to completely evaporate, the molecules interacting with the remaining water might tend to form numerous H-bonds. This not yet proved hypothesis might even explain the transition from the coexistence observed when hexane is still present at the beginning of the experiment to the dominance of the tiretrack pattern after evaporation.
- iv. The substrate-molecule energy differs for different phases. A non-negligible contribution comes from the van der Waals interactions of the substrate with the carbonated chains. For some patterns the chains do not adopt a totally flat configuration reducing thus the energy of the interaction. This effect is not accounted for in the theoretical model and would slightly vary the energetic results of the ground states. However, we believe that the supremacy of the tiretrack pattern is explained because it enhances the interaction with the solvent.

3.4 Conclusion and outlook

In this chapter, we have developed an interaction-site model which correctly predicts the ordered motifs of assembled monolayers. By reducing the degrees of freedom and considering the building-blocks as rigid bodies with a reduced set of interacting points, we have demonstrated that the self-assembly relies on very general features of the system considered. In particular, we have identified the essential aspects which encode self-assembly, namely the coupling with the substrate, the geometry of the building blocks, and their weak interactions. These are universal principles in self-organizing systems which do not depend on the special nature of the building blocks and the underlying substrate. The predictive power provided by our model may guide the synthesis of suitable building blocks to engineer arbitrary patterns for specific goals. The versatility offered to construct the building blocks makes our model especially suitable to explore a wide range of geometries. The molecular units are indeed made up of a set of smaller pieces represented by beads, which contain the interacting points and add up to originate the complete molecule.

Beyond those more applied aspects one may also study the phase behaviour of mesoscopic building blocks like Fréchet dendrons on patterned substrates. Here, we have employed Monte Carlo methods to explore the phase diagram as a function of the lattice constant of the underlying substrate and the temperature. In particular we have determined the stability of the emergent phases and the nature and critical temperature of the melting transition. We have found that a broad variety of long-range ordered phases are stable for various conformations of the building blocks and density regimes

which may indeed coexist, as it has been observed in the experiments. The melting temperatures of the ordered motifs range from approximately 500 K to 1500 K, much higher than the room temperature in which experiments were addressed. Therefore, one may consider the experimental emergent phases as the ground states of the system. We have identified the transition into a disordered phase to be discontinuous, attending to the jump in the order parameter.

There are several ways to extend these studies. Here we have considered the building blocks as rigid bodies. A natural generalization would be to make the building blocks flexible and explore the interplay between intra and inter-molecular ordering. This extension implies including at least four new degrees of freedom per molecule, the orientations of the arms, which makes the Monte Carlo simulations computationally very expensive. An interesting alternative to speed up simulations would be genetic algorithms [45, 63]. They are suitable methods to compute the ground states of two dimensional systems by minimizing the energy of single unit cells [44, 53]. The conformations and motifs resulting from this minimization can serve as input configurations for the Monte Carlo simulations to assess their stability. In this way, the interaction-site model becomes independent of external input to a larger extent. In addition, when employing genetic algorithms one can relax the constraint of the substrate. Instead considering the building blocks to be attached to the sites of a lattice, one can mimic the role of the substrate through a more realistic potential. This opens a way to investigate systems whose substrates display more complex symmetries.

Appendix A

Agent based stochastic simulations

The mafia model is carefully investigated with extensive agent-based stochastic simulations. Stochasticity is involved in two ways: update is asynchronous and agent actions are probabilistic.

We are interested in the evolution of two species, citizens and mafiosi, in a society with a fixed carrying capacity N . The density population $\rho = c + m \leq 1$, which is the sum of the number of mafiosi and citizens, is not necessarily as large as the system size $C + M \leq N$, i.e. some locations might be empty.

The initial population is randomly distributed in the N nodes available: c_0N citizens, m_0N mafiosi, and $N(1 - c_0 - m_0)$ empty nodes. The system evolves for a total time $\tau = gN$. The factor g ranges from 0.01 to 0.015, which has been proved to be enough for the system to reach a quasistationary state. At each time step $\Delta\tau$ N site updates are carried out, so that every agent updates on average once every time step.

The update process is as follows. First, a site is randomly selected among the N nodes. The possible actions are birth process for empty places and death or strategy change for citizens and mafiosi. All sites may also remain as they were. If the mobility rate does not vanish, citizens and mafiosi may also change their locations.

The probability with which one action takes place is proportional to the rates of each action— β for the birth process, 1 for the death one, ω_{mc} and ω_{cm} for the strategy change, and μ for the diffusion process. So is, for example, the probability for a citizen to be born in an empty place $\beta\Delta\tau$ at every time step. The size of the time step is taken in such a way that the sum of the probabilities for all the events is smaller than one: $\sum_{\text{events}} p_{\text{event}} = \sum_{\text{events}} r_{\text{event}}\Delta\tau \leq 1$, where r_{event} is the event's rate. $\Delta\tau$ ranges between 0.025 for simulations without mobility and 0.005 in simulations which include mobility, fulfilling the previous condition for the processes rates considered in this thesis.

While the death, birth, and mobility rates are constant, the reaction rates ω_{ij} are time and site dependent. Therefore, they must be actualized for each individual update. In a synchronous update the reaction rates would be computed simultaneously for all agents. But in the asynchronous update every updating agent computes the corresponding reaction rate when he's selected to update. In this way the agent takes into account the current strategies of his neighbours, even if they already updated in the current time step $\Delta\tau + 1$. This update seems to better resemble social actions, in which the information process is faster than the decision-making one.

A random number r , $0 \leq r \leq 1$, is generated to determine the event taking place at each step. Is the site an empty place, a citizen is born with probability $\beta\Delta\tau$, i.e. if $\beta\Delta\tau \leq r$, and remains empty otherwise. If the site is occupied with an agent, this dies if $\Delta\tau \leq r$, change his strategy if $\Delta\tau < r \leq (1 + \omega_{ij})\Delta\tau$, or move if $(1 + \omega_{ij})\Delta\tau < r \leq (1 + \omega_{ij} + \mu)\Delta\tau$. If $r > (1 + \omega_{ij} + \mu)\Delta\tau$ the individual remains with the same strategy at his initial place.

The main focus of our work relies on the different behaviours of the system in several structures. The underlying topology plays a role in the evolution process through the computation of the reaction rates ω_{ij} .

In the homogeneous mixing hypothesis all agents are *connected* to the rest of the population. Here the frequencies of citizens, mafiosi, and police entering the reaction rates are those of the whole population. Thus in our simulations it is only needed to keep both populations actualized, mafiosi and citizens frequencies, as well as the constant police fraction.

For simulating structured populations every site has a list with its nearest neighbours, as well as with the edges responsible for these connections. If the fraction of controlling elements is not zero a fraction p of the edges contains a policing element. $N_E p$ police agents are randomly distributed in the N_E edges. The nodes and edges themselves contain the information about whether they are empty or not and who is occupying the site in the case of nodes, whether it is a citizen or a mafioso. The computation of the reaction rates ω_{ij} is carried out with the fractions of citizens, mafiosi, and policing elements relative to the updating agent, i.e. those registered on his neighbours list.

If the structure is a regular lattice the nodes occupy the vertices of a grid with a constant number of nearest neighbours, 4. For the lattice, periodic boundary conditions are considered.

For the study of the dynamics in scale free networks, first the networks are generated following the algorithm implemented by Heiko Hotz described in appendix B. The connected network consists for our purpose of a list with all nodes, each of them containing sub-lists of the neighbouring nodes and the edges responsible for the links.

All the observables measured in this work are the result of averaging over 1000 simulations, which include the network construction. More than 95% of the trials to get fully connected networks were successful, so that statistical averages are at least performed over 950 measures.

In structures, individuals may have the opportunity to change their location. If an individual has been selected to displace and he moves randomly, a neighbouring site is randomly chosen and the occupants of both nodes change their locations. If migration is considered instead diffusion, this displacement only takes place if the selected site is empty.

As for intelligent mobility, the individual diffusing or migrating computes his fictitious reaction rates to change his strategy for all the neighbouring sites (or the empty ones if migration is considered) and swaps his position with the individual at the site for which his reaction rate is minimal. If the reaction rate were larger in all the neighbouring sites than in the current one, the agent remain at his place.

Appendix B

Building uncorrelated scale free networks

Although very often real networks show degree-degree correlations, it is desirable to build uncorrelated networks to study the behaviour of dynamical systems on them. One important reason for it is that whenever a system is analytically solvable it is usually only possible under the assumption that the network is uncorrelated.

As discussed in section 1.1.4 the uncorrelated configuration model allows the construction of scale free networks with arbitrary exponent, without multiple and self-connections and avoiding degree-degree correlations. The latter are related with the election of the maximal number of links per node to generate the network, the cutoff k_m .

The natural cutoff k_c is computed arguing that at most one node might have degree larger than the maximal [20]:

$$N \int_{k_c}^{\infty} P(k) dk \sim 1, \quad (\text{B.1})$$

so that $k_c(N) \sim N^{1/(\gamma-1)}$. But this cutoff leads to multiple and self-connections for $\gamma < 3$ or to uncorrelated networks if those are explicitly forbidden.

To include topological considerations, i.e. to avoid the presence of multiple and self-connections, the ratio between the edges connecting vertices of degrees k and k' , E_{kk} , and the total possible number of connections, $m_{kk'}$, between them should be smaller than one

$$r_{kk'} = \frac{E_{kk'}}{m_{kk'}} \leq 1 \quad (\text{B.2})$$

for all kind of networks. The structural cutoff is defined as the maximal degree which fulfills this condition. The number of possible connections are given by $m_{kk'} = \min\{kN_k, k'N_{k'}, N_k N_{k'}\}$. In the two first cases, kN_k and $k'N_{k'}$, the condition is directly guaranteed as $r_{kk'} = E_{kk'}/kN_k = E_{kk'}/\sum_{k'} E_{kk'} < 1$.

Making use of $\sum_{kk'} E_{kk'} = \sum_k (\sum_{k'} E_{kk'}) = \sum_k kN_k = \langle k \rangle N$ the joint probability for two random nodes with degrees k and k' to be connected is $P(k, k') =$

$E_{kk'}/N \langle k \rangle$. In addition, the joint probability for uncorrelated networks is of the form

$$P_{\text{nc}}(k, k') = P_{\text{nc}}((k|k') \cap (k'|k)) \quad (\text{B.3})$$

$$= P_{\text{nc}}(k|k') \cdot P_{\text{nc}}(k'|k) \quad (\text{B.4})$$

$$= \frac{kN_k}{\langle k \rangle N} \frac{k'N_{k'}}{\langle k \rangle N} \quad (\text{B.5})$$

$$= \frac{kk'P(k)P(k')}{\langle k \rangle^2}. \quad (\text{B.6})$$

One may thus derive the required condition $r_{kk'} \leq 1$ in the case $m_{kk'} = N_k N_{k'}$:

$$r_{kk'} = \frac{P(k, k') \langle k \rangle N}{N_k N_{k'}} \quad (\text{B.7})$$

$$r_{kk'} = \frac{kk'}{\langle k \rangle N}, \quad (\text{B.8})$$

yielding a structural cutoff $k_s(N) \sim \sqrt{\langle k \rangle N}$, which is independent of the degree distribution and the exponent γ [20].

The choice between the structural and natural cutoff is determined by the behaviour in the thermodynamic limit. So the former diverges more slowly for $\gamma < 3$, but faster for $\gamma > 3$. Therefore, the structural cutoff must be used in the first case and the natural in the second.

Heiko Hotz implemented an algorithm to build scale free networks following the scheme outlined by Catanzaro et al. [28], which has been used throughout this work.

A fixed number of N vertices are assigned a degree drawn from the scale free distribution $P(k) = \mathcal{A}k^{-\gamma}$, where the normalization factor reads $\mathcal{A} = \left(\sum_{k_0}^{k_c} k^{-\gamma}\right)^{-1}$ and the limits for the degree are given by $k_0 \leq k \leq k_c$. Every node gets as many stubs to be connected as its degree indicates.

Once all the nodes have the corresponding number of stubs the linking process starts. Two stubs are randomly selected. If they belong to different vertices which are not connected yet a permanent edge between the nodes is created and both stubs are removed. Every node adds the new neighbouring node and the edge connecting them to its neighbours list. The edge with its extremes occupants is listed in a corresponding structure.

It might happen that some stubs remain unconnected because the only possible links available are multiple or self-connections. The election of the minimal number of stubs per node $m_0 = 2$ considerably reduces the probability for this to happen. But in case the situation arises, how many trials should be performed to be sure that the networks cannot be fully connected? Hotz observed that successful networks didn't report more than ten vain attempts. Thus he imposed an upper limit of fifty failed trials, after which the network is considered not able to be fully connected.

The impossibility of creating uncorrelated connected networks with the natural cutoff for $\gamma < 3$, the correlation of the created networks, and the degree distribution were all extensively tested and found to work properly by Hotz in his diploma thesis.

Appendix C

Monte Carlo simulations

Monte Carlo (MC) methods [18, 48] are a very useful tool to investigate complex systems, for which it is not possible to evaluate the partition function $Z = \int d\mathbf{r}^N \exp(-\beta\mathcal{U}(\mathbf{r}^N))$ in the canonical (NVT) ensemble. The ratio

$$\mathcal{N}(\mathbf{r}^N) = \frac{\exp(-\beta\mathcal{U}(\mathbf{r}^N))}{Z} \quad (\text{C.1})$$

represents the probability density to find the system in a configuration \mathbf{r}^N . The number of points n_i per unit volume in the configuration space around \mathbf{r}_i^N are proportional to the fraction between $\mathcal{N}(\mathbf{r}_i^N)$ and the total number of points L —they are in last term proportional to the Boltzmann factor $\exp(-\beta\mathcal{U}(\mathbf{r}_i^N))$. This allows to compute averages of an observable A as

$$\langle A \rangle \approx \frac{1}{L} \sum n_i A(\mathbf{r}_i^N). \quad (\text{C.2})$$

To generate points in the configuration space with probabilities proportional to the Boltzmann factor one first starts with a random configuration. A new trial configuration is produced following some specific rules. Should this configuration be accepted? The most important feature the Monte Carlo method must accomplish is that whenever equilibrium is reached the system stays there. This demands that the number of accepted trials leaving equilibrium equates those accepted trials coming from neighbouring configurations and reaching equilibrium. This condition is known as detailed balance:

$$\mathcal{N}(o)\pi(o \rightarrow n) = \mathcal{N}(n)\pi(n \rightarrow o). \quad (\text{C.3})$$

The transition probability $\pi(o \rightarrow n)$ from the old to the new configuration is the product of the probability to generate this specific trial configuration $\alpha(o \rightarrow n)$ times its probability to be accepted $\text{acc}(o \rightarrow n)$. If the first is symmetric, i.e. $\alpha(n \rightarrow o) = \alpha(o \rightarrow n)$, which is an usual choice, the detailed balance reads:

$$\frac{\text{acc}(o \rightarrow n)}{\text{acc}(n \rightarrow o)} = \frac{\mathcal{N}(n)}{\mathcal{N}(o)} = \exp(-\beta(\mathcal{U}(n) - \mathcal{U}(o))). \quad (\text{C.4})$$

There are various possibilities to fulfil this requirement. The choice of Metropolis [88] which we follow in our simulations, is:

$$\text{acc}(o \rightarrow n) = \begin{cases} \frac{\mathcal{N}(n)}{\mathcal{N}(o)} & \text{if } \mathcal{N}(n) < \mathcal{N}(o) \\ 1 & \text{if } \mathcal{N}(n) \geq \mathcal{N}(o). \end{cases} \quad (\text{C.5})$$

The initial configuration in our simulations is a system with Fréchet dendrons at the vertices of a triangular lattice with a random orientation. Dendrons are represented by the interaction-site model, i.e. as a set of spheres whose centers are interacting points. The lattice constant a and the molecular conformation of the building blocks are fixed parameters of the model. The former accounts for the density of the sample $\rho = 2/\sqrt{3} a^2$. The Fréchet dendrons are in a given molecular configuration which comes from the molecular mechanics minimization. It is defined by several parameters: the distance between the molecular centre and the centers of the rings, the diameters of the rings and beads in the chains, the length of the lateral arms, and their orientations with respect to the molecular axis joining two of the rings which crosses through the molecular centre.

Systems with N ranging from some hundreds to a few thousands molecules are prepared. The molecular centers are *attached* to the lattice vertices and the rigid building blocks take a random orientation among the six equivalent possibilities in the six fold symmetric lattice.

The simulation starts at a given dimensionless temperature $k_B T/\epsilon$ and are slowly cooled down. At every temperature 500 Monte Carlo steps are performed to equilibrate the sample after which measurements are taken for 1500 MC steps in which the system has been found to be stationary. Then the temperature is lowered and the process repeated.

In a MC step all molecules update their state on average once. Trials configurations are generated with the attempt of a randomly selected molecule to perform a rotation of $\pm \pi/3$. The new configuration is accepted following the Metropolis schema described above. Within this algorithm the temperature is gradually reduced until the system reaches a stable configuration at low temperatures.

Often several arbitrary coarsening processes emerge simultaneously at different points in the ordering dynamics. The lack of a preferred direction for the ordered patterns difficult the measurement of order parameters along the cooling process. Therefore, perfect instances of the stable patterns found are specifically prepared at low temperatures and heated. Monte Carlo steps are carried out while heating the system to account for order parameters. The energy of the system is also tracked in all simulations.

To improve the efficiency of the algorithm a so-called *Verlet* list [139], associated to every site, keeps track of the neighbouring molecules every molecule interact with. To make the computation of the Lennard-Jones potential feasible the potential is truncated at a cutoff distance $r_c = 2.5 \sigma$ at which the interactions are negligible. Therefore the Verlet list contains the molecules within a distance smaller than r_c from every lattice site.

To better mimic infinite bulk phases and avoid finite size effects, periodic boundary conditions are used. The system interacts with copies of itself in all directions as long as they are within the interaction range. Every particle interacts first with the *first image* of all other particles, i.e. with the closest copy of other particles even if they are not in the same box—see the cartoon in Fig. C.1. If more distant copies, second, third images, etc. of one molecule were still within the interaction range of a second molecule, interactions with more than one copy of every particle would be possible. The length scales of the systems we investigate compared with the interaction range do not require more interactions than with the first image of molecules. Further details

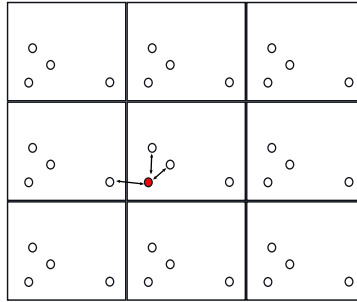


Figure C.1: Illustration of the first image algorithm. Nine copies of a system box containing four particles are shown. The coloured particle interacts with the first images of all other particles—if closer than r_c —regardless of the box they are located. The pair interactions with the first images of all particles are marked with arrows.

of the Monte Carlo technique and improvements in its implementation for molecular systems may be found in [48, 4].

Bibliography

- [1] *Soft Matter*, chapter Colloids on patterned substrates. Wiley-VCH, Weinheim, 2007.
- [2] R. Albert and A. L. Barabási. Statistical mechanics of complex networks. *Reviews of Modern Physics*, 74(1):47–97, 2002.
- [3] Faisal A. Aldaye, Alison L. Palmer, and Hanadi F. Sleiman. Assembling Materials with DNA as the Guide. *Science*, 321(5897):1795–1799, 2008.
- [4] M. P. Allen and D. J. Tildesley. *Computer simulation of liquids*. Oxford university press Oxford, 1989.
- [5] R. M. Anderson and R. M. May. Population biology of infectious diseases: Part I. *Nature*, 280:361–367, 1979.
- [6] R. M. Anderson and R. M. May. Directly transmitted infections diseases: control by vaccination. *Science*, 215(4536):1053–1060, 1982.
- [7] R. M. Anderson and R. M. May. *Infectious diseases of humans: dynamics and control*. Oxford University Press, USA, 1992.
- [8] R. Axelrod and D. Dion. The further evolution of cooperation. *Science*, 242(4884):1385–1390, 1988.
- [9] R. Axelrod and W. D. Hamilton. The evolution of cooperation. *Science*, 211(4489):1390–1396, 1981.
- [10] A. L. Barabási and R. Albert. Emergence of scaling in random networks. *Science*, 286(5439):509, 1999.
- [11] A. Barrat, M. Barthélémy, and A. Vespignani. *Dynamical processes on complex networks*. Cambridge University Press, NY, USA, 2008.
- [12] A. Barrat and M. Weigt. On the properties of small-world network models. *The European Physical Journal B*, 13(3):547–560, 2000.
- [13] Johannes V. Barth. Molecular architectonic on metal surfaces. *Ann. Rev. Phys. Chem.*, 58:375–407, 2007.
- [14] Johannes V. Barth, Giovanni Costantini, and Klaus Kern. Engineering atomic and molecular nanostructures at surfaces. *Nature*, 437:437, 671–679, 2005.

- [15] M. Barthélémy and L. A. N. Amaral. Small-world networks: Evidence for a crossover picture. *Physical Review Letters*, 82(15):3180–3183, 1999.
- [16] Marc Barthélémy and Luís A. Nunes Amaral. Erratum: Small-world networks: Evidence for a crossover picture [physical review letters 82, 3180 (1999)]. *Physical Review Letters*, 82(25):5180, 1999.
- [17] I. J. Benczik, S. Z. Benczik, B. Schmittmann, and R. K. P. Zia. Lack of consensus in social systems. *Europhysics Letters*, 82:48006, 2008.
- [18] K. Binder and D.W. Heermann. *Monte Carlo simulation in statistical physics: an introduction*. Springer Verlag, 2002.
- [19] V. Blickle, T. Speck, L. Helden, U. Seifert, and C. Bechinger. Thermodynamics of a colloidal particle in a time-dependent nonharmonic potential. *Physical review letters*, 96(7):70603, 2006.
- [20] M. Boguñá, R. Pastor-Satorras, and A. Vespignani. Cut-offs and finite size effects in scale-free networks. *The European Physical Journal B*, 38(2):205–209, 2004.
- [21] B. Bollobás and O. Riordan. The diameter of a scale-free random graph. *Combinatorica*, 24(1):5–34, 2004.
- [22] S. Bornholdt and H. G. Schuster. *Handbook of graphs and networks: From the genome to the Internet*. WILEY-VCH, 2003.
- [23] M. Brunner and C. Bechinger. Phase behavior of colloidal molecular crystals on triangular light lattices. *Physical Review Letters*, 88(24):248302, 2002.
- [24] C. Castellano, S. Fortunato, and V. Loreto. Statistical physics of social dynamics. *Reviews of Modern Physics*, 81(2):591–646, 2009.
- [25] C. Castellano, V. Loreto, A. Barrat, F. Cecconi, and D. Parisi. Comparison of voter and Glauber ordering dynamics on networks. *Physical Review E*, 71(6):66107, 2005.
- [26] C. Castellano, D. Vilone, and A. Vespignani. Incomplete ordering of the voter model on small-world networks. *Europhysics Letters*, 63(1):153–158, 2003.
- [27] X. Castelló, V. M. Eguíluz, and M. S. Miguel. Ordering dynamics with two non-excluding options: bilingualism in language competition. *New Journal of Physics*, 8:308, 2006.
- [28] M. Catanzaro, M. Boguñá, and R. Pastor-Satorras. Generation of uncorrelated random scale-free networks. *Physical Review E*, 71(2):27103, 2005.
- [29] P. Chen and S. Redner. Consensus formation in multi-state majority and plurality models. *Journal of Physics A*, 38(33):7239–7252, 2005.
- [30] P. Chen and S. Redner. Majority rule dynamics in finite dimensions. *Physical Review E*, 71(3):36101, 2005.

- [31] A. Chowdhury, B. J. Ackerson, and N. A. Clark. Laser-induced freezing. *Physical Review Letters*, 55(8):833–836, 1985.
- [32] P. Clifford and A. Sudbury. A model for spatial conflict. *Biometrika*, 60(3):581–588, 1973.
- [33] R. Cohen and S. Havlin. Scale-free networks are ultrasmall. *Physical Review Letters*, 90(5):58701, 2003.
- [34] Edwin C. Constable, Marc Haeusler, Bianca A. Hermann, Catherine E. Housecroft, Markus Neuburger, Silvia Schaffner, and Lukas J. Scherer. Self-assembled monolayers as two-dimensional crystals: relationship to three-dimensional crystals. *Crystengcomm*, 9(2):176–180, 2007.
- [35] J. T. Cox. Coalescing Random Walks and Voter Model Consensus Times on the Torus in \mathbb{Z}^d . *Ann. Probab*, 17(4):1333–1366, 1989.
- [36] L. Dall’Asta and C. Castellano. Effective surface-tension in the noise-reduced voter model. *Europhysics Letters*, 77(6):60005–62000, 2007.
- [37] M. J. De Oliveira. Isotropic majority-vote model on a square lattice. *Journal of Statistical Physics*, 66(1):273–281, 1992.
- [38] M. J. De Oliveira, J. F. F. Mendes, and M. A. Santos. Non-equilibrium spin models with Ising universal behaviour. *Journal of Physics-London-A*, 26:2317–2317, 1993.
- [39] O. Diekmann, J. A. P. Heesterbeek, and J. A. J. Metz. On the definition and the computation of the basic reproduction ratio R_0 in models for infectious diseases in heterogeneous populations. *Journal of Mathematical Biology*, 28(4):365–382, 1990.
- [40] L. A. Dugatkin and D. S. Wilson. Rover: a strategy for exploiting cooperators in a patchy environment. *American Naturalist*, pages 687–701, 1991.
- [41] K.T.D. Eames and M.J. Keeling. Modeling dynamic and network heterogeneities in the spread of sexually transmitted diseases. *Proceedings of the National Academy of Sciences*, 99(20):13330, 2002.
- [42] P. Erdos and A. Renyi. On random graphs. *Publ. Math. Debrecen*, 6(290–297):156, 1959.
- [43] P. Erdos and A. Renyi. On the evolution of random graphs. *Publ. Math. Inst. Hung. Acad. Sci*, 5:17–61, 1960.
- [44] J. Fornleitner, F. L. Verso, G. Kahl, and C. N. Likos. Genetic algorithms predict formation of exotic ordered configurations for two-component dipolar monolayers. *Soft Matter*, 4(3):480–484, 2008.
- [45] S. Forrest. Genetic algorithms: principles of natural selection applied to computation. *Science*, 261:872–878, 1993.

- [46] L. Frachebourg and P. L. Krapivsky. Exact results for kinetics of catalytic reactions. *Physical Review E*, 53(4):3009–3012, 1996.
- [47] Jean M. J. Fréchet. Dendrimers and supramolecular chemistry. *Proceedings of the National Academy of Sciences*, 99, 2002.
- [48] D. Frenkel and B. Smit. *Understanding molecular simulation: from algorithms to applications*. Academic Press, 2002.
- [49] S. Galam. Minority opinion spreading in random geometry. *The European Physical Journal B*, 25(4):403–406, 2002.
- [50] S. Galam. Heterogeneous beliefs, segregation, and extremism in the making of public opinions. *Physical Review E*, 71(4):46123, 2005.
- [51] S. Galam and F. Jacobs. The role of inflexible minorities in the breaking of democratic opinion dynamics. *Physica A: Statistical Mechanics and its Applications*, 381:366–376, 2007.
- [52] H. Glowatzki, B. Bröker, R. P. Blum, O. T. Hofmann, A. Vollmer, R. Rieger, K. Mullen, E. Zojer, J. P. Rabe, and N. Koch. "soft" metallic contact to isolated c60 molecules. *Nano Letters*, 8(11):3825–3829, 2008.
- [53] Dieter Gottwald, Gerhard Kahl, and Christos N. Likos. Predicting equilibrium structures in freezing processes. *Journal Chemical Physics*, 122:204503, 2005.
- [54] W. D. Hamilton. The genetical evolution of social behaviour. I. *Journal of Theoretical Biology*, 7(1):1, 1964.
- [55] W. D. Hamilton. Extraordinary sex ratios. *Science*, 156(3774):477–488, 1967.
- [56] M. Haran, J. E. Goose, N. P. Clote, and P. Clancy. Multiscale modeling of self-assembled monolayers of thiophenes on electronic material surfaces. *Langmuir*, 23(9):4897–4909, 2007.
- [57] C. J. Hawker and J. M. J. Fréchet. Preparation of polymers with controlled molecular architecture. A new convergent approach to dendritic macromolecules. *Journal of the American Chemical Society*, 112(21):7638–7647, 1990.
- [58] Craig J. Hawker and Jean M. J. Fréchet. A new convergent approach to monodisperse dendritic macromolecules. *Journal Chemecial Society*, 112:1010, 1990.
- [59] D. Helbing and W. Yu. Migration as a mechanism to promote cooperation. *Advances in Complex Systems*, 11(4):641–652, 2008.
- [60] D. Helbing and W. Yu. The outbreak of cooperation among success-driven individuals under noisy conditions. *Proceedings of the National Academy of Sciences*, 106(10):3680, 2009.

- [61] B. A. Hermann, L. J. Scherer, C. E. Housecroft, and E. C. Constable. Self-organized monolayers: A route to conformational switching and read-out of functional supramolecular assemblies by scanning probe methods. *Advanced Functional Materials*, 16:221–235, 2006.
- [62] J. Hofbauer and K. Sigmund. *The theory of evolution and dynamical systems: mathematical aspects of selection*. Cambridge University Press, 1988.
- [63] J. H. Holland. Genetic algorithms. *Scientific American*, 267(1):66–72, 1992.
- [64] R. A. Holley and T. M. Liggett. Ergodic theorems for weakly interacting infinite systems and the voter model. *The annals of probability*, pages 643–663, 1975.
- [65] B. A. Huberman and N. S. Glance. Evolutionary games and computer simulations. *Proceedings of the National Academy of Sciences*, 90(16):7716–7718, 1993.
- [66] Kitaigorodskii A. I. *Molecular Crystals and Molecules*. Academic Press, New York, 1973.
- [67] Boaz Ilan, Gina M. Florio, Mark S. Hybertsen, B. J. Berne, and George W. Flynn. Scanning tunneling microscopy images of alkane derivatives on graphite: Role of electronic effects. *Nano Letters*, 8(10):3160–3165, 2008.
- [68] M. Keeling. The implications of network structure for epidemic dynamics. *Theoretical Population Biology*, 67(1):1–8, 2005.
- [69] M. J. Keeling. The effects of local spatial structure on epidemiological invasions. *Proceedings: Biological Sciences*, 266(1421):859–867, 1999.
- [70] M.J. Keeling and K.T.D. Eames. Networks and epidemic models. *Journal of the Royal Society Interface*, 2(4):295, 2005.
- [71] B. Kerr, M. A. Riley, M. W. Feldman, and B. J. M. Bohannan. Local dispersal promotes biodiversity in a real-life game of rock–paper–scissors. *Nature*, 418(6894):171–174, 2002.
- [72] P. L. Krapivsky. Kinetics of monomer-monomer surface catalytic reactions. *Physical Review A*, 45(2):1067–1072, 1992.
- [73] P. L. Krapivsky and S. Redner. Organization of growing random networks. *Physical Review E*, 63(6):66123, 2001.
- [74] P. L. Krapivsky and S. Redner. Dynamics of majority rule in two-state interacting spin systems. *Physical Review Letters*, 90(23):238701, 2003.
- [75] R. Lambiotte and S. Redner. Dynamics of non-conservative voters. *Europhysics Letters*, 82(1):18007–18007, 2008.
- [76] D. P. Landau and K. Binder. *A guide to Monte Carlo simulations in statistical physics*. Cambridge University Press, 2005.

- [77] A. Langner, S. L. Tait, N. Lin, C. Rajadurai, M. Ruben, and K. Kern. Self-recognition and self-selection in multicomponent supramolecular coordination networks on surfaces. *Proceedings of the National Academy of Sciences*, 104(46):17927, 2007.
- [78] B. Latané. The psychology of social impact. *American Psychologist*, 36(4):343–356, 1981.
- [79] B. Latané, A. Nowak, and J. Szamrej. From Private Attitude to Public Opinion: A Dynamic Theory of Social Impact. *Psychological Review*, 97:362–376, 1990.
- [80] J. M. Lehn. Toward self-organization and complex matter. *Science*, 295(5564):2400–2403, 2002.
- [81] M. Lewenstein, A. Nowak, and B. Latané. Statistical mechanics of social impact. *Physical Review A*, 45(2):763–776, 1992.
- [82] T. M. Liggett. *Interacting particle systems*. Springer-Verlag, New York-Berlin, 1985.
- [83] Wael Mamdouh, Hiroshi Uji-i, Janine S. Ladislaw, Andres E. Dulcey, Virgil Percec, Frans C. De Schryver, and Steven De Feyter. Solvent controlled self-assembly at the liquid-solid interface revealed by stm. *Journal American Chemical Society*, 128:317–325, 2006.
- [84] R. M. May and R. M. Anderson. Population biology of infectious diseases: Part II. *Nature*, 280:455–461, 1979.
- [85] R. M. May and A. L. Lloyd. Infection dynamics on scale-free networks. *Physical Review E*, 64(6):66112, 2001.
- [86] R. M. May and M. A. Nowak. Evolutionary games and spatial chaos. *Nature*, 359:826–829, 1992.
- [87] J. Maynard Smith and G. R. Price. The logic of animal conflict. *Nature*, 246(5427):15–18, 1973.
- [88] N. Metropolis, A. W. Rosenbluth, M. N. Rosenbluth, A. H. Teller, and E. Teller. Equation of state calculations by fast computing machines. *The journal of chemical physics*, 21(6):1087–1092, 1953.
- [89] M. Mobilia. Does a single zealot affect an infinite group of voters? *Physical Review Letters*, 91(2):28701, 2003.
- [90] M. Mobilia and I. T. Georgiev. Voting and catalytic processes with inhomogeneities. *Physical Review E*, 71(4):46102, 2005.
- [91] M. Mobilia, A. Petersen, and S. Redner. On the role of zealotry in the voter model. *Journal of Statistical Mechanics*, 2007:08029, 2007.
- [92] M. Mobilia and S. Redner. Majority versus minority dynamics: Phase transition in an interacting two-state spin system. *Physical Review E*, 68(4):46106, 2003.

- [93] M. Molloy, B. Reed, and E. Combinatoire. A critical point for random graphs with a given degree sequence. *Random Structures and Algorithms*, 1995.
- [94] Y. Moreno, R. Pastor-Satorras, and A. Vespignani. Epidemic outbreaks in complex heterogeneous networks. *The European Physical Journal B*, 26(4):521–529, 2002.
- [95] M. Nakamaru, H. Matsuda, and Y. Iwasa. The evolution of cooperation in a lattice-structured population. *Journal of Theoretical Biology*, 184(1):65 – 81, 1997.
- [96] J. F. Nash. Equilibrium points in n-person games. *Proceedings of the National Academy of Sciences of the United States of America*, pages 48–49, 1950.
- [97] G.R. Newkome, Z. Yao, G.R. Baker, V.K. Gupta, P.S. Russo, and M.J. Saunders. Chemistry of micelles series. Part 2. Cascade molecules. Synthesis and characterization of a benzene [9] 3-arborol. *Journal of the American Chemical Society*, 108(4):849–850, 1986.
- [98] M. Nowak and K. Sigmund. A strategy of win-stay, lose-shift that outperforms tit-for-tat in the prisoner’s dilemma game. *Nature*, 364(6432):56–58, 1993.
- [99] M. A. Nowak. Five rules for the evolution of cooperation. *Science*, 314(5805):1560–1563, 2006.
- [100] M. A. Nowak, S. Bonhoeffer, and R. M. May. More spatial games. *International Journal of Bifurcation and Chaos*, 4:33–33, 1994.
- [101] M. A. Nowak, S. Bonhoeffer, and R. M. May. Spatial games and the maintenance of cooperation. *Proceedings of the National Academy of Sciences*, 91(11):4877–4881, 1994.
- [102] M. A. Nowak, A. Sasaki, C. Taylor, and D. Fudenberg. Emergence of cooperation and evolutionary stability in finite populations. *Nature*, 428(6983):646–650, 2004.
- [103] M. A. Nowak and K. Sigmund. Games on grids. *The Geometry of Ecological Interactions*, pages 135–150, 2000.
- [104] M. A. Nowak and K. Sigmund. Biodiversity: Bacterial game dynamics. *Nature*, 418(6894):138–139, 2002.
- [105] H. Ohtsuki, C. Hauert, E. Lieberman, and M. A. Nowak. A simple rule for the evolution of cooperation on graphs and social networks. *Nature*, 441(7092):502–505, 2006.
- [106] R. Pastor-Satorras and A. Vespignani. Epidemic spreading in scale-free networks. *Physical Review Letters*, 86(14):3200–3203, 2001.
- [107] R. Pastor-Satorras and A. Vespignani. Immunization of complex networks. *Physical Review E*, 65(3):36104, 2002.

- [108] G. Pawin, K. L. Wong, K. Y. Kwon, and L. Bartels. A homomolecular porous network at a Cu (111) surface. *Science*, 313(5789):961, 2006.
- [109] K. E. Plass, K. Kim, and A. J. Matzger. Two-dimensional crystallization: Self-assembly, pseudopolymorphism, and symmetry-independent molecules. *Journal American Chemical Society*, 126(29):9042–9053, 2004.
- [110] S. Redner. *A guide to first-passage processes*. Cambridge University Press, 2001.
- [111] T. Reichenbach, M. Mobilia, and E. Frey. Mobility promotes and jeopardizes biodiversity in rock–paper–scissors games. *Nature*, 448(7157):1046–1049, 2007.
- [112] C. Reichhardt and C. J. Olson Reichhardt. Colloidal dynamics on disordered substrates. *Physical Review Letters*, 2002.
- [113] C. Reichhardt and C. J. Olson Reichhardt. Ordering and melting in colloidal molecular crystal mixtures. *Physical Review E*, 2005.
- [114] C. Reichhardt and C. J. Olson Reichhardt. Stripes, clusters, and nonequilibrium ordering for bidisperse colloids with repulsive interactions. *Physical Review E*, 2007.
- [115] C. J. Rhodes and R. M. Anderson. Persistence and dynamics in lattice models of epidemic spread. *Journal of Theoretical Biology*, 180(2):125–133, 1996.
- [116] K. Tahara S. Lei, F. C. de Schryver, M. van der Auweraer, Y. Tobe, and S. de Feyter. One building block, two different supramolecular surface-confined patterns: Concentration in control at the solid-liquid interface. *Angew. Chem. Int. Ed.*, 2008.
- [117] F. C. Santos and J. M. Pacheco. Scale-free networks provide a unifying framework for the emergence of cooperation. *Physical Review Letters*, 95(9):98104, 2005.
- [118] F. C. Santos, J. M. Pacheco, and T. Lenaerts. Evolutionary dynamics of social dilemmas in structured heterogeneous populations. *Proceedings of the National Academy of Sciences*, 103(9):3490–3494, 2006.
- [119] U. Schlickum, R. Decker, F. Klappenberger, G. Zoppellaro, S. Klyatskaya, M. Ruben, I. Silanes, A. Arnau, K. Kern, H. Brune, et al. Metal-organic honeycomb nanomeshes with tunable cavity size. *Nano Letters*, 7(12):3813–3817, 2007.
- [120] J. Schnadt, E. Rauls, W. Xu, R. T. Vang, J. Knudsen, E. Laegsgaard, Z. Li, B. Hammer, and F. Besenbacher. Extended one-dimensional supramolecular assembly on a stepped surface. *Physical Review Letters*, 100(4):46103, 2008.
- [121] Nadrian C. Seeman. Dna in a material world. *Nature*, 421:427 – 431, 2003.

- [122] J. Shao, S. Havlin, and H. E. Stanley. Dynamic opinion model and invasion percolation. *Physical Review Letters*, 103(1):18701, 2009.
- [123] D. X. Shi, W. Ji, X. Lin, X. B. He, J. C. Lian, L. Gao, J. M. Cai, H. Lin, S. X. Du, F. Lin, et al. Role of lateral alkyl chains in modulation of molecular structures on metal surfaces. *Physical Review Letters*, 96(22):226101, 2006.
- [124] F. Silly, U. K. Weber, A. Q. Shaw, V. M. Burlakov, M. R. Castell, G. A. D Briggs, and D. G. Pettifor. Deriving molecular bonding from a macromolecular self-assembly using kinetic Monte Carlo simulations. *Physical Review B*, 77(20):201408, 2008.
- [125] C. Sire and S. N. Majumdar. Coarsening in the q-state potts model and the ising model with globally conserved magnetization. *Physical Review E*, 52(1):244–254, 1995.
- [126] F. Slanina and H. Lavicka. Analytical results for the Sznajd model of opinion formation. *The European Physical Journal B*, 35(2):279–288, 2003.
- [127] V. Sood, T. Antal, and S. Redner. Voter models on heterogeneous networks. *Physical Review E*, 77(4):41121, 2008.
- [128] V. Sood and S. Redner. Voter model on heterogeneous graphs. *Physical Review Letters*, 94(17):178701, 2005.
- [129] K. Suchecki, V. M. Eguíluz, and M. S. Miguel. Conservation laws for the voter model in complex networks. *Europhysics Letters*, 69(2):228–234, 2005.
- [130] K. Suchecki, V. M. Eguíluz, and M. San Miguel. Voter model dynamics in complex networks: Role of dimensionality, disorder, and degree distribution. *Physical Review E*, 72(3):36132, 2005.
- [131] K. Sznajd-Weron and J. Sznajd. Opinion evolution in closed community. *International Journal of Modern Physics C*, 11(6):1157–1166, 2000.
- [132] C. Tao, Q. Liu, B. C. Riddick, W. G. Cullen, J. Reutt-Robey, J. D. Weeks, and E. D. Williams. Dynamic interfaces in an organic thin film. *Proceedings of the National Academy of Sciences*, 105(43):16418, 2008.
- [133] C. J. Tessone and R. Toral. System size stochastic resonance in a model for opinion formation. *Physica A: Statistical Mechanics and its Applications*, 351(1):106–116, 2005.
- [134] D. A. Tomalia, H. Baker, J. Dewald, M. Hall, G. Kallos, S. Martin, J. Roeck, J. Ryder, and P. Smith. A new class of polymers: starburst-dendritic macromolecules. *Polymer Journal*, 17(1):117–132, 1985.
- [135] S.M. Ulam. A collection of mathematical problems. *New York-London*, 1960.
- [136] M. H. Vainstein, A. T. C. Silva, and J. J. Arenzon. Does mobility decrease cooperation? *Journal of Theoretical Biology*, 244(4):722–728, 2007.

- [137] F. Vázquez and V. M. Eguíluz. Analytical solution of the voter model on uncorrelated networks. *New Journal of Physics*, 10(6):063011, 2008.
- [138] F. Vázquez, P. L. Krapivsky, and S. Redner. Constrained opinion dynamics: Freezing and slow evolution. *Journal Physics A: Mathematical and General*, 36(3):L61–L68, 2003.
- [139] L. Verlet. Computer experiments on classical fluids. ii. equilibrium correlation functions. *Physical Review*, 165(1):201–14, 1968.
- [140] J. Von Neumann and O. Morgenstern. *Theory of games and economic behavior*. Princeton University Press, 1944.
- [141] A. Šarlah, T. Franosch, and E. Frey. Melting of colloidal molecular crystals on triangular lattices. *Physical Review Letters*, 95(8):088302, 2005.
- [142] Andreja Šarlah, Erwin Frey, and Thomas Franosch. Spin models for orientational ordering of colloidal molecular crystals. *Physical Review E*, 75(2):021402, 2007.
- [143] D. J. Watts and S. H. Strogatz. Small world. *Nature*, 393:440–442, 1998.
- [144] Shuxia Yin, Chen Wang, Xiaohui Qiu, Bo Xu, and Chunli Bai. Theoretical study of the effects of intermolecular interactions in self-assembled long-chain alkanes adsorbed on graphite surface. *Surface and Interface Analysis*, 32(1):248–252, 2001.
- [145] S. Zhang, D. M. Marini, W. Hwang, and S. Santoso. Design of nanostructured biological materials through self-assembly of peptides and proteins. *Current Opinion in Chemical Biology*, 2002.

List of publications

Parts of the material of this thesis have been prepared for publishing in the following works:

- Rohr, C.; Balbás Gamba, M.; Gruber, K.; Constable, E.; Frey, E.; Franosch, T.; and Hermann, B. Molecular jigsaw: pattern diversity encoded by elementary geometrical features. Published in *Nanoletters*, DOI:10.1021/nl903225j. Contains results of chapter 3.
- Hermann, B. A.; Rohr, C.; Balbás Gamba, M.; Gruber, K.; Malecki, A.; Constable, E. C.; Frey, E.; and Franosch, T. Predicting the ground state in an unprecedented pattern diversity. In preparation, contains results of chapter 3.
- Balbás Gamba, M.; Frey, E. Understanding the role of structures in social dilemmas: the mafia model. In preparation, contains results of chapter 2.

Acknowledgements

You have this manuscript in your hands thanks to the contribution of many great persons which made it possible, both in a professional and a personal sense. To all of them I am kindly grateful.

First of all, I wish to thank Erwin Frey for having given me the possibility to work with him. That was the first step, but by far not the most important. From him I learned how passion can build physical models. I have found great pleasure, like a student in her first lessons, by listening to him in a lecture, a talk, or at his desk, explaining, thinking, creating. Or even dreaming? Thanks for your enthusiasm. For the fruitful discussions, for the thousand ideas.

Thanks as well to Thomas Franosch, who stimulated and advised me in the project of self-assembly at the early stages of my work. This project would have made no sense without the nice and fruitful collaboration with Kathrin Gruber, Bianca Hermann, and Carsten Rohr. Thank you.

Along this time in the group, I was always impressed by its stimulating dynamics. Erwin has managed to set up the best human in vivo lab to test how nicely cooperation works. But this is definitely not enough. Very good players made the rest. Thank you all for the lively and beautiful atmosphere during these seasons. In particular, big thanks to my office-mate, Tobias Reichenbach, for the many enjoyable conversations and thoughts shared.

Special thanks to Isabel Guerra, Cristina Pop, Álvaro Tejero, and Frederik Wagner for the long conversations to improve general understanding and proofreading the manuscript. Thousand thanks to Wolfgang Pietsch and Wolfram Möbius for the chase of *martismus* in the German version of the abstract.

Heiko Hotz generously provided me with his code and explanations to generate the networks used in this work. Thank you.

My computational education was once patiently initiated by Álvaro Tejero. From programming to typesetting and back, pursuing minimalism and functionality. After the intensive beginners course some colleagues and friends were always ready to answer my innumerable technical questions. Daniel Peña, Frederik Wagner, Tobias Munk, Wolfram Möbius, Peter Colberg, and Bruno Rino. Thank you all. If the result is not good enough, I'm the only responsible.

Two persons could have written volumes of "Admin for dummies" by collecting their patient explanations to put some order in my computer. Many thanks for your time, Frederik Wagner and Ralph Simmler.

I want to express my gratitude to *Fundació La Caixa* and the *Deutscher Akademischer Austausch Dienst* for the financial support during two years of this work. I specially want to acknowledge their professionalism and excellent coordination.

This thesis would have not existed without someone who at the worst moment believed and made me believe. He encouraged me to step forward and face a new challenge. Thanks, Álvaro.

José Luis was the first who drew me closer to the fascinating world of physics years and years ago, as he also brought my attention to many other fields which became passions. Thanks, for all the wonderful discoveries.

Thanks to José Manuel Udías, who continuously supported me to step further. Together with other colleagues he lit the hope to believe and fight for better conditions, both social and cultural in our department in Madrid and scientific to approach investigation abroad later.

During the Munich adventure the most valuable luggage was undoubtedly that of the good friends. Without you it would not have been possible. In the distance or in the daily life. Some of you were the stimulus to move back to Munich. Others became the reason to stay. Here and there my old friends, who feed my spirit in our encounters and in the distance, or even almost daily in the *foro*; who supported my worst moments with the joyful *buenos días* arriving from everywhere. And of course, the philosophers, bringing me out of the *Höhle* for the lunches to realize that it is Wednesday, again! And to enjoy your smiles. To you all, a big and heartfelt thanks.

Mi mayor gratitud es para mi familia. Ellos son los responsables del aprendizaje más importante. Y de que hoy pueda estar aquí. Gracias a mis irrepetibles tíos. A Julián, por su humanidad. A mi hermano, Gorka, con el que he compartido tantos magníficos momentos del camino que recorrimos tan a menudo de la mano. Gracias a todos por las interminables conversaciones de sobremesa, por las inquietudes compartidas y transmitidas. Por vuestra alegría. Gracias por arrojarme y hacerme saber querida.

Y especialmente gracias a ti, mamá. Por tu lucha constante. Sólo tú sabes —a veces yo creo intuir— las vicisitudes con las que has lidiado para poder mostrarnos un mundo ilusionante lleno de posibilidades. Para todos. Yo hago mía tu percepción; realidad o quimera es la única que me estimula en cada paso. Espero haber heredado al menos un poquito de ese espíritu que no teme a los gigantes. Muchas gracias.